Universidade Nova de Lisboa

Instituto de Higiene e Medicina Tropical

Trypanosoma brucei effect on leukocyte differentiation and activation

Tatiana Raquel Dias Guerreiro

DISSERTATION IN SUPPORT OF CANDIDATURE FOR A MASTER DEGREE IN BIOMEDICAL SCIENCES, BY THE UNIVERSIDADE NOVA DE LISBOA, INSTITUTO DE HIGIENE E MEDICINA TROPICAL

(MARCH, 2018)

Universidade Nova de Lisboa

Instituto de Higiene e Medicina Tropical

Trypanosoma brucei effect on leukocyte differentiation and activation

Author: Tatiana Raquel Dias Guerreiro

Bachelor of Science (BSc) in Biochemistry (FCT-UNL)

Supervisor: Prof. Dr. Gabriela Santos-Gomes (IHMT-UNL)

Co-supervisor: Prof. Dr. Marcelo Sousa Silva (UFRN - Brazil, and IHMT-UNL)

Dissertation in support of Candidature for a Master Degree in Biomedical Sciences, by the Universidade Nova de Lisboa, Instituto de Higiene e Medicina Tropical

Às pessoas mais importantes da minha vida:

MÃE. PAI. ❤

ACKNOWLEDGMENTS

Em primeiro lugar quero agradecer à minha orientadora, Professora Doutora Gabriela Santos-Gomes, por me ter recebido no seu grupo de investigação. Agradeço-lhe o facto de ter acreditado em mim e por todo o apoio incansável demonstrado. Obrigada por todos os conselhos e rigor, que sem dúvida me fizeram aprender muito, quer pessoal quer profissionalmente. Certamente nunca me irei esquecer de "fazer as rezas" e acreditar que tudo acaba bem. O meu sincero obrigada.

Ao meu co-orientador Dr. Marcelo Sousa-Silva, por toda a partilha de conhecimentos e por toda a atenção disponibilizada.

À Doutora Dinora Lopes, ao senhor Vitor e à dona Rosário pelo trabalho desempenhado no biotério, por toda a simpatia e dedicação.

À Professora Graça Alexandre-Pires, por toda a disponibilidade e ajuda. Obrigada por manifestar ao longo de todo o trabalho, uma constante preocupação e cuidado. Sem a sua ajuda grande parte desta tese não teria sido possível realizar.

Ao professor Doutor Celso Cunha, Doutor João Tavanez, Marina e Rafael por toda a partilha de material, sempre que necessário, e pela simpatia e bom ambiente vivido no laboratório.

À Patrícia por toda a paciência, ajuda e companheirismo. Obrigada por todos os momentos de partilha dentro e fora do laboratório. Foste sem dúvida uma ajuda fundamental neste ano. Nunca me vou esquecer dos nossos momentos e serás sempre uma pessoa muito importante para mim. Desejo-te o melhor do mundo!

À Joana. A minha grande companheira desta aventura. Nem sempre foi fácil, mas contigo por perto todos os problemas se tornaram menores. Nunca me vou esquecer do ano incrível que tivemos no laboratório, nem do quanto a tua presença foi essencial. Ficarás sempre a minha mana, a minha grande companheira. Obrigada pela amizade que permaneceu! Obrigada por tudo!

À Áurea e David Gabriel, por toda a partilha de conhecimentos e ajuda com a edição das fotografias.

Ao Filipe. Por ser o melhor amigo que alguém poderia ter. Obrigada pela ajuda com a edição das fotografias. Por toda a paciência e preocupação. Por todas as conversas e momentos que só nós entendemos. À nossa telepatia. Obrigada por teres sempre uma palavra certa para o momento certo e por me fazeres rir. Obrigada por provares que a distância não significa nada. Amigo não precisa estar, precisar ser! E tu és! Único! Sem ti não teria sido tão fácil o desenvolvimento deste trabalho. Obrigada por tudo!

Ao Hugo e ao Flávio. Por todos os nossos momentos tão únicos. Por estarem sempre lá para tudo. Por toda a ajuda e preocupação. Pelas nossas gargalhadas incríveis. À nossa amizade verdadeira, que sei que se irá manter igual passem os anos que passarem.

À Luísa, por nunca deixar que a distância mude nada, e por ser tão verdadeira! Por ter sempre uma palavra certa para o momento certo e por me encorajar.

À Rita, uma grande companheira da escrita da tese! Contigo por perto tudo se tornou mais fácil. Foste sem dúvida um grande pilar nesta etapa e nunca me vou esquecer. Obrigada pela tua amizade, preocupação e pelos nossos momentos e aventuras por Lisboa.

Rita, Inês, Patrícia, Catarina, Susana, Mariana, sei que mesmo "longe" sempre desejaram que tudo corresse bem. Obrigada pela vossa amizade, e por mostrarem que mesmo separadas por alguns quilómetros nada muda. Obrigada por todos os nossos momentos e cumplicidade, que sem dúvida foram muito importantes para me dar forças para continuar!

À minha prima Daniela, que acompanhou todas as minhas preocupações e superações. Sei o quanto te preocupaste para que esta etapa fosse bem-sucedida. Obrigada pela tua amizade!

Às minhas colegas de casa, Rute e Filipa, por demonstrarem sempre preocupação e interesse. Obrigada por acompanharem as minhas preocupações e superações.

Ao meu Algarve. Pelas lindas praias e paisagens, que me permitiram "renovar energias"! É uma energia única, que sem dúvidas me transmitiu muita força e vontade para continuar.

À minha família, especialmente tios e avós. Sei o quanto se preocuparam e quanto desejaram que tudo corresse bem. Acredito que de alguma maneira a vossa energia chegou sempre até mim e nunca me deixou desistir.

Por último, o meu maior e mais sincero agradecimento, aos meus pais. Por sempre me apoiarem, que mesmo longe estiveram sempre tão presentes ao longo desta etapa. A realização deste mestrado só foi possível com o vosso apoio e suporte e por isso a vocês dedico esta tese. Palavras não são suficientes para demonstrar o quando agradeço o que têm feito por mim. Obrigada por serem o meu grande pilar!

RESUMO

Tripanossomíase Africana ou doença do sono é uma doença zoonótica causada por *Trypanosoma brucei*, um protozoário parasita transmitido pela mosca tsetse ou *Glossina*. A introdução do parasita no hospedeiro vertebrado provoca uma sucessão de eventos que envolvem a imunidade inata e adaptativa. Os macrófagos (MΦ) apresentam um papel fundamental na defesa inata por serem células apresentadoras profissionais de antigénio (APC) e células fagocíticas, importantes na eliminação dos tripanossomas. A imunidade adaptativa é assegurada pelos linfócitos, nomeadamente pelos linfócitos T. Contudo, o papel desempenhado por estas células imunitárias ainda não se encontra completamente clarificado. Assim, este estudo teve como objetivo analisar a atividade dos MΦ na infeção por *T. brucei*, avaliando os níveis de ureia e óxido nítrico (NO) e a expressão membranar das moléculas de classe I (MHCI) e classe II (MHCII) do complexo principal de histocompatibilidade. A diferenciação das populações linfocitárias, T *helper* (Th), T citotóxicas (Tc) e T reguladoras foi também avaliada. MΦ de murganho foram expostos a tripomastigotas de *T. brucei* e estimulados com antigénio total e exossomas de *T. brucei*. A caracterização da ativação macrofágica através de ensaios colorimétricos demonstrou que ambos os fenótipos M1 e M2 foram expressos e foi evidenciada correlação positiva entre a produção de ureia e de NO. Adicionalmente, os resultados da citometria de fluxo indicaram que o parasita prejudica a diferenciação das subpopulações de $M\Phi MHCI^+$ e $M\Phi MHCII^+$ mas induz o aumento de moléculas MHCI. Contrariamente, os exossomas demonstraram estimular as funções APC através das moléculas MHCI e MHCII. Os rácios MHCI/MHCII indicaram que o contacto com o parasita favorece a apresentação antigénica às células $TCD4^+$, enquanto que os exossomas direcionam a apresentação antigénica para as subpopulações de linfócitos $TCD4^+$ e $TCD8^+$. A caraterização das populações linfocitárias através da citometria de fluxo demonstrou que *T. brucei* causa a diminuição das populações de linfócitos Th e Tc. Contrariamente, a estimulação com o antigénio total ou com os exossomas induziram a expansão de ambas as subpopulações linfocitárias. *T. brucei* parece promover a expansão das subpopulações linfocitárias $CD8^-CD25^+FoxP3^-$ e $CD8^+CD25^+FoxP3^-$. A expansão da subpopulação celular $CD25^-FoxP3^+$ foi observada na fração celular $CD8^-$ após estimulação do antigénio e na fração celular $CD8^+$ estimulada por exossomas. Além disso, os exossomas também promoveram a expansão da subpopulação de linfócitos T $CD8^+CD25^+FoxP3^+$. Curiosamente, apesar da contração celular *T. brucei* induziu o aumento das moléculas FoxP3. Em conjunto, os resultados obtidos indicam que o parasita e os exossomas parecem exercer efeitos opostos nas células analisadas. Os parasitas parecem minimizar a apresentação antigénica e evitam induzir a expansão das subpopulações de linfócitos T, facilitando a sua permanência no hospedeiro. Por outro lado, os exossomas segregados por *T. brucei* parecem estimular a apresentação antigénica e mediar a expansão dos linfócitos Th, possivelmente deslocando o foco da atividade do sistema imunitário dos parasitas para os exossomas. Estes resultados permitiram clarificar alguns dos princípios subjacentes à resposta imunitária inata e adaptativa na fase inicial da infeção. A compreensão destes mecanismos pode vir a contribuir para o desenvolvimento de novas estratégias de controlo e eliminação da Tripanossomíase Africana.

Palavras-chave: Tripanossomíase Africana; *Tripanossoma brucei brucei*; Exossomas; Macrófagos; Linfócitos T; Células T reguladoras

ABSTRACT

African trypanosomiasis or sleeping sickness is a zoonotic disease caused by *Trypanosoma brucei*, a protozoan parasite transmitted by tsetse fly or *Glossina*. Parasite introduction into mammal hosts, triggers a succession of events, involving both innate and adaptive immunity. Macrophages (MΦ) have a key role in innate defense, since they are antigen-presenting cells (APC) and have a phagocytosis function essential for trypanosomes clearance. Adaptive immune defense is carried out by lymphocytes, in particular by T lymphocytes. However, the exact role of these immune cells remains not completely understood. Thus, this study aimed to assess the role of MΦ in *T. brucei* infection by measuring the urea and nitric oxide (NO) levels, and by evaluating membrane expression of class I (MHCI) and class II (MHCII) molecules of major histocompatibility complex. The differentiation of T helper (Th), T cytotoxic (Tc) and T regulatory cell subsets was assessed. Mouse MΦ were exposed to *T. brucei* trypomastigotes and stimulated by *T. brucei* extract and *T. brucei* exosomes. Characterization of MΦ activation with colorimetric assays have indicated that both M1 and M2 phenotypes were expressed, evidencing a positive correlation between urea and NO levels produced. Additionally, results of flow cytometry indicated that *T. brucei* impairs the expansion of both $MHCI^+$ and $MHCII^+$ MΦ subsets, but enhanced MHCI molecules. On the contrary, *T. brucei* exosomes stimulated APC functions through MHCI and MHCII molecules. MHCI/MHCII rates indicated that *T. brucei* shift the antigen presentation to $CD4^+$ T cells, while exosomes directed the antigen presentation to both $CD4^+$ and $CD8^+$ T cells. Characterization of lymphocyte subsets by flow cytometry demonstrated that *T. brucei* impairs both Th and Tc lymphocytes. On the contrary, cell stimulation by extract and exosomes promote the expansion of both T cell subpopulations. *T. brucei* seem to promote the expansion of $CD8^-CD25^+FoxP3^-$ and $CD8^+CD25^+FoxP3^-$ T cell subsets. The expansion of $CD25^-FoxP3^+$ T cell subset was observed in $CD8^-$ cell fraction antigen stimulated and in the $CD8^+$ cell fraction exosome stimulated. Moreover, exosomes also induced the expansion of $CD8^+$ $CD25^+FoxP3^+$ T cell subset. Interestingly, despite cell decrease *T. brucei* seemed to increase FoxP3 molecules. Taken together, these findings indicate that parasite and parasite exosomes seem to have opposite effects on the evaluated cells. Parasites seem to minimize antigen presentation and avoid inducing the expansion of T cell subsets, facilitating its permanence in the host. On the other hand, *T. brucei* secreted exosomes seems to induce APC functions and mediate the expansion of Th lymphocytes, probably focusing the immune activity on the exosomes and not on the parasites. These findings allowed to understand some underlying principles of the innate and adaptive immune response in the early-stage of infection. Comprehension of these mechanisms can endorse the development of new strategies for control and elimination of African Trypanosomiasis.

Keywords: African Trypanosomiasis; *Trypanosoma brucei brucei*; Exosomes; Macrophages; T lymphocytes; Regulatory T cells

TABLE OF CONTENTS

LIST OF FIGURES

LIST OF TABLES

ABBREVIATION LIST

×g – Times gravity

aaMΦ – Alternatively activated macrophages

Abs – Antibodies

APt – Alternative pathway

AT – African trypanosomiasis

AAT – Animal African trypanosomiasis

ACD – Anemia of chronic disease

ACK – Ammonium-chloride-potassium

AdC – Adenylate cyclase

APC – Antigen-presenting cells

APOL1 – Apolipoprotein L-1

BSA – Bovine serum albumin

caMΦ – Classically activated macrophages

CATT – Card agglutination test for Trypanosomiasis

CD – Cluster of Differentiation

CEDOC – Chronic Diseases Research Center

CO_2 – Carbon dioxide

CP – Cell percentage

CPt – Classic pathway

CPDA – Citrate-phosphate-dextrose solution with adenine

CNS – Central nervous system

CbSF – Cerebrospinal fluid

CSF – Colony stimulating factor

CPDA – Citrate-phosphate-dextrose solution with adenine

CTL-4 – Cytotoxic T lymphocyte-associated antigen 4

DCs – Dendritic cells

DEAE – Diethylaminoethyl

DF – Dilution factor

DMSO – Dimethyl sulfoxide

EDTA – Ethylenediaminetetraacetic acid

EV – Extracellular vesicles

FBS – Fetal bovine serum

FI – Fluorescence intensity

FITC – Fluorescein isothiocyanate

FoxP3 – Forkhead transcription factor box P3

FSC – Forward scatter light

GIP – Glycosylinositolphosphate

GIP-sVSG – Glycosylinositolphosphate attached to Variant surface glycoprotein

GITR – Glucocorticoid-induced tumour necrosis factor receptor family-related gene

GPI – Glycosylphosphatidylinositol

GPI-PLC – Glycosylphosphatidylinositol-phospholipase C

HAT – Human African trypanosomiasis

HDL – High-density lipoproteins

HIF-1α – Hypoxia-inducible factor-1α

Ig – Immunoglobulins

IHMT – Instituto de Higiene e Medicina Tropical

IL-1β – Interleukin-1β

IFN-γ – Interferon-γ

IM – Intramuscularly

IV – Intravenously

kDNA – Kinetoplast DNA

LAG-3 – Lymphocyte activation gene-3

LPt – Lectin pathway

MΦ – Macrophages

MAC – Membrane attack complex

MHC – Major histocompatibility complex

MHCI – Major histocompatibility complex class I molecules

MHCII – Major histocompatibility complex class II molecules

MyD88 – Myeloid differentiation primary response protein 88

NC – Negative control

NECT – Nifurtimox-eflornithine combination therapy

NHS – Normal human serum

NO – Nitric oxide

NO_2^- – Nitrite

NO_3^- – Nitrate

NOS2 – Nitric oxide synthase 2

NTD – Neglected tropical disease

OA – Oral administration

OD – Optical density

PAMPs – Pathogen-associated molecular pattern molecules

PBS – Phosphate-buffered saline

PBSG – Phosphate-buffered saline with glucose

PC – Positive control

PE – Phycoerythrin

PerCP – Peridinin Chlorophyll Protein Complex

PPRs – Pattern-recognition receptors

PMA – Phormol myristate acetate

PMBC – Peripheral mononuclear blood cells

RNA – Ribonucleic acid

ROI – Reactive oxygen intermediates

RPMI - Roswell Park Memorial Institute

RT – Room temperature

RTD – Rapid diagnostic-test

ScEM – Scanning electronic microscopy

SEM – Standard error of mean

SIF – Stumpy-induction factor

SIRS – Systemic immune response syndrome

SRA – Serum resistance-associated

SR-A – Type A scavenger receptors

SSC – Side scattered light

TbKHC-1 – *Trypanosoma brucei*-derived kinesin heavy chain

TGF-β – Transforming growth factor

Tc – T citotoxic

Th – T helper

TLF – Trypanolitic factor

TLTF –Trypanosome-derived lymphocyte triggering factor

TSIF – Trypanosome suppression immunomodulating factor

TNF-α – Tumor necrosis factor alpha

Treg – Regulatory T cells

VAT – Variable antigenic type

VS – Volume sample

VSG – Variant surface glycoprotein

WHO – World Health Organization

1. INTRODUCTION

1.1. African Trypanosomiasis

1.1.1. General concepts

African trypanosomiasis (AT), otherwise termed sleeping sickness, is a vector-borne disease caused by an extracellular Kinetoplastida parasite belonging to Trypanosomatidae family, genus *Trypanosoma* and species *Trypanosoma brucei* (Barrett et al., 2003, Vincendeau and Bouteille, 2006, Malvy and Chappuis, 2011, Franco et al., 2014).

This endemic parasitic disease is restricted to the intertropical regions of Africa, where the parasite is transmitted by a unique vector, the tsetse fly or *Glossina* (Vincendeau and Bouteille, 2006). This disease exhibits high morbidity and mortality rates and according the World Health Organization (WHO) is classified as a neglected tropical disease (NTD) (WHO, 2012).

T. brucei (*T. b.*) is divided into three subspecies, where *T. b. rhodisiense* and *T. b. gambiense* cause human infections and *T. b. brucei* is only infective for animals. Furthermore, *T. congolense* and *T. vivax* are also infective for animals (Steverding, 2008).

Since parasites that cause Human African Trypanosomiasis (HAT) are very similar to *T. b. brucei* and there are few murine HAT models, *T. b. brucei* is the most used parasite in the majority of AT research (Keita et al., 1997).

1.1.2. Geographical distribution and Epidemiology

There are described more than 360 active foci, and the majority is in rural areas where sanitary and hygiene conditions are underprivileged and health care systems are fragile and difficult to reach (Cattand et al., 2001, Franco et al., 2014). Although this disease has a focal distribution, there are some areas where the habitats present suitable conditions to support vector life cycle, but where it was never reported any case of AT (Malvy and Chappuis, 2011).

The majority of data reported on HAT cases includes infections by *T. b. gambiense* and *T. b. rhodesiense*. These two parasites are described as causing two

different diseases, with different epidemiological and clinical patterns and different treatment. *T. b. gambiense* infection gives rise to a chronic disease and is found in Western and Central Africa, while *T. b. rhodesiense* leads to the acute form and is found in Eastern and Southern Africa (**Fig. 1**).

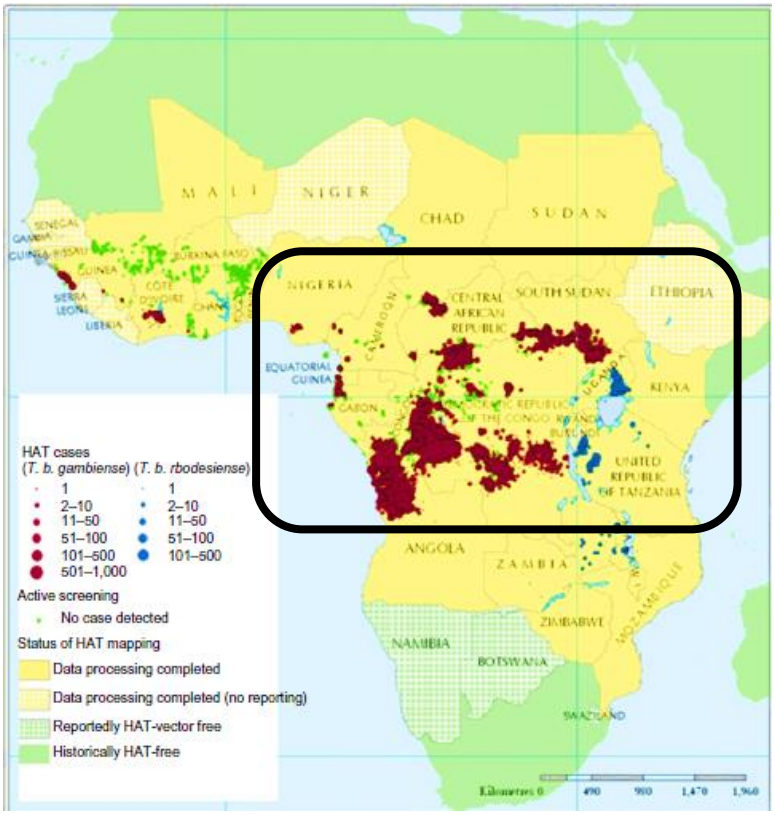

Figure 1 – Geographical distribution of HAT. Surrounded area comprises the majority of detected HAT cases**,** between 2000-2009 [Adapted from (Franco et al., 2014)].

The risk factors associated with this disease are mainly determined by the exposition of humans and animals to the infected tsetse fly. However, there are other transmission routes described. Vertical transmission has been reported in children, which mothers became infected during pregnancy. The infection can also be acquired through blood transfusion, although the reported cases are very rare. Even though once reported, sexual contact is also a possible transmission (Rocha et al., 2004). Although never reported, it is also possible that the transmission can occur by organ transplantation. Along with all of these atypical transmission routes, accidental mechanical transmission can also occur in laboratory work (reviewed in Franco et al., 2014).

In the late nineteenth century occurred the first epidemic, being reported 300,000-500,000 deaths in Africa (Malvy and Chappuis, 2011). Between 1920 and 1940 the second great epidemic induced colonial authorities to invest in vector control. This investment promotes the reduction of disease incidence in a progressive way until mid-1960s, when disease was almost eliminated (Malvy and Chappuis, 2011, Franco et al., 2014). In the late 1990s, it was observed a disease resurgence related to post-independence period and associated with reduction of control and surveillance programs due to civil conflicts. HAT increase placed WHO in the coordination of control programs and, as a result, since 2000 the number of notifying cases has been decreasing **(Fig. 2**). In, 2012, this organization intended to achieve the elimination of gambiense HAT as a public health problem in 2020, and the sustainable elimination (interruption of the transmission of gambiense HAT) of the disease is previewed in 2030 (Franco et al., 2014).

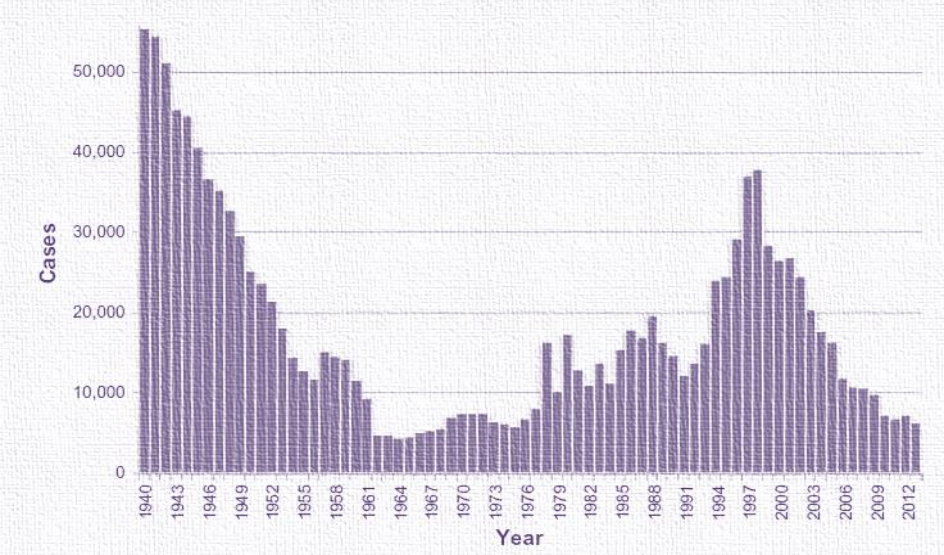

Figure 2 – Epidemiological pattern of African trypanosomiasis. Total number of new cases reported between 1940 and 2012 [Adapted from (Franco et al., 2014)].

Clinical data show that gambiense-HAT cases represent 98% of the total HAT cases, while cases of rhodesiense-HAT remain in ~2%. It is possible that in the future an overlap of the two forms of HAT can occur, since refugees from endemic areas of gambiense are moving into areas occupied by the rhodesiense clinical form (Franco et al., 2014).

1.2. *Trypanosoma*

1.2.1. General features

The genus *Trypanosoma* can be divided into two groups: salivaria and stercoraria (**Fig. 3**). African parasites are included in the first group, which means that the salivaria parasites are able to settle in the stomach of their vector, but they never take place at the intestinal track (Baral, 2010).

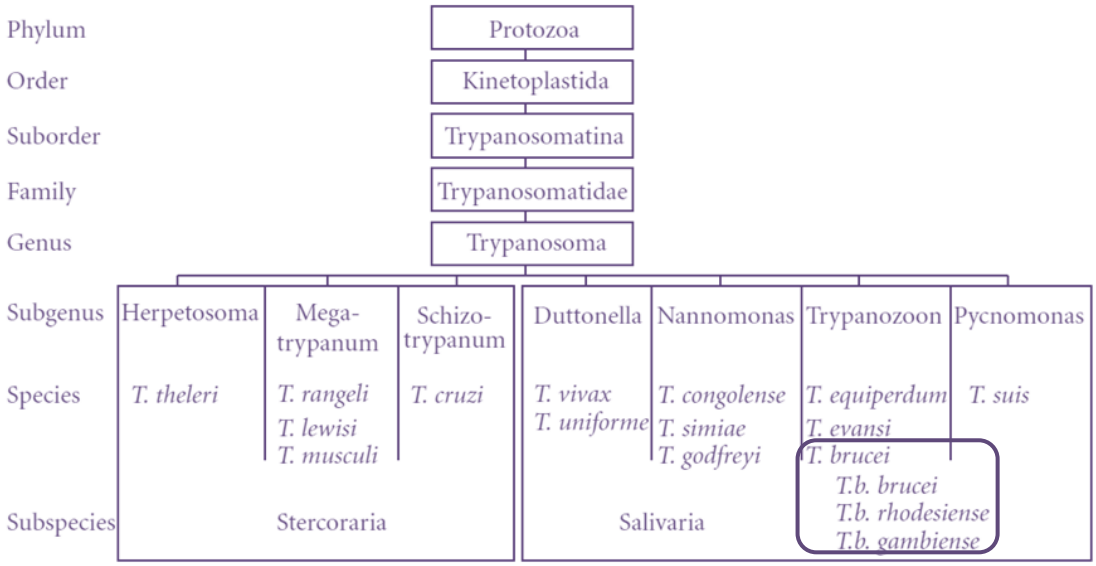

Figure 3 – Simplified classification of *Trypanosoma* species. The genus *Trypanosoma* includes seven subgenera that comprises fourteen species, where it is included the species *T. brucei*, which encloses three subspecies (Adapted from Baral, 2010).

The size of *Trypanosome* varies according to the environment and the morphological form (**Fig. 4A**). If in the mammal host, trypomastigote form present size ranging from 16-42 µm, while in the vector, their epimastigote form has a length between 10-35 µm (Sharma et al., 2009).

Once this parasite is a eukaryote, it contains an elongated mitochondria. This mitochondria exhibits a highly condensed DNA that is recognized as the kinetoplast (kDNA) (**Fig. 4B**) (Baral, 2010). In the trypomastigote form, kinetoplast is localized in the posterior region of parasite and so kDNA has a post-nuclear position, while in the epimastigote form, it is located in an anterior position relative to the nucleus, evidencing a pre-nuclear kDNA (Maslov et al., 2013).

This parasite also contains a flagellar pocket (**Fig. 4C**) that is an invagination of the plasma membrane and is the place where the flagellum is attached to. The flagellum is responsible for (i) cell motility that is required for the viability of the bloodstream forms; (ii) attachment of the parasite in host surfaces; (iii) morphogenesis and cell division (Baral, 2010). In both trypomastigote and epimastigote forms the flagellum emerges from a lateral opening of a flagellar pocket (Maslov et al., 2013).

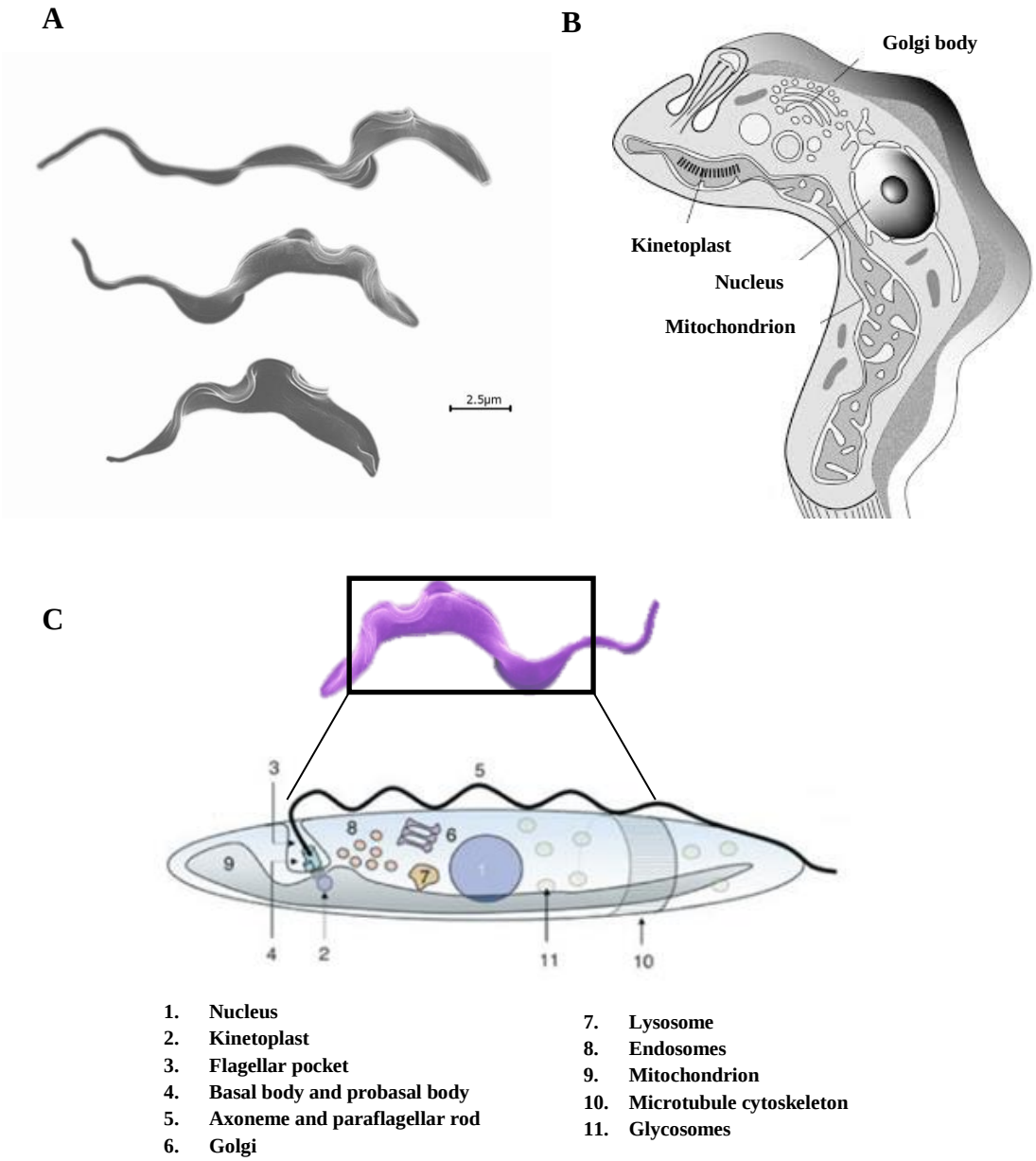

Figure 4 - ***Trypanosome*** **schematic representation. A –** Variation of parasite size. Scale bar: 2,5 µm; **B –** Representation of the parasite posterior region**; C –** Structural main components of *Trypanosome* (Adapted from Matthews, 2005).

Like mammal cells, trypanosomes secrete extracellular vesicles (EV), such as microvesicles and exosomes (Raposo and Stoorvogel, 2013) (**Fig. 5A**). Exosomes are nanovesicles that are released into the extracellular space upon fusion with the plasma membrane. Exosomes contain molecular components of the cell, such as proteins, ribonucleic acid (RNA), deoxyribonucleic acid (DNA) and lipids (Stoorvogel et al., 2002). It is reported that *T. brucei* releases exosome-like vesicles with 50-100 nm (**Fig. 5B**). EV seems to play a key role in both parasite-parasite and parasite-host interactions, being able to induce an effect in host immune systems (Marcilla et al., 2014).

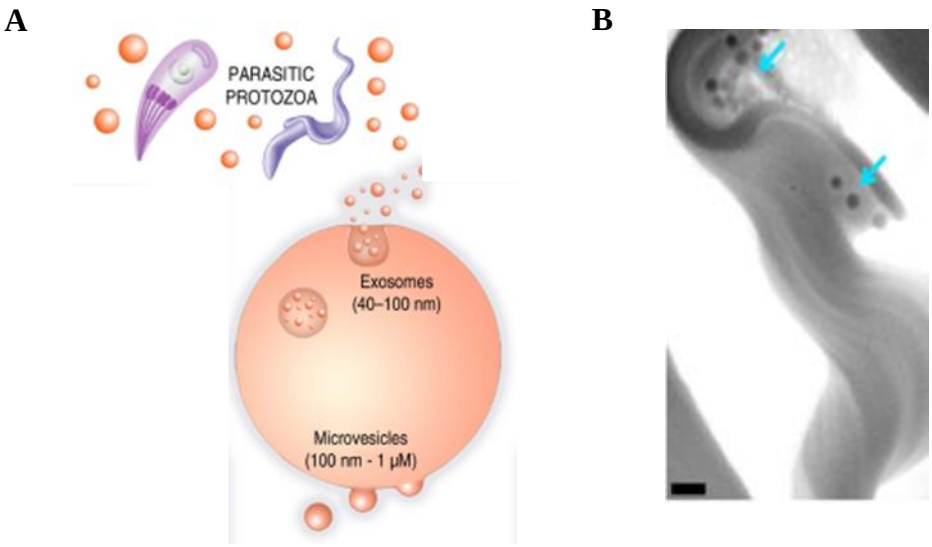

Figure 5 – Extracellular vesicles associated to parasitic diseases. A- Schematic representation of exosomes and microvesicles released by parasitic protozoa. B- EV at *T. brucei* surface, indicated by blue arrows. Scale bar: 400 nm [Adapted from (Szempruch et al., 2016)].

1.2.2. Life cycle

African trypanosomes are characterized by having an heteroxenous life cycle, that alternates between the intestine of their hematophagous vector and the blood of the mammalian host (Achcar et al., 2014).

To acquire the energy necessary, trypanosomes need to absorb nutrients such as proteins, fats and carbohydrates, as well as oxygen and iron, that are present in the blood fluids of their hosts (Stijlemans et al., 2015, Basu et al., 2016). While in mammal host, the principal source of energy is glucose and in their vector is the proline. Once in the vertebrate host, bloodstream forms can be found in different host fluids, such as lymph and cerebro-spinal fluid (CbSF), and often can cross the placenta (Brun et al., 2010). When reaches the brain, after crossing choroid plexus, parasite replication by mitosis takes about 5-10 h (Turner et al., 1995).

Trypanosomes multiply by binary fission, but sometimes sexual reproduction can occur in the salivary gland of their invertebrate host. Hence, they yield the possibility of genetic exchange and the rapid trade of virulence factors or drug resistance associated genes (Peacock et al., 2011).

It is described that *T. brucei* parasites can be monomorphic, which means they exhibit only their long-slender dividing form, or pleomorphic, when exists the slender form and the short stumpy non-dividing form (**Fig. 6**) (Breidbach et al., 2002). Both forms are covered by variant surface glycoprotein (VSG). When within the tsetse fly the parasite is covered by a procyclin coat and the VSG coat is only acquired upon differentiation into metacyclic form, the infective form (Barry et al., 1998, Maslov et al., 2013).

To allow the reestablishing of life cycle once ingested by the tsetse fly, these parasite release a stumpy induction factor (SIF) that only triggers the production of non-replicating forms (Fenn and Matthews, 2007). Only these forms can develop in the vector while the slender forms totally disappear, probably due to lack of glucose. Once infected, the tsetse fly remains infected for all their lifetime, where the parasite life-cycle inside the vector takes about 18-35 days (Vickerman et al., 1988).

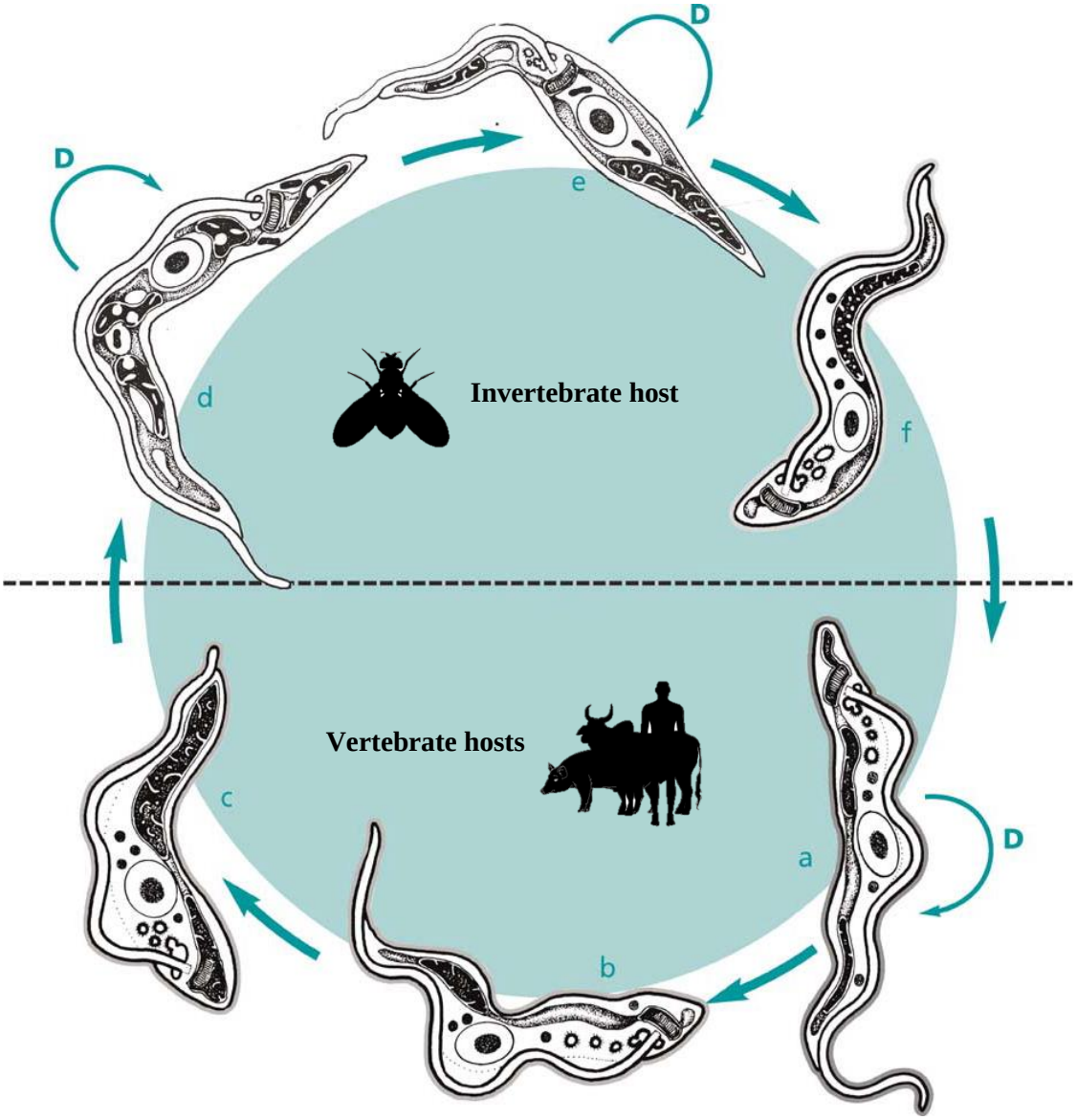

Figure 6 - **Life cycle of *T. brucei.*** Parasite life cycle can be divided into two phases that allow their survival into the both hosts (vertebrate and invertebrate). Transmission of parasites occurs by the bite of an infected tsetse fly. During a blood meal on the host, the vector injects metacyclic trypomastigotes (f). The parasite enters the haemolymphatic system and pass into the bloodstream and can even invade the central nervous system (CNS). Inside the host, the parasite transforms into the proliferative slender bloodstream forms (a) and continue the replication by binary fission, via an intermediate form (b) into a non-proliferative stumpy form (c). The tsetse fly becomes infected with this form, that is pre-adapted to survive inside the vector, having the capacity to differentiate into procyclic forms (d) that multiply by binary fission in the fly's midgut. These forms leave the midgut and differentiate into epimastigote forms (e) that reach the fly's salivary glands and continue to replicate by binary fission and then differentiate into metacyclic trypomastigotes (f). **D** indicates the replicative forms (Adapted from Barrett et al., 2007).

1.3. Human and Animal African Trypanosomiasis

Sleeping sickness is an example of a reemerging zoonosis, and is hallmarked by a fragmented sleep pattern, where sleep and wakefulness disturbances occurs. (Lundkvist et al., 2004).

1.3.1. Clinical Features

The inoculation of the parasite into mammal hosts causes a series of events that involves in the early-stage innate immunity and, in late-stage, adaptive immunity. (Vincendeau and Bouteille, 2006).

After being introduced into the host dermis, the parasites start to replicate giving origin to the initial lesion or the inoculation chancre that is characterized by a local erythema, heat, edema, tenderness and a lack of any suppuration (Barrett et al., 2003, Vincendeau and Bouteille, 2006). After two or three weeks, the chancre tends to disappear, and the disease can evolve in two distinct successive phases (Vincendeau and Bouteille, 2006).

The phase I or the hemolymphatic stage is characterized by successive waves of invasion of the blood and lymphatic system by the trypanosomes, which causes intermittent fever (Lundkvist et al., 2004, Vincendeau and Bouteille, 2006). Cardiovascular alterations, headaches, irregular fever, exhaustion, anorexia, extreme thirst, muscle and joint pains, pruritus, anemia, rash and frequently deep hyperesthesia are the principal clinical features that characterize this first stage (Vincendeau and Bouteille, 2006). This phase of the disease is sometimes undiagnosed since fever can be absent and this way does not allow the correct diagnosis, and consequently the disease stays untreated (Ponte-Sucre, 2016).

In the phase II or the meningoencephalitis stage, the general clinical features associated to stage I do not completely disappear. The typical symptoms of sleeping sickness occur at stage II. Patients exhibit daytime somnolence and nocturnal insomnia (Vincendeau and Bouteille, 2006). This disturbed sleep pattern is accompanied by headaches, confusion, mood swings, aggressive behavior, euphoria, tremor, extreme lethargy, poor condition and, lastly coma (Lundkvist et al., 2004, Vincendeau and

Bouteille, 2006). Apart from the disruptions of the circadian rhythm, other biological rhythms are disturbed, like the body temperature, cortisol and prolactin or growth hormone secretion, glucose depletion featuring a diabetes like-state, as well as of plasma renin activity (Lundkvist et al., 2004, Vincendeau and Bouteille, 2006). Patients exhibit a progressive aggravation of the neurological symptoms. At the terminal phase of the disease, demyelination and atrophy of CNS occur. Moreover, consciousness disturbances can occur, as well development of dementia with incoherence, incontinence and epileptic fits (Vincendeau and Bouteille, 2006). The patient remains in a state known as cachexia and when not treated, an encephalitic reaction can appear leading to death (Vincendeau and Bouteille, 2006, Cnops et al., 2016). The patient dies due to physiological collapse or heart failure (Ponte-Sucre, 2016).

In the case of African Animal Trypanosomiasis (AAT), also called Nagana, all the domestic animals can be infected, and the symptoms described are fever, listlessness, emaciation, hair loss, discharge from the eyes, edema, anemia and paralysis. With the progression of the disease the animals become unfit, and so this explains the disease name “N’gana” (a Zulu word which means “powerless/useless”) (Steverding, 2008).

1.3.2. Diagnosis

To establish HAT diagnosis three principles need to be followed: (i) screening; (ii) parasitological confirmation and (iii) staging. According to Malvy and Chappuis, (2011) the Card Agglutination Test for Trypanosomiasis (CATT) is a simple and rapid serological screening test, and its use is universal. Despite all of the advantages, CATT has some limitations, such as limited sensitivity (Kennedy, 2013). Other serological tests are available, like immunofluorescence or ELISA, but their use in endemic countries faces limitations (Malvy and Chappuis, 2011).

To confirm the presence of parasites, it is common to proceed to their search in the chancre lesion and on cervical lymph node fluid by puncture, or in the blood by microscopic visualization. Once there are few circulating parasites, blood concentration techniques are used, like microhematocrit centrifugation or capillary tube centrifugation

technique. Although these techniques are widely used, the sensitivity is low. For trypanosome detection, the most sensitive technique is the miniature-anion-exchange centrifugation that separates parasites from venous blood and allows the concentration by centrifugation, although it is more expensive and requires more time (Malvy and Chappuis, 2011).

Once the patient is confirmed with HAT, staging by CbSF examination is essential because treatment differs according the stage. Stage II is confirmed by using the threshold criteria of 5 white blood cells/μL and/or parasites in the CbSF (Malvy and Chappuis, 2011). In the late stage occurs the appearance of morular cells, also known as Mott cells, which are plasma cells containing IgM inclusions, and so a high IgM concentration in CbSF is also a reliable marker of CNS involvement (Malvy and Chappuis, 2011, Kennedy, 2013). Also, CbSF protein is increased (>25 mg per 100 mL) (Barrett et al., 2003).

T. congolense, T. vivax and *T. brucei* share a high level of homology, leading to limitations in AAT diagnosis. Diagnostic methods of AAT can be divided into two categories: detection of parasite or its antigens and/or DNA and detection of antibodies. The first one allows the detection of a current infection while the second has one limitation, is not able of distinct the infection stage (Jongejan et al., 1988).

1.3.3. Treatment

Although many studies have been done in order to establish an effective treatment, the actual drugs used to treat HAT are facing some limitations. Drugs used in both early and late stages are not available for oral use, sometimes exhibiting a toxic effect and often are ineffective, and no vaccines are available yet (Kennedy, 2013, Geiger et al., 2016). As mentioned before, the diagnosis need to be rigorous, once the treatment depends on the stage of the disease. Also, it is important to identify which of the subspecies was responsible for the infection, once the treatment is different for an infection caused by *T. b. gambiense* or by *T. b. rhodesiense* (**Table 1**).

Table 1 – Anti-trypanosomal treatment currently in use. Drugs used in first- and second line-treatment for both early- and late-stage of Human African trypanosomiasis (Adapted from Malvy and Chappuis, 2011 and Kennedy, 2013).

Stage	Parasite	First-line treatment	Dosing	Second-line treatment	Dosing
Early-Stage	*T. b. gambiense*	Pentamidine	4 mg/kg/day IM or IV 7 days	Suramin	IV/IM
	T. b. rhodesiense	Suramin	4-5 mg/kg/day IV (1st day), then 20 mg/kg/day IV 5 weeks	Pentamidine	IM
Late-Stage	*T. b. gambiense*	NECT (Eflornithine + Nifurtimox)	E: 400 mg/kg/day IV 7 days N: 15 mg/kg/day OA 10 days	Melarsoprol	2.2 mg/kg/day IV 10 days
	T. b. rhodesiense	Melarsoprol	2.2 mg/kg/day IV 10 days	NA	

IM: intramuscular; **IV:** intravenous; **NECT:** nifurtimox-eflornithine combination therapy; **OA:** oral administration: **NA:** not available

First-line treatment for early-stage *T. b. gambiense* rely on pentamidine. It is administered intramuscularly (IM) or intravenously (IV). Although its effectiveness has been confirmed, some complications are associated such as hypotension, hyperglycaemia or hypoglycaemia, and rarely can occur anaphylaxis and clinical pancreatitis. For late-stage, is the nifurtimox-eflornithine combination therapy (NECT) that is used currently. In this therapy nifurtimox is orally administered (OA) while eflornithine is delivered IV. Nifurtimox was originally used for Chagas' Disease, or American Trypanosomiasis (caused by *T. cruzi*). Eflornithine (also known as α-difluoromethylornithine or DFMO) is a trypanostatic drug, which means it affects trypanosome metabolism, but at the same time is cytostatic, since it affects the host cells. NECT emerged to replace the eflornithine monotherapy, that can cause bone marrow toxicity, alopecia and gastrointestinal disturbances. Although these side-effects can also occur in combination therapy, the rates of mortally post-treatment are 0.7%, comparing to monotherapy that reached values of 2.1% (Malvy and Chappuis, 2011, Kennedy, 2013, Keating et al., 2015).

For early-stage of *T. b. rhodesiense* disease, currently suramin is IV administered. This drug is defined as very effective, but also can cause some side-effects to the patient, like renal failure, anaphylactic shock, skin lesions and peripheral neuropathy. Melarsoprol is available to treat late-stage disease. However, this drug is poorly tolerated by most patients and presents a widely range of secondary effects, such

as hepatic toxicity, acute phlebitis, vein sclerosis and encephalopathic syndrome (Malvy and Chappuis, 2011).

In the early-stage of disease, there are alternative treatments or second-line treatment that basically relies on a drug alternation. Thus, in alternative treatment, *T. b. gambiense* first-line treatment is applied for *T. b. rhodesiense* treatment, and in turn alternative treatment for *T. b. rhodesiense* corresponds of *T. b. gambiense* first-line treatment. The same occurs in the late-stage, where *T. b. gambiense* second-line treatment corresponds to *T. b. rhodesiense* first-line treatment. However, for rhodesiense form there is no available second-line treatment for late-sage, since melarsoprol still is the only effective drug (Kennedy, 2013, Keating et al., 2015).

Despite all of these described treatments, many studies have been done in order to improve the treatment, and for further disease elimination. Murine model recent studies reported that an orally active drug, called SCYX-7158, was able to cure the late-stage of both disease forms. According to Nare et al., (2010), this compound that belongs to the oxaborole class drug has been used in clinical trials phase I and continued studies evidenced positive results, pointing this class of drugs as a possible new treatment. Most recently, Field et al. (2017) reviewed anti-trypanosomatid drugs and reported that this compound in now in the phase II of tests. Also, fexinidazol is being tested at clinical trial phase III.

Contrary to HAT, where NECT seems to show great results, in AAT no drugs combinations are currently being used. Instead, the treatment alternates between two compounds, diminazene and isometamidium. These two compounds are called “sanative pairs” and although their use is essential, there are reported some cases of inefficiency related to multiple drug-resistant trypanosomes (Giordani et al., 2016).

1.3.4. Trypanotolerance

As mentioned before, if no treatment is applied against this infection, death can occur. However, Jamonneau et al. (2012) followed the infection of a few patients infected with *T. b. gambiense* that refused to accept treatment and reported that with time these patients reverted for an asymptomatic stage. These patients had no blood

circulating parasites and a decrease of antitrypanosome antibody titers was observed. In some cases, patients became seronegative. Other asymptomatic patients had no detectable parasitemia, but continued seropositive (Jamonneau et al., 2004, 2012). This asymptomatic status is defined as trypanotolerance, which means that the patient is able to control the infection (Kennedy, 2013).

Although these preliminary studies raise some unanswered questions about this phenomenon, trypanotolerance is well described in animals, such as cattle and experimentally infected mice (Ponte-Sucre, 2016).

1.4. Immune response against trypanosomes

The immune system is constituted by innate and acquired responses. Taken together these responses are responsible for host defense by (i) recognition of foreign antigens for further elimination, (ii) generation of immune memory and (iii) development of tolerance to self-antigens (Luckheeram et al., 2012).

From parasite point of view, it is crucial to induce an equilibrated immune response that can destroy and eliminate the excessive amount of parasites, maintaining a lower parasitemia to guarantee their persistence, and at the same time preventing the host to be killed so they can continue their life cycle (Stijemans et al., 2007).

1.4.1. Innate immune response

The innate immune system is the first line of host defense, which means that in the presence of a pathogen, its function is crucial for early recognition and triggering of a proinflammatory response. Epithelial barrier of the skin, the alternative complement cascade and other lytic serum components, dendritic cells (DC), oxygen and toxic nitrogen metabolites of macrophages (MΦ) and other phagocyte cells constitutes the principal components involved in innate defense (Mogensen, 2009).

DC display many dendrites that capture antigens and stimulate lymphocytes. These cells are found in nonlymphoid tissues, but are able to migrate to lymphoid organs through the afferent lymph or bloodstream, initiating the adaptive immune

response. MΦ are mononuclear cells that can engulf foreign antigens through endocytosis processes such as phagocytosis. Both these cells are antigen-presenting cells (APC) (Geiger et al., 2016). APC functions include the (i) antigen uptake, (ii) process native antigens in the acidic compartment of the endocytic pathway and (iii) the final presentation of resultant antigenic peptides to T cells (Chaplin, 2010).

Also, alternative complement activation has a key role in the first line of defense. Complement system is composed of cell surface and plasma proteins and can be activated through three different pathways (i) classical pathway (CPt), (ii) alternative pathway (APt) and (iii) lectin pathway (LPt) (Chaplin, 2010). When activated, three major types of effector components are generated: (i) anaphylatoxins (C3a and C5a), proinflammatory molecules that are able to attract and activate lymphocytes; (ii) opsonins (C3b, iC3b and C3d) that attach covalently to target surface to allow their transport and further elimination; (iii) the membrane attack complex (MAC) (Noris and Remuzzi, 2013). In the presence of pathogens, occurs the activation of complement cascade and as consequence C3 molecules are generated. When activated by proteolytic cleavage promoted by C3 convertases, C3b molecules are produced and will bind covalently to the surface of the parasite. Consequently, these molecules allow the MAC to assemble and attack on parasite membrane, causing parasite lysis (Geiger et al., 2016, Joiner, 1988).

Similarly, natural killer (NK) cells play a critical role in innate immune response, due to its lysis effect on extracellular parasites. NK are granular lymphocyte-like cells that are able to synthesize chemokines, and consequently initiate an inflammatory response by secreting interferon (IFN)-γ and tumor necrosis factor (TNF)-α (Mogensen, 2009). Together with DC and γδ T cells, which role in trypanosomiasis is not completely understood, NK establish a bridge between innate and adaptive immune responses.

This response is not specific and is characterized by the recognition of pathogen-associated molecular pattern molecules (PAMPs), that are conserved structures present on the surface of different organisms. Within the progression of an infection, PAMPs are recognized by pattern-recognition receptors (PPRs) followed by the activation of

signaling pathways. Consequently, immune mediators are produced by innate immune cells, leading T-lymphocyte to initiate their functions (Mogensen, 2009).

1.4.1.1. Parasite recognition

Trypanosomes are surrounded by a dense surface coat where a single polypeptide is the major component, the Variant Surface Glycoprotein (VSG). These immunogenic coats have 12-15 nm and are present at the cell surface as homodimers and anchored in the membrane by glycosylphosphatidylinositol (GPI) (Namangala, 2011, Horn, 2014). GPI-anchored with VSG homodimers constitutes the PAMPs that are recognized by PPRs and down-regulate the host innate immunity (Paulnock et al., 2010).

1.4.1.2. Parasite/host interaction

During infection, GPI anchors suffers cleavage when an endogenous GPI-phospholipase C, localized along the parasite flagellum, is activated (Paulnock and Coller, 2001, Paulnock et al., 2010). VSG is released from the membrane with glycosylinositolphosphate (GIP) residues attached (GIP-sVSG) (Paulnock et al., 2010). Studies have shown that the release of GPI-sVSG is rapidly detectable in host tissues and seems to occur in episodes of high parasite burden and define them as the first to activate cells of innate response. GIP-sVSG has an affinity for type A scavenger receptors (SR-A) that are present on MΦ and DCs membranes (Paulnock et al., 2010).

Although MΦ receptor -binding *T. brucei* has not been identified yet, in case of *T. congolense*, most recent studies reported that immune activation occurs through the binding of the parasite to the toll-like receptor 2 (TLR2) expressed on MΦ (Kuriakose et al., 2016). In *T. brucei* infection, it has been demonstrated that the activation of the innate response is dependent of the myeloid differentiation primary response protein 88 (MyD88) (Drennan et al., 2005).

MΦ are crucial to initiate and maintain anti-*Trypanosome* response, due to their phagocytosis ability, which is the principal mechanism for clearance of trypanosomes from the blood stream (Namangala, 2012). Studies performed in *T. brucei*-infected mice

showed that the expansion of MΦ population occurs in liver, spleen and bone marrow (Vincendeau and Bouteille, 2006).

When GIP-sVSG interacts with MΦ, they are classically activated (caMΦ), also denominated M1-MΦ type, and start to produce proinflammatory molecules, like TNF-α, IL-6 (denominated type I cytokines) and, nitric oxide (NO) (Baral, 2010). Furthermore, early studies with purified GPI have shown that GPI triggers MΦ to secrete proinflammatory cytokines that can be responsible for the cachexia that hallmarks this disease (Tachado and Schofield, 1994). Moreover, MΦ are also responsible for phagocytosis and clearance of opsonized parasites (Kuriakose et al., 2016).

TNF-α presents a major role in activation, proliferation and differentiation of B cells, through a sequence of events that contributes to further parasite elimination. Moreover, it was reported that in *T. b. brucei*-infected mice TNF-α levels increase in brain after treatment with anti-trypanosomal drugs (Hunter et al., 1991). However, high levels of this cytokine are known to be responsible for fever, asthenia, hypergammaglobulinemia and cachexia that are very common characteristics of this disease (Ponte-Sucre, 2016). In fact, TNF-α seems to be responsible for the general state of inflammation, that can lead to meningoencephalitis in late-stage, as well for anemia and tissue necrosis, a hallmark of this parasitosis (**Fig. 7**) (Magez et al., 2002, Sternberg, 2004). Furthermore, it has been also proposed that TNF-α is used for trypanosomes to penetrate through the blood brain barrier (Enanga et al., 2002). Previous studies with *T. evansi* showed that neither TNF or NO seemed to control the infection, while in *T. brucei*, TNF seems to control parasitemia (Ponte-Sucre, 2016). Relatively to IL-4, their role remains poorly described and understood. Some studies with *T. gambie*nse showed that this cytokine controls the infection, while other authors reported that knockout mice lacking IL-4, did not show any alteration in infection control.

To subvert the effect of M1-MΦ, trypanosomes release some components, such as *Trypanosoma brucei*-derived kinesin heavy chain (TbKHC-1) and adenylate cyclase (AdC). These parasite components trigger myeloid cells to produce IL-10 and arginase that in turn induce polyamine production, which are nutrients necessary for parasite

survival. Furthermore, IL-10 prevents TNF production (Salmon et al., 2012, De Muylder et al., 2013).

Upon interaction with trypanosome soluble factors, MΦ synthesizes reactive oxygen intermediates (ROI), such as hydrogen peroxide and hypochlorous acid that are oxygen species, whose trypanosomes are sensitive to (Vincendeau and Bouteille, 2006).

In order to reduce the inflammation that when sustained can cause pathology, the host down regulates caMΦ and the production of pro-inflammatory cytokines, leading MΦ to be alternatively activated (aaMΦ), or M2-MΦ type, becoming anti-inflammatory. Type II cytokines, like IL-4, IL-10 and IL-13 are produced, avoiding tissue damage (Baral, 2010). It is described that during infection, MΦ also release immunosuppressive cytokines, like transforming growth factor (TGF)-β that seems to inhibit IL-4, which plays a key role in B cell proliferation and differentiation (Fargeas et al., 1992, Vincendeau and Bouteille, 2006).

Type I inflammatory response is critical in the early stage of infection and the shift to the type II response plays a critical role in late stage (Baral, 2010). This switch from M1-MΦ to M2-MΦ occurs 4 weeks after infection, when the late stage of the disease takes place (Namangala, 2012). However, the role of some cytokines that are released within disease progression is not completely understood (Baral, 2010).

In *T. brucei*-infected mice, it has been demonstrated that Th2 cytokines allow a longer survival. Moreover, when IL-6 and IL-10 are produced seems to protect neuroinflammatory pathology. Therefore, it is suggested that hyperactivated M1-MΦ and the consequent persistence of type 1 immune response are associated with trypanosusceptibility, featuring systemic immune response syndrome and anemia. On the other hand, trypanotolerance is associated with animals that can switch to type 2 immune response by inducting aaMΦ (Stijemans et al., 2007).

Although complement activation occurs in the early-stage of the disease, it is described that sometimes it is observed “hypocomplementemia” (Devine et al., 1986). This phenomenon has been demonstrated with *T. b. gambiense* exposed to human serum. These authors reported that through VSG, parasite inhibits activation of the alternative pathway. This occurs when this parasite is covered by C3 and C3 convertase.

Hence, the terminal complex (C5-C9) responsible for trypanolysis become impaired, no lytic activity is triggered, and consequently the complement cascade stops (Devine et al., 1986, Stijlemans et al., 2016). Moreover, it is also reported that the release of C3a and C5a, that occurs in the early stage of the infection, contributes to initiate immune response since both complement components act like chemotactic agents, attracting phagocytes to the infection site and inducing mast cells to produce histamine, with the consequent increase of microvascular permeability, thereby contributing to parasite extravasion into the blood circulation (Stijlemans et al., 2017).

Studies with *T. brucei*-infected mice demonstrated that in the first stage of infection, there are no detectable changes in NK activity, but with disease progression, more precisely after the 9^{th} day, NK activity is severely reduced (Vincendeau and Bouteille, 2006).

1.4.2. Adaptive immune response

Unlike the innate response, the adaptive immune response is antigen specific. This response is carried out by white blood cells that can be thymus-derived lymphocytes (T lymphocytes) and mediate cellular immunity, or bone-marrow-derived lymphocytes (B lymphocytes) that support humoral immunity (Luckheeram et al., 2012, Rock et al., 2016).

T cells are responsible for cytokine production and can be divided into $CD4^+$ T cells, or helper T cells (Th) and $CD8^+$ T cells, also denominated cytotoxic cells (Chaplin, 2010).

Although T cells help in pathogen elimination, they are unable to recognize their surface. To overcome this limitation, antigen presentation pathways have evolved and so T cells have at their surface receptors, known as the T cell receptor (TCR), to recognize antigens, but only in context of class I molecules of major histocompatibility complex (MHC I) or class II molecules of major histocompatibility complex (MHCII). When bound to MHC molecules, antigens can be recognized, and T cells can distinguish which ones are self and non-self (Eckle et al., 2013).

As mentioned before, MΦ and DC are APC and all of the antigens that are internalized into endocytic compartments of these cells are presented to $CD4^+$ T cells in the context of MHCII. On the other hand, antigens in the cytosol are presented to $CD8^+$ T cells in the context of MHCI (Buus et al., 1987, Rock et al., 2016). These molecules expressed in immune cells bound to antigen peptide fragments, so they can be recognized by antigen receptors present in the surface of T cells (Roche and Furuta, 2015, Rock et al., 2016).

$CD4^+$ T cells perform distinct functions in the immune system, including regulation of MΦ function, support antibody (Abs) production by B cells, regulation and control of autoimmunity. Once their functions are lost, immune response becomes impaired and so the individual is more susceptible to infectious disorders, like parasitic diseases (Zhu et al., 2010). Besides Th, $CD4^+$ T cell subpopulation also comprises regulatory T cells (Treg), where $CD25^+$ and forkhead transcription factor box P3 (FoxP3) are recognized as Treg cell markers (Corthay, 2009).

$CD8^+$ T cells recognize the antigen presented through MHCI and release granules that contain perforin and granzymes, which are cytotoxic proteins that contributes to lysis of target cells (Chaplin, 2010). These cells can also release TNF-α and IFN-γ and moreover can induce apoptosis, which means programmed cell death of the target cells (Harty et al., 2000).

B cells constitutes only 15% of the leukocytes and are responsible for production of Abs, also denominated immunoglobulins (Ig) (Chaplin, 2010). There are described five classes of Abs in mammals, IgA, IgD, IgE, IgM, IgG, and each of them presents different biological properties. IgM is the first Abs that is expressed although IgG is the predominant Ig circulating in blood (Schroeder and Cavacini, 2010).

1.4.2.1. Parasite virulent factors

As mentioned before, adaptive immune response comprises both cellular and humoral responses. Since this parasite multiplies extracellularly, it is expected that humoral response plays the main role in infection control (Baral, 2010). Although B-

cell response is strongly protective it is limited by their specificity to VSG that changes in every infection peak (Magez et al., 2008).

Early studies in *T. brucei*-infected mice indicated that T-cell independent anti-VSG IgM response is the first line of humoral immune response against parasites (Magez et al., 2008). Although the role of Abs remains poorly described (Vincendeau and Bouteille, 2006) it is known that VSG-specific IgM levels present a fold increase of 3-4 after infection and are responsible for parasite elimination, contrary to VSG-specific IgG that seems to have no effect in parasite clearance. These findings are supported by the fact that IgM Abs starts to appear after the end of a parasitemia peak, which means, after the variable antigen type (VAT) has been eliminated and another VSG is being expressed. On the other hand, Stijemans et al. (2007) reported that in *T. brucei*-infected mice, IgG Abs were involved in parasitemia reduction, while IgM Abs does not play any role and were dispensable. These findings culminate with the association between trypanotolerance and increased IgG levels.

Taken together, these data show that the relationship between the type of Abs that are produced against the parasite depends of the trypanosome species. It is described that IgM is the main Ig produced during a *T. evansi* infection, while for *T. congolense* and *T. brucei* IgG plays the key role. It has also been reported that clearing capacity of *T. congolense*-infected mice is dependent of MΦ phagocytosis Abs-mediated, including the Kupffer cells, the main phagocytic population resident in liver (Shi et al., 2003).

Experimental evidences shown that African trypanosomes releases *Trypanosome*-derived lymphocyte triggering factor (TLTF). This molecule has the potential to induce secretion of IFN-γ by T-lymphocytes, more specifically by $CD8^+$ T cells (Hamadien et al., 1999). IFN-γ is described as a growth factor for trypanosomes and is also an inductor of MΦ activation **(Fig. 7)**, directing prostaglandins production, and impairing IL-2 production by $CD4^+$ T cells that culminate in T cell unresponsiveness (Lucas et al., 1993). However, the role of IFN-γ in trypanosomiasis is not completely understood. Studies with IFN-γ-deficient mice indicated that this proinflammatory cytokine is required for resistance to *T. brucei* infection (Hertz et al., 1998). On the other hand, in *T. congolense*-infected mice was reported susceptibility

and early mortality. Mice died of a Systemic Inflammatory Response Syndrome (SIRS) that seems to be mediated by IFN-γ (Shi et al., 2003). This seems to be a consequence of MΦ overactivation due to excessive production of IFN-γ combined with absence of IL-10, leading to liver pathology and then to death of the infected mice (Shi et al., 2003, Guilliams et al., 2007).

Despite TLTF there is another molecule released from this African *Trypanosome*, the *T. brucei*-derived Trypanosome Suppression Immunomodulating Factor (TSIF) (Gomez-Rodriguez et al., 2009). It is reported that this molecule is released during the later stage of infection and seems to interfere with IL-10 production and block T-cell proliferation, consequently inhibiting B-cell development and impairing humoral response. Therefore, it seems that parasite use this molecule to guarantee their own survival, once in the absence of this trypanosome derived factor, infected mice died after 2 days (Gomez-Rodriguez et al., 2009, Stijlemans et al., 2016).

With disease progression, a dramatic increase of Ig occurs, however presents specificity to autoantigens. It is reported that components released by trypanosomes triggers B cells to produce autoantibodies. In HAT patients, autoantibodies have been described against red blood cells, liver, components of CNS myelin and against cell structure components, such as intermediate filaments, with consequent tissular lesions (**Fig. 7**) (Reviewed by Vincendeau and Bouteille, 2006).

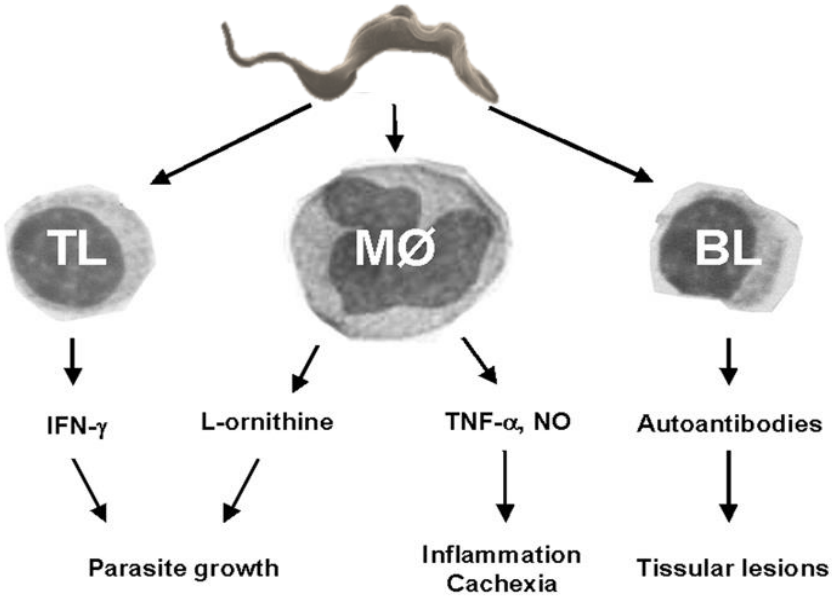

Figure 7 – Interaction of components released from trypanosomes with the activation of immune cells. TL- T lymphocyte, MΦ- macrophages**,** BL- B lymphocyte [Adapted from (Vincendeau and Bouteille, 2006)].

Studies of *T. b. brucei*-infected mice have shown a decrease of B-cell development in bone marrow, as well as the abolishment of splenic B-cell maturation (Bockstal et al., 2011). Moreover, it was recently reported that IFN-γ mediates depletion of follicular B-cells that are responsible for memory cells (Radwanska et al., 2008, Cnops et al., 2015). The fact that this parasite expresses different VAT, process that will be further detailed, also contributes to the failure of B-cells. Once the parasite is always suffering changes in their surface, the Abs that are generated will consequently be different, impairing memory generation. As a result of B lymphocytes dysfunction, the mice become more susceptible to repetitive infections (Radwanska et al., 2008, Bockstal et al., 2011, Lejon et al., 2014).

Treg cells seems to play a significant role in other infectious diseases, however their role in AT remains controversial. Some studies indicate that $CD4^+$ $CD25^+$ $Foxp3^+$ are responsible for the resistance of *T. congolense*-infected mice. It was demonstrated that these cells impair IFN-γ production and hence downregulate MΦ and their production of proinflammatory cytokines (Guilliams et al., 2007). However, there are studies pointing Treg cells as responsible for susceptibility in this disease (Wei and

Tabel, 2008). Another study, also with *T. congolense*, showed that depletion of Treg cell subset enhance infection control in susceptible mice. According to these authors, Treg cell depletion allows parasitaemia control while in the presence of Treg cells there are overproduction of IFN-γ and IL-6, and consequently parasitaemia increase (Okwor et al., 2012).

As a conclusion remark, this disease is characterized by parasitaemia peaks that are associated with a T cell suppression and, at the same time with B cells activation, that although is associated with clearance of the different trypanosome variants, have no memory, and consequently parasitaemia control is impaired and the patient remains in an immunosuppression state (Pays and Vanhollebeke, 2009). Although it is known that $CD4^+$ and $CD8^+$ T cells are the principal producers of IL-10 and IFN-γ, the role of these cells in this disease is not well understood yet (Liu et al., 2015).

1.4.3. Immunosuppression

Suppression of the immune response is a hallmark of this disease, where high susceptibility to opportunistic infections can occur. Although several studies have been done in order to understand immunosuppression, remains the question if it is mediated by MΦ, T cells, or by both cell populations (Baral, 2010).

As mentioned before, these parasites can modulate APC functions, allowing them to escape immune system action and further contribute to immunosuppression (Geiger et al., 2016). Moreover, it is known that in the chronic stage of disease with the continuous T cell activation occurs exhaustion and consequently the immune response becomes impaired, also contributing for host immunosuppression (Wherry, 2011). In AT many parasitemia peaks are generated, hence T cells are constantly being activated, and so their exhaustion can occur, and this may explain the state of immunosuppression of HAT patients.

1.5. Immune evasion strategies of *Trypanosoma brucei*

It is known that *T. brucei* never enter into the host cells and multiply only extracellularly, and so the exposure to the immune system is constant (Namangala, 2011). In order to guarantee their survival and transmission and overcome the latter's clearance, trypanosomes adopted several strategies that allow them to evade or subvert host's immune response (Schwede and Carrington, 2010, Geiger et al., 2016).

1.5.1. Antigenic variation

Upon the bite of the tsetse fly in the mammalian host, their saliva contains some components that induce a local inflammatory immune response. Hence, is triggered the mast cell degranulation, where histamine is released and consequently occurs vasodilatation, that allows the parasites to disseminate and circulate in blood.

Firstly, bloodstream forms of trypanosomes continuously change their major antigen, VSG. In the ascending phase of parasitemia, parasites are denominated homotype, which means they have the same antigenic type. When the immune system recognizes the parasites, specific antibodies are generated, and the majority of parasites is eliminated. At the same time, there are some heterotype parasites that are expressing another VAT and remain untargeted. These new parasites can escape from the immune system, replicate and become the new homotype, generating this way a new wave of parasitemia. Here begins a cycle, new antibodies are generated for this homotype, some can escape and multiply expressing a new VAT, resulting in parasite successive waves and in a long-lasting chronic infection (**Fig. 8**) (Baral, 2010, Geiger et al., 2016).

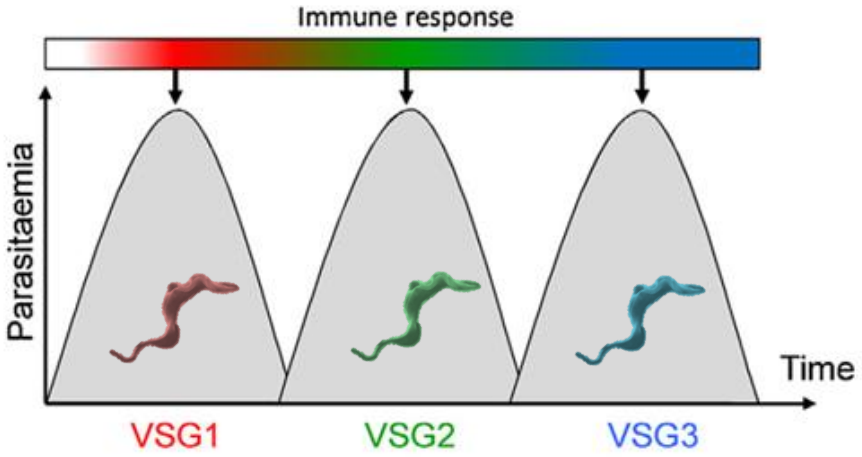

Figure 8 - Switching VSG expression. Parasitemia waves and corresponding variants last approximately 7-10 days. Within a progression of a new wave, trypanosomes oscillate between distinct life stages. Metacyclic forms start to proliferate, become proliferative slender, and the peak of infection is achieved when parasites acquire their non-proliferative stumpy-form (Adapted from Baral, 2010).

1.5.2. Alteration of antigen presenting cell functions

Another well documented evasion mechanism is the induction of alterations in immune system of the host (Namangala, 2011). As mentioned before, this parasite interferes with APC cell functions. Due to the connection of GIP residues with the cells of the immune system, occurs regulation of cytokine profiles and consequently changes in the APC functions.

Although many studies have been done in order to explain how this parasite alters APC functions, this mechanism remains unclear. However, there are cumulative evidences that MHCII antigen presentation is impaired in infected mice. Studies reported by Namangala et al. (2000) showed that MΦ from spleen, lymph nodes and peritoneal cavity reduced MHC molecules. These findings suggest that this can be due to the release of biological active factors by living trypanosomes that damage vesicular traffic within MΦ. Moreover, these parasites release degradable components, like phospholipids, that may affect the connection between MHCII and the antigens that are processed, and consequently the function of these molecules is reduced (Namangala et al., 2000).

1.5.3. Trypanolitic factor of human blood serum

Normal human serum (NHS) is composed by trypanolitic factors (TLF1 and TLF2) that are associated with high-density lipoprotein (HDL) and complexed with apolipoprotein L-I (APOL1) (Namangala, 2011). *T. b. gambiense* and *T. b. rhodesiense* developed mechanisms to overcome TLF functions and became resistant, and this is the main reason why they are infective to human beings (Baral, 2010, Namangala, 2011). These human infective strains developed different mechanisms to avoid TLF action. While first express *T. gambiense*-specific glycoprotein (TgsGP) that downregulate APOL1 and consequently prevents parasite lysis, *T. b. rhodesiense* expresses a serum resistance associated (SRA) gene, that also interacts with APOL1, preventing parasite death (Lecordier et al., 2014).

1.5.4. Macromolecular trafficking mechanism

As mentioned before, trypanosomes need to acquire nutrients from their host, and so they are known to exhibit a high endocytosis rate. Engstler et al., (2007) described a phenomenon on the surface of the parasite that is used as a strategy for evading the mammalian humoral immune system. Their experiments found out a macromolecular trafficking mechanism, where the antibodies produced against VSG, that are disposed on the entire parasite cell surface, are endocytosed in the flagellar pocket. These results show that parasite also uses their endocytosis rate to escape the complement-mediated killing (Engstler et al., 2007, Baral, 2010).

1.5.5. Secretion of aromatic ketoacids

Experimental evidences indicate that at high parasitemia occurs amino acid depletion of serum, especially tryptophan. This depletion is accompanied by excretion of the correspondent aromatic α-ketoacid (Newport et al., 1977).

Most recently, McGettrick et al., (2016) reported that bloodstream forms of *T. b. brucei* excretes some of this aromatic ketoacids, including indolepyruvate that is a transamination product of tryptophan. When innate immunity is activated, hypoxia-

inducible factor-1α (HIF-1α) is responsible for the induction of MΦ genes encoding interleukin-1β (IL-1β), a proinflammatory cytokine. Results obtained by McGettrick et al., (2016) indicate that indolepyruvate reduces HIF-1α protein levels, leading to an IL-1β reduction, although its exact role is not completely understood in *T. brucei* infection. These data confirm the evidence of indolepyruvate as a modulator in a mechanism of innate immune evasion.

1.6. Objectives

The main goal of the current study is to characterize leukocyte activation when exposed to *T. b. brucei* bloodstream forms, to the respective extract and to parasite exosomes.

The specific aims are:

- **Analyze activation of cell line MΦ P388D1 when exposed to *T. brucei* and stimulated by parasite extract and parasite exosomes**

  The study of MΦ activation was evaluated by measuring urea and NO levels after exposition to *T. brucei*. Moreover, membranar expression of MHC molecules (MHCI and MHCII) after contact with parasite was assessed by flow cytometry. To visualize the interaction of parasite with cell, scanning electron microscopy (ScEM) was performed.

- **Investigate differentiation of the lymphocyte subpopulations Th ($CD4^+$), T cytotoxic ($CD8^+$) and Treg ($CD25^+$) after exposition to *T. brucei* and stimulation by parasite extract and parasite exosomes**

  Immunophenotyping of lymphocyte subsets were performed in two steps: first lymphocytes were magnetically separated in $CD8^-$ and $CD8^+$ cell fraction and then cells were marked with CD3, CD25 and FoxP3 monoclonal antibodies linked to a fluorescent molecule and evaluated by flow cytometry.

2. MATERIALS AND METHODS

2.1. Experimental design

The current study aims to characterize leukocyte response generated by *T. brucei* viable trypomastigotes.

To obtain trypomastigotes, CD1 mice were infected with a crioconserved strain of *Trypanosoma brucei brucei.* To evaluate the parasite effect on mouse leukocytes, MΦ and lymphocytes were *in vitro* exposed to trypomastigotes, mimicking the natural infection. In parallel, trypomastigote antigenic extract was performed and exosomes[1] previously isolated from cultured trypomastigotes were also added to cells.

Macrophage activity was assessed at several time points through urea and NO production. Moreover, antigenic presentation was indirectly investigated by the expression of membranar MHC molecules (MHCI and MHCII). Differentiation of T cell subpopulations, including $CD3^+CD8^-$ Th cells, $CD3^+CD8^+$ T cytotoxic cells (Tc), regulatory $CD3^+CD8^+CD25^+$ and $CD3^+CD8^-CD25^+$ T cell subsets, and effector $CD3^+CD8^+CD25^-$ and $CD3^+CD8^-CD25^-$ T cells were also evaluated (**Fig. 9**).

[1] Exosomes were isolated by Joana Marques during her MSc thesis

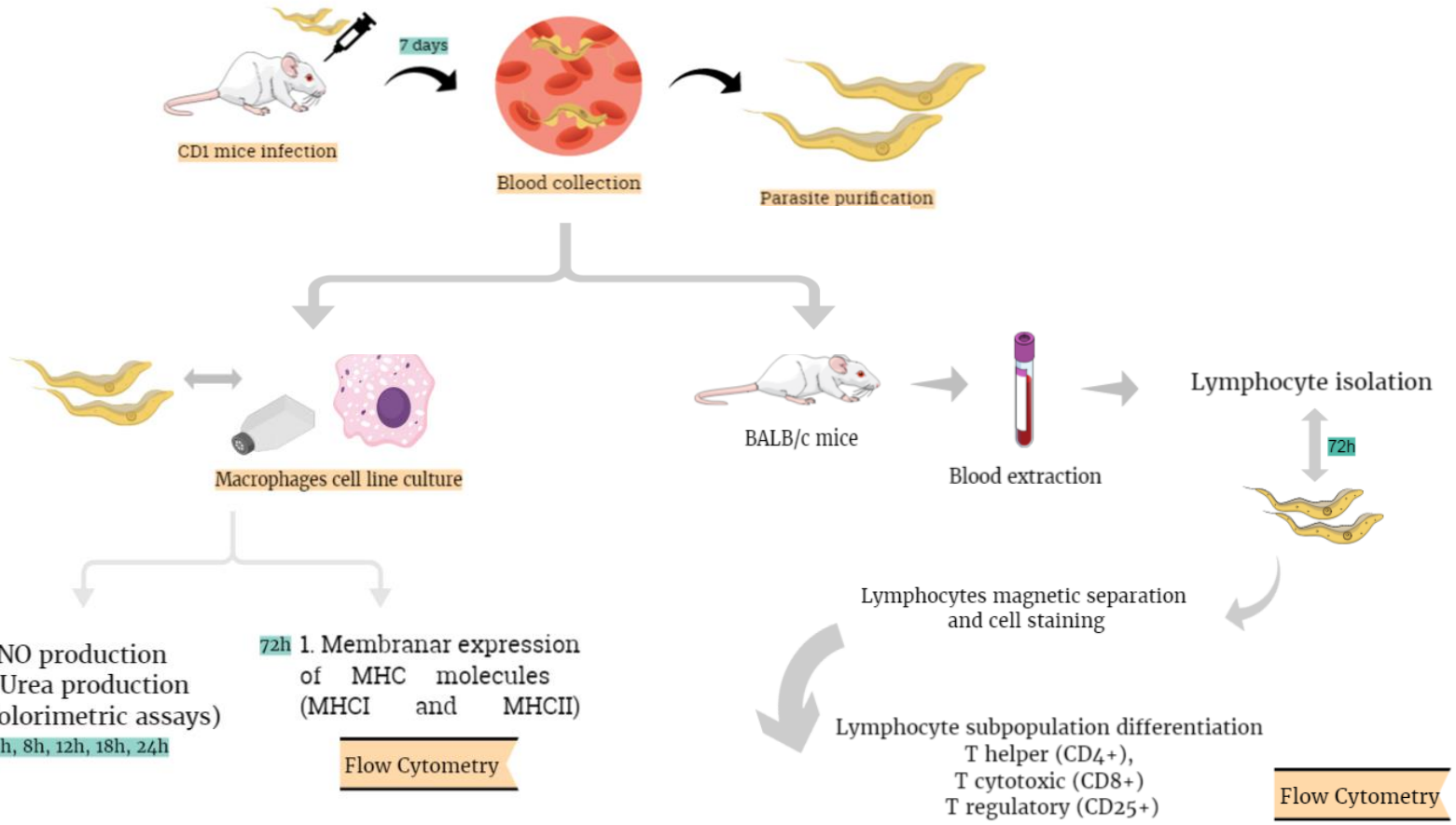

Figure 9 – Schematic representation of experimental design. CD1 mice were infected with *T. brucei brucei* trypomastigotes by intraperitoneal injection. After one week, total blood was collected and parasites were purified and maintained in culture. Parasites were used for antigenic extract preparation. Lymphocytes and MΦ were exposed to trypomastigotes. NO and urea released by MΦ were measured at different time points and the expression of MHC molecules (MHCI and MHCII) characterized. Differentiation of Th ($CD3^+CD8^-$), Tc ($CD3^+CD8^+$) and Treg ($CD3^+CD25^+$) cell subsets were also evaluated.

2.2. Parasite isolation and purification

Six- to eight-week-old male and female *Mus musculus* mice, CD-1 strain were infected with *Trypanosoma brucei brucei* G.V.R. 35 strain.

Parasites stored at -80ºC were used for mouse infection by an intraperitoneal injection of 500 µl of parasites diluted in phosphate-buffered saline (PBS) 20 mM glucose (PBSG). All animals were maintained in IMHT's animal house and handled according to institutional guidelines and the experiments were performed in compliance with EU requirements (2010/63/EU). Manipulation of parasites was done in containment level 2, ensuring biosafety and biosecurity in compliance with Portuguese law (Portaria n.o 405/98 and EU directive 2000/54/EC).

Infection was periodically monitored by tail-blood and controlled by morphological visualization of blood samples under an optical microscope (Motic®). Positive blood samples were fixed with methanol (VWR, USA) for 5 min at RT and stained with Giemsa solution (1:10) (VWR) for 10 min. Then, the dye was removed and slides were dry. Samples were observed by optical microscopy and digital images were acquired. Giemsa solution that is widely used for parasite coloration stains the DNA phosphate groups, allowing the visualization of endocytic compartments rich in DNA, such as the kinetoplast and the nucleus.

At parasitemia peak, cardiac blood was collected with the anticoagulant citrate-phosphate-dextrose solution with adenine (CPDA) (Sigma-Aldrich, USA). Blood was inoculated in Schneider's Drosophila medium (Lonza, USA) and incubated at 24 ºC for 24 h. Then, to promote erythrocytes lysis ammonium-chloride-potassium lysis buffer (ACK lysis buffer) was carefully added to blood suspension (1:5) and incubated for 5 min at room temperature (RT). The suspension was centrifuged at 300 ×g for 5 min at RT. Supernatant was discarded, pellet resuspended in 5 mL of PBS and centrifuged at 300 ×g for 5 min at 4ºC. The pellet was washed with PBS one more time and then resuspended in culture medium.

To obtain a purified parasite suspension, a diethylaminoethyl (DEAE)-cellulose column (Sigma-Aldrich) equilibrated with PBSG was used according to (Lanham and Godfrey, 1970). Blood was diluted in PBSG (1:2) and passed over the column. Under

these conditions, blood components adhere to the column matrix while parasites are eluted. Once purified, parasites were transferred to Schneider medium supplemented with 20% of heat-inactivated fetal bovine serum (FBS) (Sigma-Aldrich) and incubated at 24 ºC.

2.3. Parasite crude antigen (extract)

To obtain a parasite lysate, trypomastigotes were harvested from cultures by centrifugation at 2000 ×g for 10 min at 4ºC. The supernatant was discarded, and the pellet washed twice with PBS 2 mM EDTA. A new centrifugation (2000 ×g for 10 min at 4 ºC) was performed and the obtained pellet was resuspended in PBS. Parasites were then disrupted by eight freeze thawing cycles of -20 ºC at RT. Protein content ($mg.mL^{1}$) was quantified in a Nanodrop 1000 Spectrophotometer (Thermo Scientific, EUA) and the obtained lysate stored at -20 ºC until further use.

2.4. Macrophages

Macrophage (MΦ)-like P388D1 cell line (ATCC, EUA) was used in the present study. This cell line was isolated from a mouse lymphoma and was cryopreserved at -180 ºC until use. It is constituted by cells with MΦ characteristics that when in culture remain in suspension.

Cells (8.9×10^{6} cell/well) were cultured in Roswell Park Memorial Institute medium (RPMI) 1640 (Lonza, Switzerland) supplemented with 10% (v/v) of heat-inactivated FBS, 2mM L-glutamine (MERCK, Germany) and penicillin-streptomycin (Sigma-Aldrich) at 100 U/mL and 100 $\mu g.mL^{-1}$, respectively and adjusted to pH 7.2 (complete RPMI medium). Cells were grown at 37 ºC in a humidified atmosphere with 5% CO_2. Every 2-3 days, medium was removed from cell cultures and replaced with fresh medium, and cell viability was ascertained by the trypan blue exclusion method. Alive cells with intact cell membranes can exclude different compounds, including dyes like trypan blue (vital dye). Therefore, in a cell suspension the viable cells remain clear while nonviable cells become stained, presenting a blue coloration of cytoplasm. After ascertaining viability, the cell concentration was estimated in a Neubauer-counting chamber, under an optical microscope.

Cultured MΦ were incubated for 6 h with trypomastigotes at a rate of three parasites per cell. In parallel, cells were also incubated with antigenic extract and parasite exosomes (10 $\mu g.mL^{-1}$). Cultures were washed with PBS by centrifugation at 1800 ×g for 10 min at RT. After cytocentrifugation at 1600 ×g for 10 min (StatSpin® Cytofuge, USA) followed by coverslip fixation and Giemsa staining (VWR, EUA), slides were observed by optical microscopy and images were acquired.

In order to characterize the effect of parasite exposure in MΦ microbicid metabolism, production of urea and NO were evaluated. Parasites were incubated with MΦ (1:3) for 6 h, 8 h, 12 h, 18 h and 24 h at 37ºC in a humidified atmosphere with 5% CO_2. In parallel, non-stimulated MΦ and phormol myristate acetate (PMA)-stimulated MΦ were used as negative and positive control, respectively. PMA has been described as an activator of protein kinase C, a protein responsible for trigger ROS production.

At each time point, cell suspensions were centrifuged at 500 ×g for 10 min at 4ºC and supernatants were collected and stored at -20 ºC until further analysis. To indirectly evaluate the role of MΦ in driving acquired immune response, cells were also used to evaluate the expression of membranar MHCI and MHCII.

2.4.1. Urea production

In the presence of pathogens, MΦ can metabolize arginine, an essential amino acid, driving the production of ornithine and urea (Mills, 2001) (**Fig. 10**).

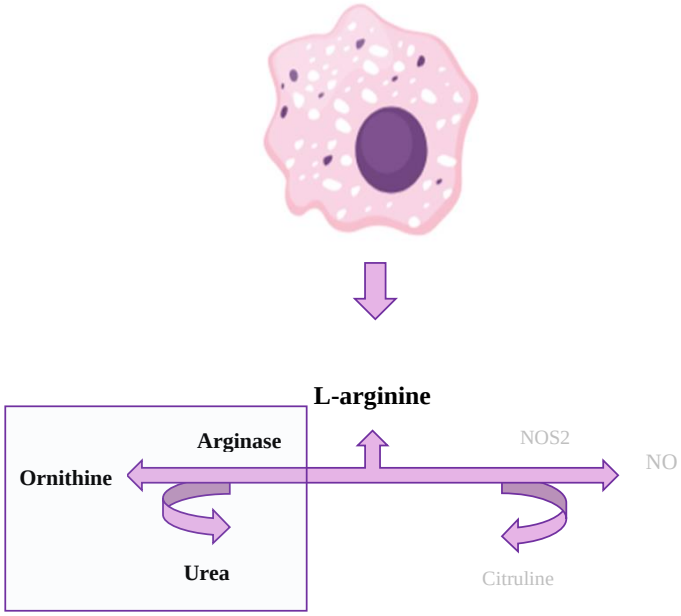

Figure 10 – Arginine metabolism in M2-MΦ. MΦ differently express nitric oxide synthase 2 (NOS2) and arginase, thereby inducing different immune functions. In the presence of anti-inflammatory signals, arginase is activated, and L-arginine is metabolized in ornithine with consequent release of urea.

In the present study, urea levels were measured using the commercial kit QuantiChrom™ Urea Assay Kit-DIUR-100 (BioAssay System). This kit allows the measurement of urea directly in biological samples without requiring any pre-treatment. A chromogenic reagent that forms a colored complex with urea was used and it was assumed that color intensity is directly proportional to the urea concentration present in the sample.

Crioconserved MΦ supernatants were thawed and resuspended, and 50 µl of each sample were plated in triplicate in a sterile 96-well plate. Standard urea concentration (50 $mg.dL^{-1}$) diluted in RPMI medium (1:10) and the blank (water) were also plated according with manufacturer's instructions. The intensity of color was measured at 430 nm in a microplate reader (BioRad-680, BioRad, USA) and urea concentration was determined according to **equation 1**.

Equation 1:

$$[Urea](mg.dL^{-1}) = \frac{OD_{sample} - OD_{blank}}{OD_{standard} - OD_{blank}} \; x \; n \; x \; 5$$

Where *OD* indicates optical density, *n* is the dilution factor (*n*=1) and 5 corresponds to standard urea concentration (1 mg.dL^{-1} of standard urea corresponds to 167 µM of urea).

2.4.2. Nitric oxide production

Instead metabolize arginine, MΦ can activate a different pathway producing citrulline and nitric oxide (NO) (Mills, 2001) (**Fig. 11**).

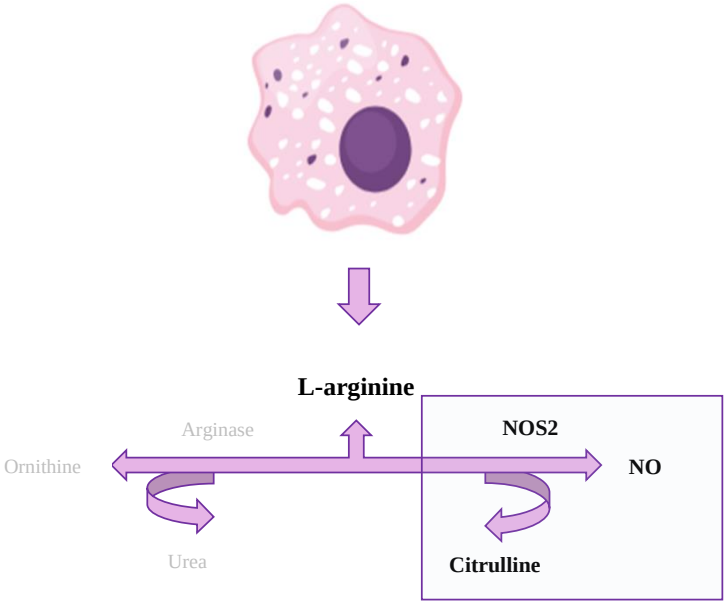

Figure 11 - Arginine metabolism in M1-MΦ. MΦ differently express nitric oxide synthase 2 (NOS2) and arginase, thereby inducing different immune functions. In the presence of pro-inflammatory signals, NOS is activated, leading to NO synthesis and citrulline release.

To measure NO, it was used a commercial kit Nitrate/Nitrite Colorimetric Assay kit (Abnova). This kit allows the measurement of total nitrate/nitrite present in samples in just two steps. First, is added nitrate reductase, an enzyme that converts nitrate to

nitrite, and then the Griess Reagent that converts nitrite into a deep purple azo compound. This compound exhibits a maximum absorbance at 540-550 nm.

Stored supernatants were thawed and resuspended, and 80 µl of each sample were plated in triplicate in a sterile 96 well plate. Serial dilutions of a nitrate standard solution (200 µM), ranging from 0 µM to 35 µM were used to raise a standard curve, and the blank was constituted by the assay buffer. The reaction was performed according to manufacturer's instructions. Color intensity was measured at 570 nm in a microplate reader and NO concentration was determined according to **equation 2**.

Equation 2:

$$[Nitrate + Nitrite]\ (\mu M) = (OD_{570nm} - slope\ standard\ cuve)\ x\ VS\ x\ DF$$

Where *OD* is the optical density, *VS* is the volume of sample and *DF* the dilution factor (DF=1).

2.4.3. Scanning Electron Microscopy of macrophages and trypomastigotes

Cultured-MΦ exposed to trypomastigotes for 6 h at a rate of three parasites per cell were used to perform Scanning Electron Microscopy (ScEM). ScEM uses high-energy electrons that after contact with the surface of a solid sample, can provide information about sample surface dimensional topography, through high-resolution images (Cochrane, 1996).

Coverslips were emerged with poly-D-Lysine overnight to increase sample adherence. MΦ exposed to parasite adhered to coverslips were fixed with PBS 4% paraformaldehyde (VWR, International), overnight at 4ºC. Coverslips were post-fixed with PBS 2.5% glutaraldehyde (Merck, Germany), for 30 min at 4ºC. Then, coverslips were rinsed three times with distillate water and treated with 0.5% osmium tetroxide (Sigma-Aldrich), for 30 min. The washing process was repeated, and the coverslips were incubated with a fixative solution of 1% tannic acid (Sigma-Aldrich), during 30 min, creating conditions that enhance electron density. Afterwards coverslips were washed, and the process of dehydration was initiated by the sequential addition of 30%,

50%, 70%, 80% and 90% ethanol for 5 min each. Once this process finished, the coverslips were stored immersed in 100% ethanol, at 4ºC until further use. At the Unidade de Microscopia, FCULisboa (Lisbon, Portugal), the samples were dried using the critical point drying method, coated with gold palladium and mounted on stubs. Cells were then observed under a scanning electronic microscope (Hitachi SU8010) and images were acquired with the generous collaboration of Professor Graça Alexandre-Pires (FMVULisboa, Lisbon, Portugal).

2.4.4. Macrophage expression of MHCI and MHCII

In order to better understand the effect of parasite in the membranar expression of MHC molecules (MHCI and MHCII) in MΦ, flow cytometry was applied.

MΦ exposed to viable parasites, extract and exosomes stimulated MΦ and, non-stimulated MΦ (**Table 2**) were centrifuged at 370 ×g for 10 min, at 4ºC and then resuspended in PBS 2% FBS 0.01% sodium azide to prevent antibodies (Abs) capping, avoiding the aggregation of fluorescently tagged Abs. FITC-conjugated anti-MHCI and PE-conjugated anti MHCII (BioLegend, USA) monoclonal antibodies were added to cell samples according to **Table 3**.

Table 2 – List of different stimuli used in cultured MΦ.

Stimulus	*T. brucei*			PMA (Positive control)
	Viable trypomastigotes	Extract	Exosomes	
Rate (Parasite:Cells)	1:3			
Final concentration			10 µg.mL^{-1}	

Table 3 – Mouse monoclonal antibodies, fluorochromes, concentrations and volumes used in cultured MΦ.

Monoclonal antibody	**Fluorochrome**	**Concentration**	**Volume added (µL)**
anti-MHCI (H-2Kb)	FITC	0.5 mg.mL^{-1}	1.64
anti-MHCII (I-A/I-E)	PE	0.2 mg.mL^{-1}	4.5

Cells were incubated in the dark for 1 h at 4 ºC. Then, 200 µL of PBS were added and cells were centrifuged at 600 ×g for 5 min at RT. Resuspended cells were fixed in PBS 0.2% formaldehyde and incubated for 20 min in the dark at RT. Afterwards, PBS was added and cells were centrifuged twice at 400 ×g for 5 min at 4 ºC. Cells were washed, fixed and resuspended in PBS 2% FBS 0.01% sodium azide (like described above) and stored at 4 ºC in the dark until further flow cytometry analysis.

2.5. Differentiation of lymphocyte subsets after exposure to *T. brucei* trypomastigotes

2.5.1. Lymphocytes isolation

Six- to eight-week-old male BALB/c mice (*Mus musculus*) were purchased from the Instituto Gulbenkian de Ciência and maintained in IHMT's animal house.

Cardiac blood obtained from the mouse was carefully laid on top of the cell separation solution (Biocoll, VWR) (1:2). Tubes were centrifuged at 925 ×g during 20 min at RT. Biocoll is a lymphocyte separation medium and its density [1.077 $g.mL^{-1}$] is lower than erythrocytes and granulocytes and higher than mononuclear cell. This way, after centrifugation erythrocytes and polymorphonuclear cells remains in the bottom of the tube, while in the interface between plasma and Biocoll, is visible a cellular ring enriched in lymphocytes (**Fig. 12**).

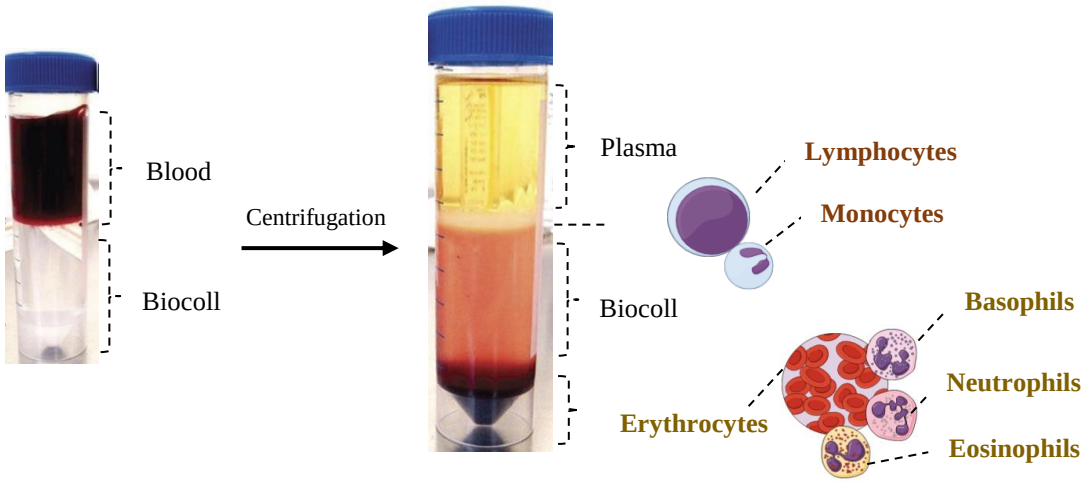

Figure 12 - Representative scheme of the underlaying principle of blood peripheral mononuclear cells isolation by density gradient. After centrifugation, erythrocytes and granulocytes (basophil, neutrophil and eosinophil) remains in the sediment. Above the Biocoll there is visible a ring enriched in peripheral mononuclear blood cells (PMBC), composed by lymphocytes and monocytes.

Mononuclear cells were carefully removed and washed 3× with PBS by centrifugation at 370 ×g for 10 min at 4 ºC. Supernatant was discarded, and the pellet resuspended in PBS. Cell viability was determined by trypan blue (as above described). After ascertaining viability, the cell concentration was estimated in a Neubauer-counting chamber, under an optical microscope.

2.5.2. Cell stimulation

Blood mononuclear cell suspension, which include mainly lymphocytes and also some monocyte/MΦ was plated in a sterile 96-well plate (7.6×10^7 cells/well). Viable parasites (1:3), parasite extract and parasite exosomes (10 µg.mL^{-1}) were added to cells (**Table 4**). Plates were then incubated for 72 h at 37 ºC in a humidified atmosphere with 5% CO_2. In parallel, resting/non-stimulated cells (negative control) and Concanavalin A (Con A) stimulated cells (positive control) were also incubated. Con A is a lectin, which means, a carbohydrate-binding protein that has the ability to bind to T cell receptors, stimulating these cells to proliferate.

Table 4 - Stimuli used to activate lymphocytes.

Stimulus	*T. brucei*			Concanavalin A (Positive control)
	Viable trypomastigotes	Extract	Exosomes	
Rate (Parasite:Cells)	1:3			
Final concentration				10 μg.mL^{-1}

2.5.3. Magnetic separation of cells

The principle of MACS® separation relies on the use of antibody-coated magnetic MicroBeads that can label the cells. These microbead-cell complexes can be separated from other non-labelled cells in a magnetic field.

The cell suspension was centrifuged at 300 ×g for 10 min at 4 ºC and the supernatant was discarded. The obtained pellet was resuspended in cold PBS (pH 7.2) 0.5% bovine serum albumin (BSA) 2 mM EDTA (90 μL of buffer per 1×10^7 total cells). CD8a (Ly-2) microbeads (MACS®, Miltenyi Biotec, Germany) were added to the cell suspension according to a standard protocol provided by the manufacturer (10 μL per 1×10^7 cells) and incubated in the dark for 15 min at 4 ºC. Cells were then washed with PBS by centrifugation at 300 ×g for 10 min and resuspended again in PBS.

Then, the cell suspension that included microbeads bound to CD8a molecules present at the cell surface was loaded into a column that was placed in the magnetic field of a MACS® Separator. The magnetically labeled CD8a$^+$ cells stay retained in the magnetic column (positive selection), while the unlabeled cells CD8a$^-$ run out freely. Once the column was removed from the magnetic field, the retained CD8a$^+$ cells were eluted. At the end of magnetic separation, two cell fractions were obtained, CD8$^+$ cells and CD8$^-$ cells. The CD8$^-$ cell fraction included cells with CD4$^+$ phenotype.

2.5.3.1. Magnetic separation control

After cell magnetic separation, a control was included with unstimulated cells. Thus, CD8$^-$ cell fraction was stained with anti-CD3 FITC and anti-CD4 PerCP, and

$CD8^+$ cell fraction with anti-CD3 FITC and anti-CD8 PerCP. This control was performed in duplicate for each sample and was used to confirm the success of magnetic separation.

2.5.4. Cell labelling

Cell fractions were centrifuged at 370 ×g for 10 min at 4 ºC and then resuspended in PBS 2% FBS 0.01% sodium azide. FITC-conjugated anti-CD3 and PerCP/cy-5.5-conjugated anti-CD25 (BioLegend, San Diego, California, EUA) were added to the samples according to **Table 5**.

Table 5 – Mouse monoclonal antibodies, fluorochromes, concentrations and volumes used in lymphocyte subset characterization.

Monoclonal antibody	Fluorochrome	Concentration	Volume added (µL)
anti-CD3	FITC	0.5 $mg.mL^{-1}$	2
anti-CD25	PerCP/cy-5.5	0.2 $mg.mL^{-1}$	2.6
anti-FoxP3	PE	0.2 $mg.mL^{-1}$	2.6

Cells were incubated in the dark for 1 h at 4 ºC and then washed twice with 200 µL of PBS at 600 ×g for 5 min at RT. Cells were fixed in PBS 0.2% formaldehyde and incubated for 20 min in the dark at RT. Afterwards, cells were washed twice with PBS at 400 ×g for 5 min at 4 ºC.

Since FoxP3 is a nuclear factor, to mark this factor cell permeabilization is required. After cell fixation and wash, cells were resuspended in permeabilization buffer, containing PBS 1% FBS 0.1% sodium azide 0.5% Triton, and incubated for 20 min at RT. Cells were then washed twice with permeabilization buffer by centrifugation at 400 ×g for 5 min at 4 ºC. The pellet was resuspended in the residual volume and cells were incubated with the monoclonal antibody in the dark (**Table 5)** for 1 h at RT and then cells were washed.

For further subset gatting, also a fluorochrome minus one (FMO) control was included. This control contains all the fluorochromes except the one that is being

analyzed to identify and gate cells. Then, the point where it is observed absence of fluorescence, corresponds to the beginning of gate that will include the respective subset marked with the fluorochrome that was not included in the FMO.

Cells and controls were resuspended in 200 µL of PBS 2% FBS, 0.01% sodium azide and stored at 4ºC in the dark until further analysis by flow cytometry.

2.6. Flow cytometry

Flow cytometry was used to evaluate the expression of membranar MHCI and MHC II molecules of MΦ, and also to assess lymphocyte subsets after being *in vitro* exposed to *T. brucei* trypomastigotes and stimulated by parasite extract and parasite exosomes,

The flow cytometry acquisition was performed in a 4-color flow cytometer (BD FACSCalibur, BD Biosciences, USA) at Chronic Diseases Research Center (CEDOC), NOVA Medical School, UNL (Lisbon, Portugal) with the generous collaboration of Professor Graça Alexandre-Pires. Forward scatter-height (FSC-H) *vs*. side scatter-height (SSC-H) gate was used to remove cell debris. Data was analyzed using Flowjo V10 (Tree Star Inc., USA).

2.6.1. Flow Cytometry Basic concepts

Flow cytometry is a widely used laser-based technique able to analyze properties of cells and particles. By using specific Abs against surface cell markers, such as antibodies against a specific Cluster of Differentiation (CD), conjugated with fluorescent molecules (fluorochromes), cell subsets can be identified (Schlossman, 1984).

The cytometer has detectors that receive the fluorescence emitted from stained cells after being excited by appropriated lasers. Furthermore, when the laser reaches each cell of a heterogenous cell population the detectors also get the diffracted light (or the slight amount of light that passes around each cell), determining the size (forward scatter light) and complexity (volume and granulosity - side scatter light) of each cell.

Taken together, fluorescence levels, cell size and cell complexity allow the characterization of cell populations (**Fig. 13**).

SAMPLE – To perform flow cytometry procedure, particles or cells can be used. With this technique, multiple physical and chemical characteristics can be assessed. The sample used in flow cytometry need to be suspended in buffer, so each cell can individual flow through laser light.

LABELLING – Cells can be stained with fluorescent dyes. Fluorescent dyes are conjugated with antibodies that will recognize cell antigens. Fluorescent emission of each cell can be detected by flow cytometer sensors and analyzed, being determined the fluorescent intensity of each cell and the frequency of fluorescent cells in a given cell population.

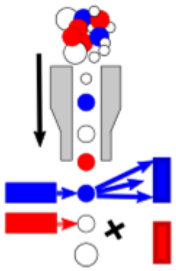

FLOW – Once in the cytometer, light scattering and fluorescence are the cell properties studied. Forward scatter (FSC), also known as low-angle light scatter, corresponds to the amount of light that is refracted in the forward direction. Side-scattered light (SSC) is measured by a located 90º from the laser path detector. The light intensity is converted into voltage, which magnitude is proportional to the cell size, in the case of FSC, and proportional to cell granularity, in SSC. A fluorescent signal is emitted, when the laser light strikes the fluorochrome-conjugated antibodies. Taken together, the data of fluorescence and of FSC/SSC allow to perform a multiparametric analysis of particle/cells of interest.

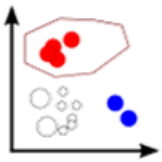

ANALYSIS – Once obtained, data can be analyzed according to a single parameter, represented in histogram, or according two parameters, represent by a FSC-H vs. SSC-H dot plot. The latter is commonly used for "gatting", which means delineate one or more regions of interest, according to cell properties.

Figure 13 – Representative scheme of the underlaying working principle of flow cytometry.

In the case of blood samples, is possible to distinguish (i) granulocytes, since they are larger and granular; (ii) monocytes, that although large cells, do not present granularity; and (iii) lymphocytes, since they are agranular small cells (**Fig. 14**).

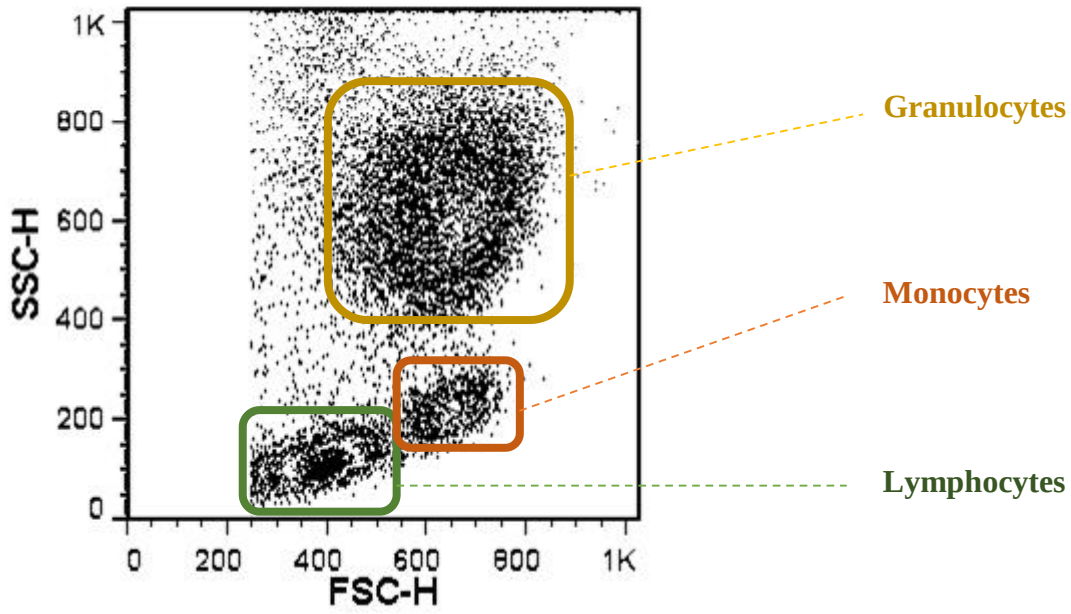

Figure 14 – Representative dot-plot of forward and side scatter. FSC-H *vs*. SSC-H allows to distinguish different subsets of a cell population, since they are proportional to size and cell complexity, respectively. For example, in a mixed population of white blood cells is possible to distinguish lymphocytes, monocytes and granulocytes, due their different complexity and size.

2.7. Data analysis

The obtained values of urea and NO were divided by the value of resting-MΦ at different times, in order to determinate *de novo* production. In turn, the sum of the *de novo* urea levels and *de novo* NO levels, were used to determine accumulation rates, at different incubation times.

Data of both *de novo* urea and *de novo* NO production obtained at different times of exposure and stimulation was used to generate a linear regression between these two-independent data.

A ratio between MHCI and MHCII expression was calculated according to **equation 3**, using the results of both fluorescence intensity (FI) and cell percentage (CP). This ratio allowed to correlate these two-independent parameters, in a way to express an indirect indication of the predominance of antigen presentation to $CD8^+$ T cells or to $CD4^+$ T cells.

Equation 3:

$$FI.CP = \frac{FI_{MHC\ I}}{FI_{MHC\ II}} . \frac{CP_{MHC\ I}}{CP_{MHC\ II}}$$

Where, *FI* represents the median of fluorescence intensity and *CP* corresponds to cell percentage that expressed MHC cell markers ($MHC^+M\Phi$).

Despite CP, also FI was assessed in lymphocytes subset characterization, in a gate performed in CD3.

In order to define a correlation between T cell subset frequencies and FI, regression lines were generated. In the case of CD25, CP was assessed by the sum of respective positive quadrants, Q2 and Q3, and in the case of FoxP3 by the sum of Q1 and Q2. For each regression line, were included data of negative control (NC) and different stimuli used, to establish a variation between non-stimulated lymphocytes and lymphocytes after 72 h of exposure, respectively. Thus, the slope of the linear regression allows to define a positive or negative correlation, and consequently allow the better comprehension of parasite effect in modulation of the studied cell subsets.

2.8. Statistical analysis

Data analysis was performed using GraphPad Prism version 6.01 (GraphPad Software, San Diego, CA). Significant differences between groups were determined using the non-parametric Wilcoxon test. A significance level of 5% ($p < 0.05$) was used to evaluate statistical significance. Results from three independent experiments evaluated in triplicate are represented by box-plots (with median, maximum and

minimum) or by graph bars (as mean and standard error). Tables were also used to describe obtained data by mean plus standard error of the mean (SEM). Spearman correlation (ρ) that ranges between -1 and +1, thus indicating a positive or inverse correlation, was also used to analyze data relation.

3. RESULTS

3.1. Detection of *T. b. brucei*-bloodstream form

Mice blood samples stained with Giemsa solution were used for morphological observation, confirming the presence of parasite bloodstream form. Parasite identity was confirmed, since it was found free in bloodstream as expected, and evidenced its unique characteristic, an undulating membrane (**Fig. 15A**).

Microscopic observation of cultured-MΦ exposed to trypanosomes showed that although parasites remain extracellular, seem to evidence a tropism for these cells, due the proximity verified (**Fig. 15B, C and D**).

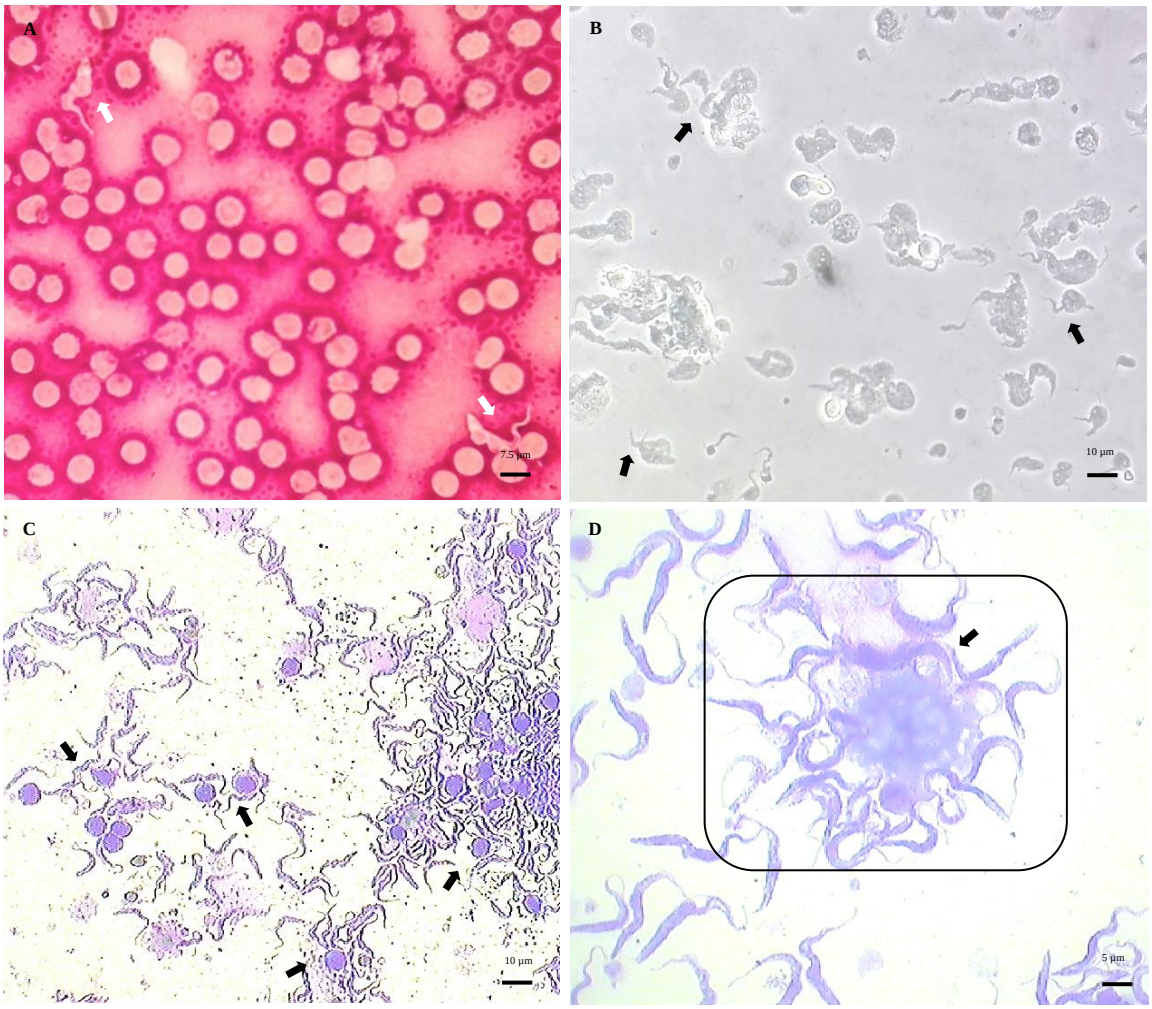

Figure 15 – *T. b. brucei* trypomastigotes in mouse blood and in contact with macrophages. Infected blood (A) and MΦ exposed to parasite for 6 h were observed by optical microscopy and images were acquired. B – fresh preparation of MΦ exposed to trypomastigotes (size bar: 10 µm, 1000× magnification), C and D – MΦ exposed to trypomastigotes Giemsa stained- A: size bar: 7.5 µm, 400× magnification; C: size bar: 10 µm, 400× magnification; D: size bar: 5 µm, 1000× magnification. White arrows – *T. b. brucei* trypomastigotes; Black arrows – apparent parasite tropism to MΦ.

Scanning electron microscopy (ScEM) allowed to observe the cultured-MΦ morphology. The cells exhibited their typical spherical shape, with prominent surface and expected size (10-14 µm). Moreover, as observed in optical microscopy, also ScEM images allowed to evidence a tropism of parasite for cultured-MΦ (**Fig. 16A**). The unique morphology of trypomastigote form with an undulant membrane confirms parasite identity. Although the size of parasite varies according with the environment, ranging between 16-42 µm, the observed trypomastigote form presents an expected size **(Fig. 16B)**. However, it was observed an unexpected parasite fragility, since flagellum was the only structure that maintained total integrity (**Fig. 16A, B, C**). It was also possible to observe some prominent structures on the parasite surface with size ranging about 100 nm, thus suggesting the possibility of extracellular vesicle secretion (**Fig. 16D**).

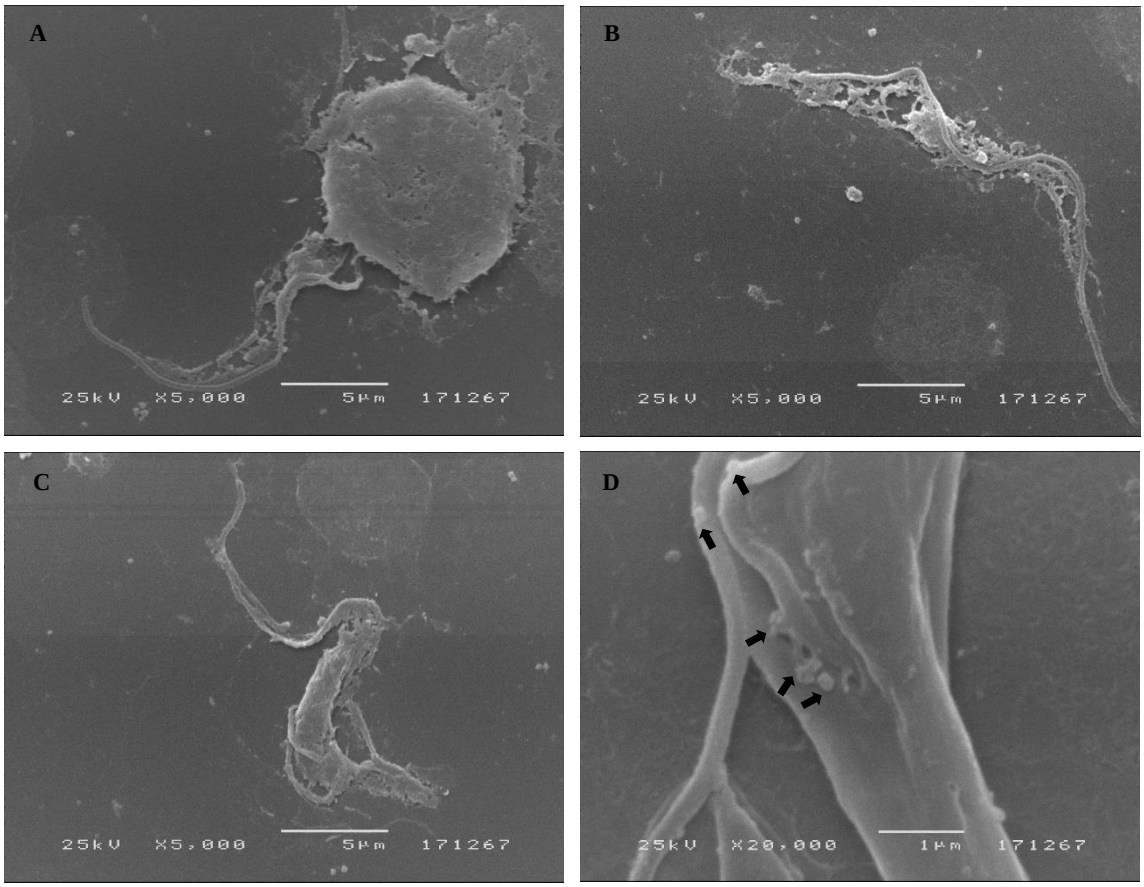

Figure 16 – Cultured MΦ exposed to *T. b brucei*. MΦ were incubated with *T. b. brucei* trypomastigotes for 6 h and were observed by ScEM. A - *T. b. brucei*-exposed MΦ; B, C – *T. b. brucei*-bloodstream form; D – Apparent vesicle secretion by *T. b. brucei* trypomastigote (black arrows).

3.2.*T. b. brucei* induces the differentiation of M1- and M2-MΦ

In order to investigate how MΦ react to *T. brucei* parasites, urea production and NO were evaluated at different time points.

As expected, resting-MΦ presented residual levels of urea production. However, when stimulated with PMA these cells produced high levels of urea, that were significantly different from resting-MΦ (**Fig. 17**) at all time points evaluated ($p = 0.0313$), indicating that cells were viable and functional.

When exposed to parasites, MΦ produce high levels of urea ($p_{6h} = 0.0313$) that peaked after 8 h of exposure ($p = 0.0078$). This peak was followed by successive decreases, reaching a minimum of urea after 24 h of exposure. Even so, urea production was significantly higher when compared with the amount of urea released by resting-MΦ ($p_{12h} = 0.0078$; $p_{18h,\ 24h} = 0.0313$, **Fig 17A).**

Parasite extract also induced cells to produce increased levels of urea that were significantly different from resting-MΦ ($p_{6h} = 0.0313$). Parasite antigen stimulated cells exhibited a maximum of urea production after 8 h of incubation ($p_{8h} = 0.0078$). This peak was followed by successive decreases, reaching a minimum of urea after 24 h of exposure. These values still were significantly high when compared with the urea produced by resting-MΦ ($p_{12h,\ 18h,\ 24h} = 0.0313$, **Fig. 17B).**

MΦ exposed to exosomes also revealed a high production of urea significant different from resting-MΦ ($p_{6h} = 0.0156$; $p_{8h,\ 12h} = 0.0313$) that peaked after 18h of incubation ($p_{18h} = 0.0313$). This peak was followed by a significant urea decrease that still was significantly higher than the amount of urea released by resting-MΦ ($p_{24h} = 0.0313$, **Fig. 17C**).

These results showed that alive parasites, parasite extract and parasite exosomes induce MΦ to produce high urea levels. The highest urea production was observed in *T. brucei* exposed cells, followed by antigenic extract and then by exosomes. Furthermore, all urea values were significantly superior when compared with the equivalent positive control ($0.0078 > p < 0.0313$).

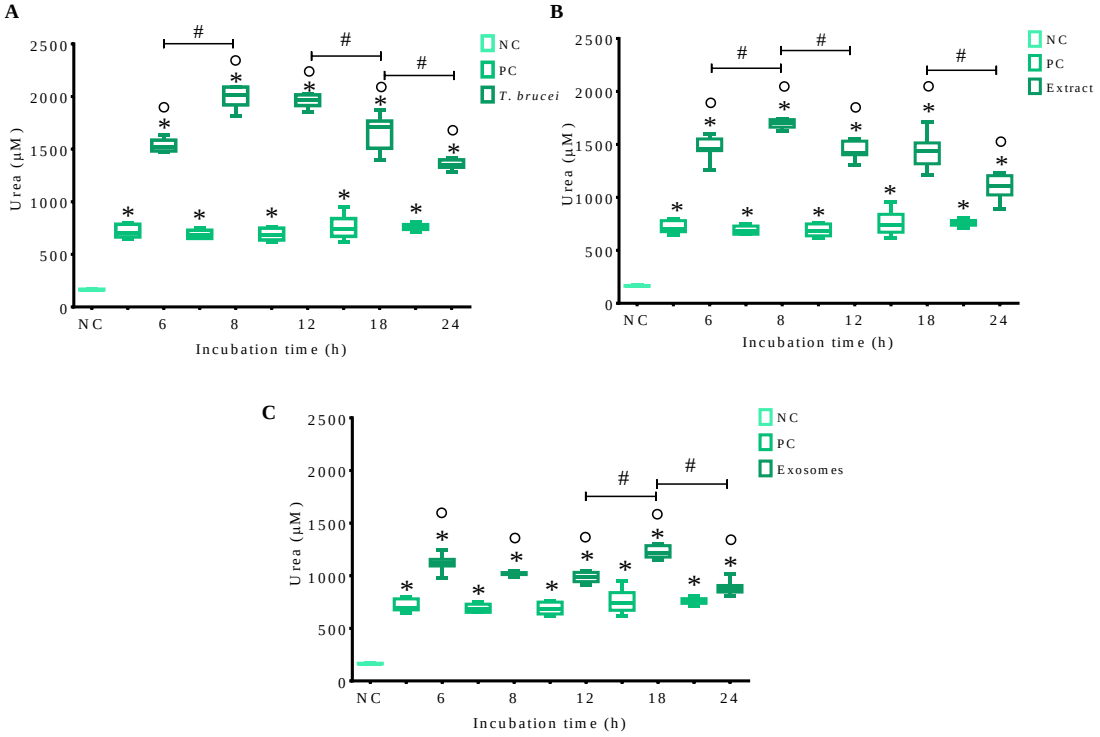

Figure 17 – Urea production by *T. brucei* exposed-MΦ. Urea production by MΦ was evaluated after 6 h, 8 h, 12 h, 18 h and 24 h of exposure to *T. brucei* (A) and of stimulation by parasite extract (B) and parasite exosomes (C). Urea produced by resting MΦ (negative control, NC), and PMA-stimulated MΦ (positive control, PC) were also evaluated. Results of three independent experiments and of three replicates per sample are represented by box-plot indicating median, minimum and maximum values. The non-parametric Wilcoxon test was used for statistical comparisons ($p<0.05$). * represents significant values when comparing resting-MΦ with the other conditions; ○ represents significant differences between PC and exposed- or stimulated-MΦ, and # indicates significant differences when comparing MΦ at different time points.

Resting-MΦ demonstrated a residual NO synthesis. However, PMA-stimulated MΦ revealed a significant increase of NO (**Fig. 18**) when compared with resting-MΦ at all time points evaluated ($p = 0.0313$), indicating that cells were functional.

After exposure to viable parasites, a significant increase of NO production ($p_{6h} = 0.0156$; $p_{8h,\ 12h} = 0.0313$) was observed. A peak of urea production ($p_{18h} = 0.0156$) was verified 18 h after parasite exposure. This peak was followed by a significant decrease, nonetheless the values still were significantly high when compared with resting-MΦ ($p_{24h} = 0.0313$, **Fig 18A**).

Parasite extract induced a fluctuation in NO production by MΦ over time that reached significant different values (p_{6h} = 0.0078; p_{8h} = 0.0156; p_{12h} = 0.0391; $p_{18h, 24h}$ = 0.0313) when compared with the negative control (**Fig 18B**).

Parasite exosome-stimulated MΦ produced similar NO levels at all time points, ($p_{6h, 8h, 12h, 24h}$ = 0.0156) except at 18 h of stimulation where a slight NO increase was observed (p_{18h} = 0.0313, **Fig. 18C**).

Likewise, as urea production, also MΦ present a similar response to different stimuli, producing increased NO that were significantly higher than negative and positive controls (0.0156 > p < 0.0313). The highest NO production was observed in cells exposed to *T. brucei*, followed by antigen and by exosomes.

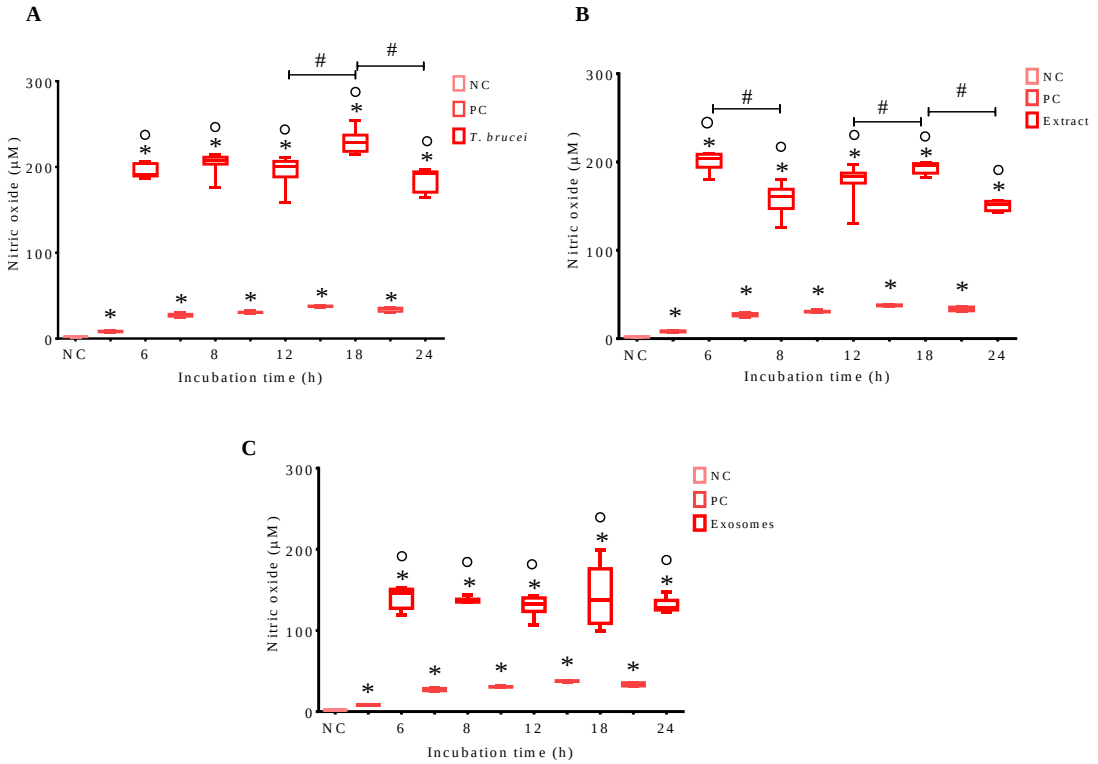

Figure 18 – NO production by *T. brucei* exposed-MΦ. NO production by MΦ was evaluated after 6 h, 8 h, 12 h, 18 h and 24 h of exposure to *T. brucei* (A), and of stimulation by parasite extract (B) and parasite exosomes (C). NO produced by resting-MΦ (negative control, NC) and by PMA-stimulated MΦ (positive control, PC) were also evaluated. Results of three independent experiments and of three replicates per sample are represented by box-plot, median, minimum and maximum values. The non-parametric Wilcoxon test was used for statistical comparisons ($p<0.05$). * represents values of statistical significance when compared resting-MΦ with the other conditions; ○ represents significant differences between PC and exposed- or stimulated-MΦ, and # indicates significant differences when comparing MΦ at different time points.

3.3. High levels of *de novo* nitric oxide and urea are produced after *T. brucei* exposure

Values obtained for the resting-MΦ were used to determinate *de novo* NO production, as well NO accumulation rates.

PMA stimulated-MΦ (positive control) presented similar levels of *de novo* NO production over time. In the case of parasite exposure and of parasite antigen and parasite exosome stimulation, MΦ synthesized similar amounts of NO over time. Furthermore, NO production was in all cases significantly higher that positive control ($p_{parasite}$ = 0.0156; $p_{exosomes,\ extract}$ = 0.0313, **Fig. 19A**). Moreover, it was also possible to observe that *T. brucei*, parasite extract and parasite exosomes induced a fold increase in NO production around of 100×, 90× and 75×, respectively, when compared to resting-MΦ (**Fig. 19A**).

Compared with PMA-exposed MΦ, that exhibit a gradual accumulation along incubation time, MΦ exposed to *T. brucei* alive trypomastigotes and stimulated by parasite exosomes and parasite antigens showed an intense urea accumulation over time ($p_{parasite}$ = 0.0156; $p_{exosomes,\ extract}$ = 0.0313, **Fig. 19B**).

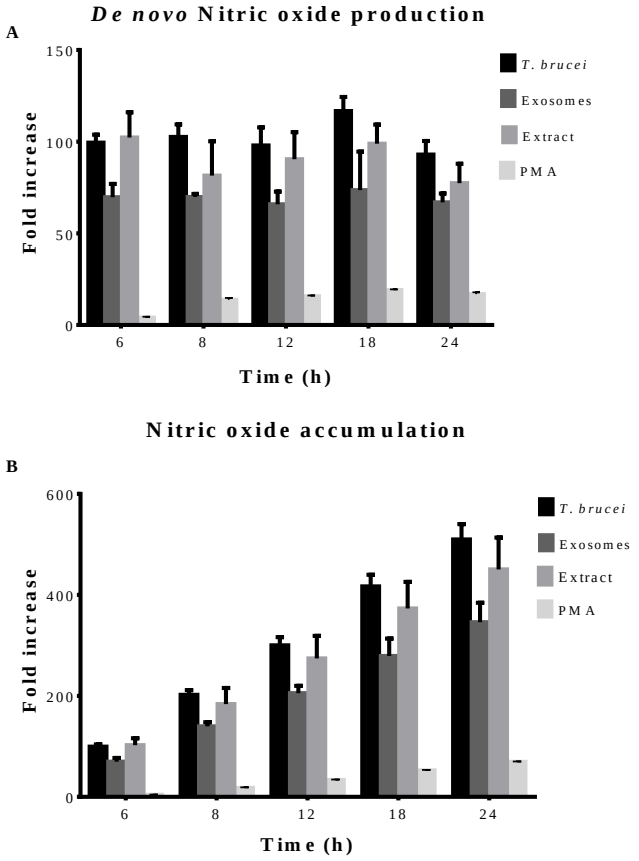

Figure 19 - Nitric oxide *de novo* production by MΦ exposed to *T. brucei* and NO accumulation. After 6 h, 8 h, 12 h, 18 h and 24 h de novo synthesized NO (A) and the respective accumulation rate (B) was estimated in MΦ exposed to parasites and stimulated by parasite extract and parasite exosomes. PMA-stimulated MΦ were used as positive control. Values are represented as mean plus standard error of samples performed in triplicate.

Urea accumulation and *de novo* urea production rates were also assessed using values obtained for resting-MΦ.

De novo urea production by PMA stimulated-MΦ revealed similar levels over time. In the case of parasite exposure and extract-simulation, MΦ synthesized significant high levels of urea over incubation time ($p_{parasite,\ extract}$ = 0.0313) when compared with the positive control (**Fig. 20A**). A significant high accumulation of urea was also observed in MΦ exposed to parasites and in extract stimulated MΦ when compared with positive control ($p_{parasite,\ extract}$ = 0.0313, **Fig. 20B**).

Moreover, *T. brucei* was responsible for inducing a fold increase around of 12×, while antigenic extract triggered a fold increase of approximately 10×, and parasite exosomes induced an enhancement of about 7.5× in urea *de novo* production, when compared with resting-MΦ (**Fig. 20A**).

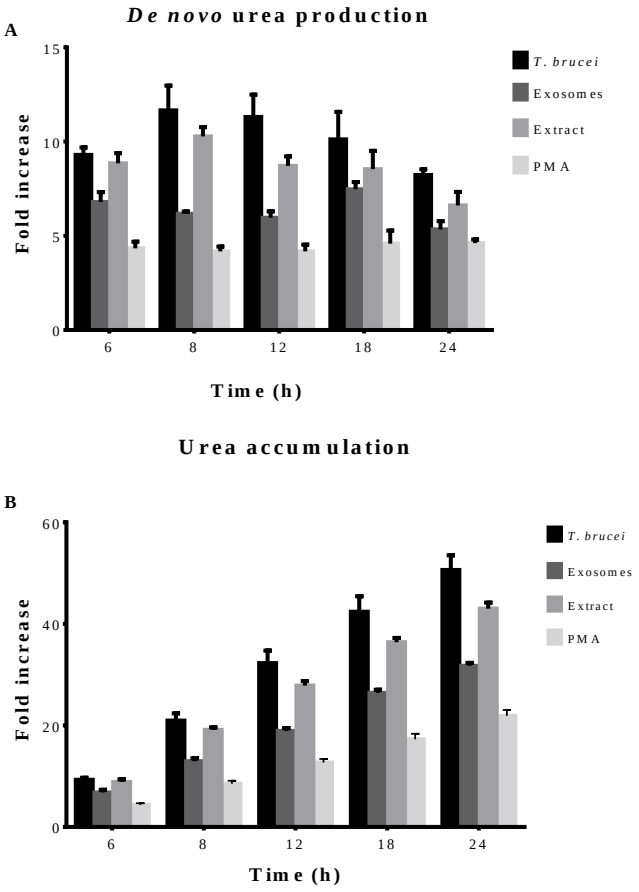

Figure 20 - Urea *de novo* production by MΦ exposed to *T. brucei* and urea accumulation. After 6 h, 8 h, 12 h, 18 h and 24 h *de novo* synthesized urea (A) and the respective accumulation rate (B) were estimated in MΦ exposed to parasites and stimulated by parasite extract and parasite exosomes. PMA-stimulated MΦ were used as positive control. Values are represented by mean plus standard error of samples performed in triplicate.

3.4. *De novo* NO and urea are simultaneously produced by *T. brucei*-exposed MΦ

To evaluate the relation between urea-producing MΦ and NO-producing MΦ, a linear regression was generated using *de novo* NO values and *de novo* urea levels over time. A positive linear correlation was obtained to *T. brucei* exposed MΦ and to parasite antigens- and parasite exosomes-stimulated MΦ. Thus, these results indicate that NO and urea levels increased simultaneously for 24 h. A significant positive correlation was observed in parasite exposed-MΦ (p=0.0223, **Fig. 21A**). This positive correlation was followed by parasite exosome stimulated-MΦ (**Fig. 21B**). However, MΦ stimulated by parasite extract (**Fig. 21C**) showed a stable urea production.

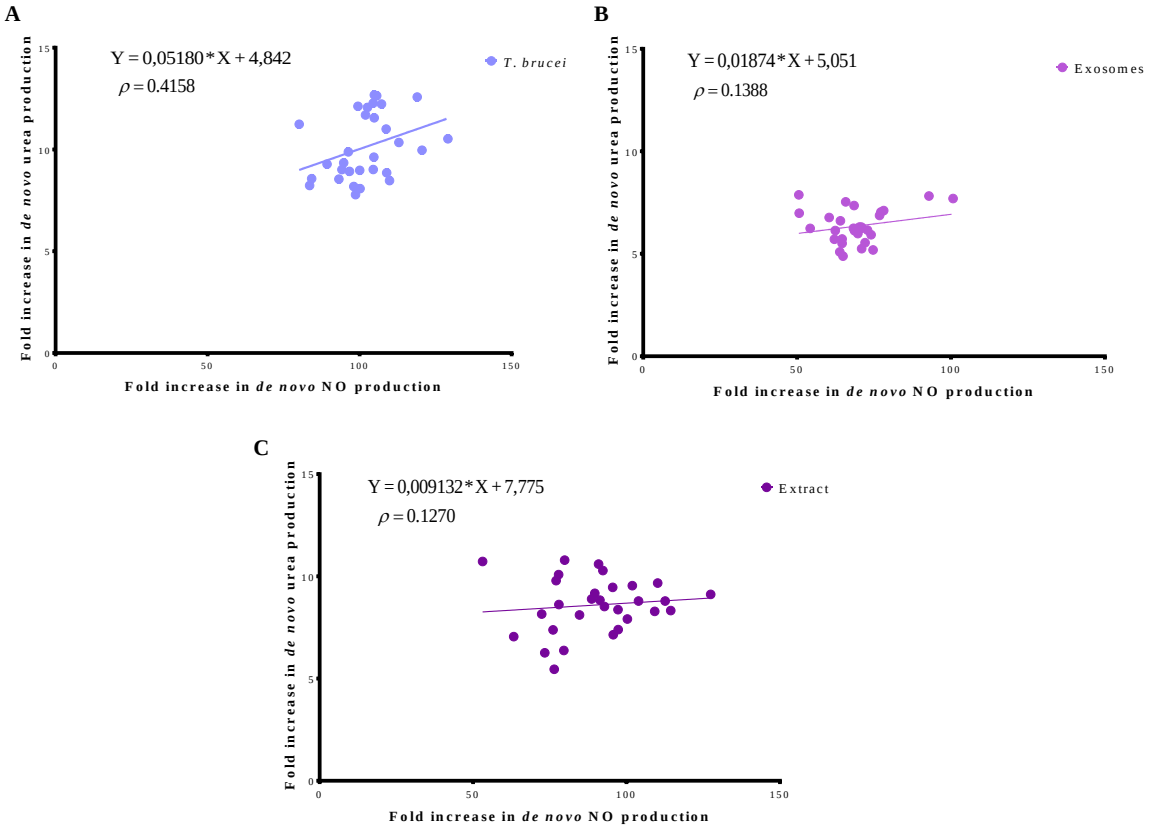

Figure 21 – Correlation between NO and urea production. A linear regression was generated using *de novo* NO and *de novo* urea values obtained from *T. brucei* exposed MΦ (A) and from parasite antigen- (C) and parasite exosome-stimulated MΦ (B), during 24 h.

3.5. Antigen presentation

3.5.1. *T. b. brucei* impairs MHC expression on MΦ and parasite exosomes increases MHC$^+$MΦ

The ability of *T. b. brucei* trypomastigotes to induce MΦ to present exogenous antigens was indirectly evaluated. Levels of MHCI and MHCII fluorescence were assessed in fluorochrome minus one (FMO) histograms (**Fig. 22**).

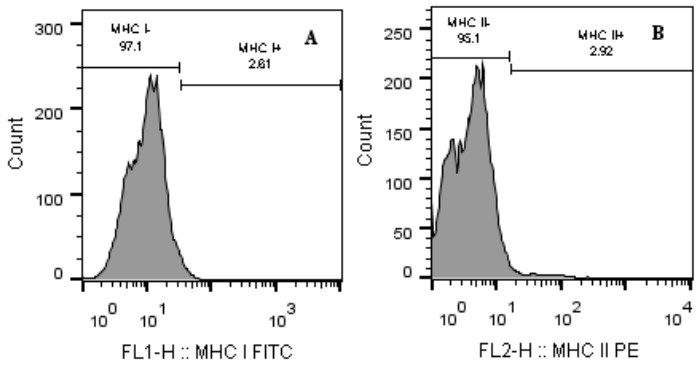

Figure 22 – Representative histograms of flow cytometry analysis of MHC molecules. The histograms FL1-H *vs* number of events (count) and FL2-H vs number of events (count) were used to determine MHCI$^+$ (A) and MHCII$^+$ cells (B), respectively.

When compared to resting-MΦ (**Fig. 23A and 24A**), PMA-stimulated MΦ (**Fig. 23B and 24A**) revealed a significant increase of MHCI$^+$MΦ ($p = 0.0078$). In the case of *T. brucei* exposure (**Fig. 23C and 24A**), MHCI$^+$MΦ nearly was completely inhibited ($p = 0.0156$). On the other hand, when stimulated by *T. brucei* extract ($p = 0.0195$, **Fig. 23D and 24A**) and by parasite exosomes ($p = 0.0273$, **Fig. 23E and 24A**) MHCI$^+$MΦ presented a significant increase. Even so, only less than 5% of the cells expressed MHCI molecules.

In the case of membranar MHCII molecules, it was observed that PMA-stimulated MΦ (**Fig. 23B and 24B**) increased significantly their APC capacity ($p = 0.0078$) when compared to resting MΦ (**Fig. 23A and 24B**). Results of *T. brucei*-stimulated MΦ showed an impaired capacity of MΦ to present antigens ($p = 0.0313$, **Fig. 23C and 24B**). Along with these findings, also APC function seemed to be impaired by *T. brucei* extract ($p = 0.0313$, **Fig. 23D and 24B**). However, in exosome-

stimulated MΦ, it was observed a significant increase in MHCII$^+$ cells (p = 0.0234, **Fig. 23E and 24B**).

Despite significant increases in capacity of these cells to present antigens were observed, in general the cell percentage did not reach 10%. In all the cases, the amount of double positive cells (MHCI$^+$MHCII$^+$ cells) was very low, presenting the majority of the cells double negative phenotype (MHCI$^-$ MHCII$^-$ cells, **Fig. 23**).

Taken together, these results shown a similar expression pattern for both MHC class I and II molecules. In both cases, *T. brucei* inhibited the MΦ capacity to present antigens. However, exosomes seemed to stimulate the APC function of MΦ cells through MHCII molecules and also increase the potential to present antigens via MHCI.

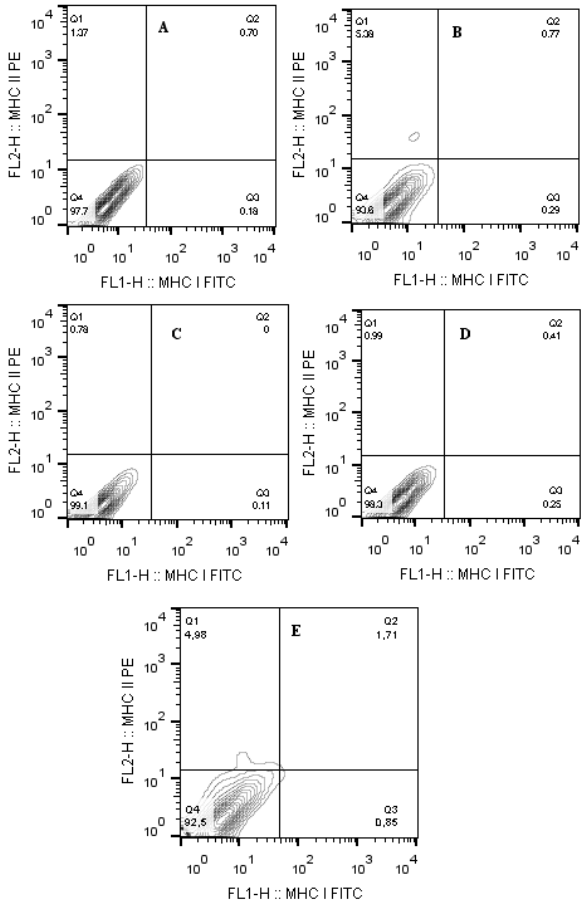

Figure 23 - Representative dot-plots of flow cytometry analysis of MHC molecules. After 72 h of incubation, levels of MHCI and MHCII were evaluated in resting-MΦ (A), PMA-stimulated MΦ (B), MΦ exposed to *T. b. brucei* (C) and, in MΦ stimulated by parasite extract (D) and by parasite exosomes (E).

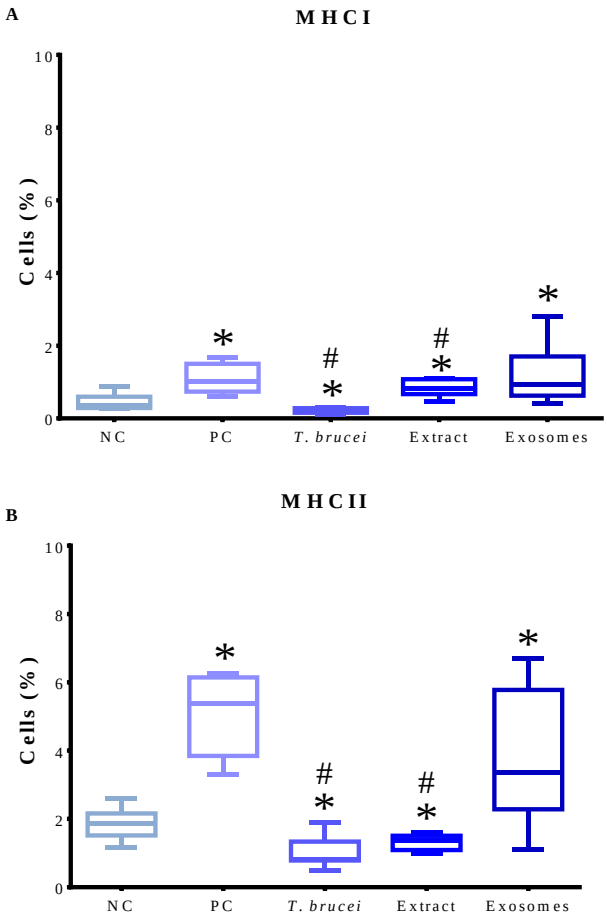

Figure 24 – MHCI and MHCII surface expression on *T. b. brucei*-exposed MΦ. After 72 h of incubation, levels of $MHCI^+$ (A) and $MHCII^+$ cells (B) were evaluated in MΦ exposed to *T. b. brucei* and, in MΦ stimulated by parasite extract and by parasite exosomes. In parallel, resting-MΦ (negative control, NC) and PMA stimulated-MΦ (positive control, PC) were also evaluated. Results of three independent experiments and of three replicates per sample are represented by whisker box-plot, median, minimum and maximum values. The non-parametric Wilcoxon test was used for statistical comparisons ($p<0.05$). * represents values of statistical significance when comparing NC *vs* the other conditions and, # represents significant differences when comparing PC *vs* the other conditions.

3.5.2. Density of MHCI molecules increases after *T. b. brucei* exposure

The intensity of fluorescence, reflecting the density of MHC molecules on the cell surface was also evaluated (**Fig. 25**).

When comparing with resting-MΦ, MHCI density significantly increased after PMA stimulation ($p = 0.0156$). A considerable augment of MHCI density was also

observed in cells exposed to *T. brucei* (p = 0.0313) and to parasite extract (p = 0.0313, **Fig. 25A**). However, exosomes did not seem to promote the increase of MHCI.

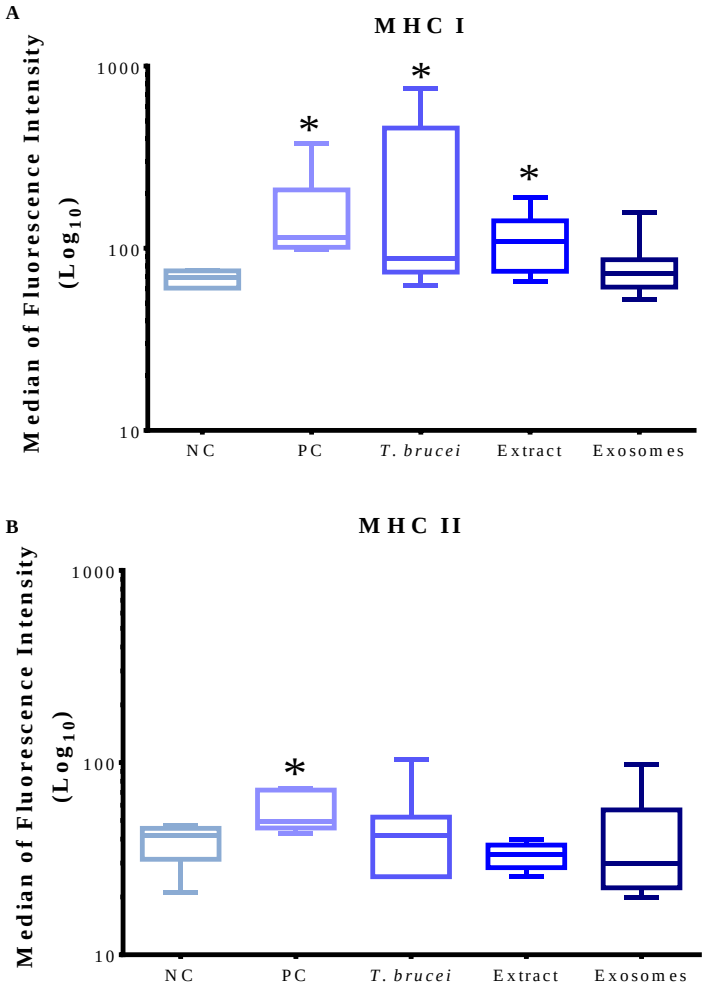

Figure 25 – Density levels of membranar MHCI and MHCII on *T. b. brucei*-exposed MΦ. MΦ exposed to *T. brucei* and stimulated by parasite extract and parasite exosomes were used to evaluate the membranar density of MHCI (A) and MHCII (B). Resting-MΦ (NC) and PMA-stimulated MΦ (PC) were also evaluated. Results of three independent experiments and samples triplicates are represented by box-plot, median, minimum and maximum values. The non-parametric Wilcoxon test was used for statistical comparisons ($p<0.05$). * represents values of statistical significance when comparing resting-MΦ with the other conditions.

3.5.3. An increase of MHCI/MHCII ratio was observed after *T. b. brucei* exposure and exosome stimulation

A ratio of MHCI *vs* MHCII was calculated, taking into account both Fluorescence Intensity (FI) and Cell Percentage (CP), as previously described in data analysis sub-heading. In the case of resting-MΦ (mean = 0.393) and extract stimulated-MΦ (mean = 0.341) all MHCI/MHCII ratio values were <1. In *T. brucei* exposed-MΦ (mean = 0.508) the majority of values were ≤1, pointing towards a predominant antigen presentation to $CD8^-$ T cells. In exosomes stimulated-MΦ (mean=1.098) was observed that some values were <1 and the others were >1, thus suggesting an antigen presentation to both $CD8^-$ and $CD8^+$ T cells. Furthermore, MHCI/MHCII ratio values were significantly increased when compared with resting MΦ ($p_{T.\ brucei}$ = 0.0313, $p_{exosomes}$ = 0.0391, **Fig. 26**).

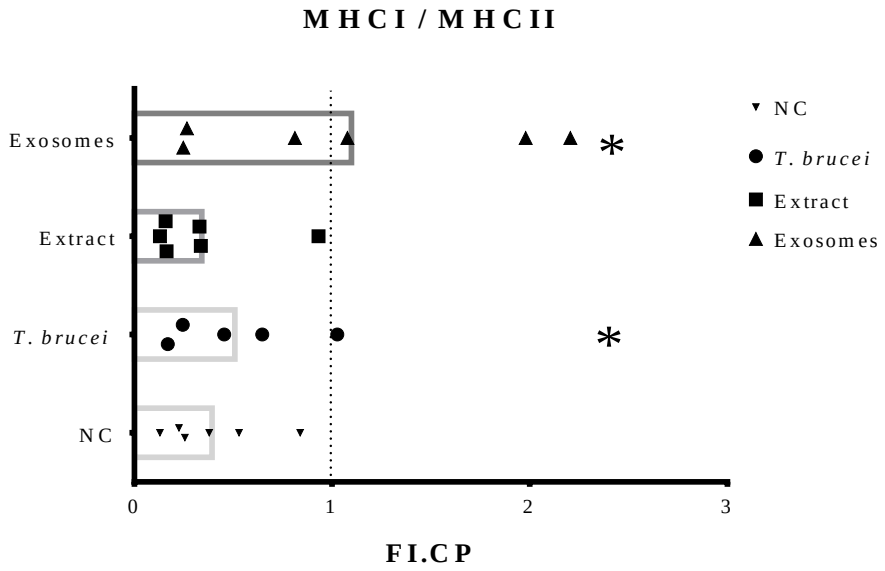

Figure 26 – MHCI/MHCII ratio of *T. b. brucei* exposed MΦ and of parasite extract- and exosomes-stimulated MΦ. The ratio $MHCI^+$ *vs* $MHCII^+$ were determined in MΦ exposed to parasites and in MΦ stimulated by parasite extract and exosomes. FI.CP of resting MΦ (NC) were also estimated. Results are represented by column graphs of three independent experiments performed in triplicate. The non-parametric Wilcoxon test was used for statistical comparisons ($p<0.05$). * represents values of statistical significance when comparing resting MΦ (NC) with the other conditions.

3.6. Characterization of lymphocyte subsets

In order to characterize lymphocyte subsets, after exposure to *T. b. brucei* trypomastigotes, parasite antigen and parasite exosomes, cells were magnetically separated in two fractions ($CD8^-$ and $CD8^+$) and analyzed by flow cytometry. CD3 gate was applied in FMO histograms for further immunophenotyping of cell subsets (**Fig. 27**).

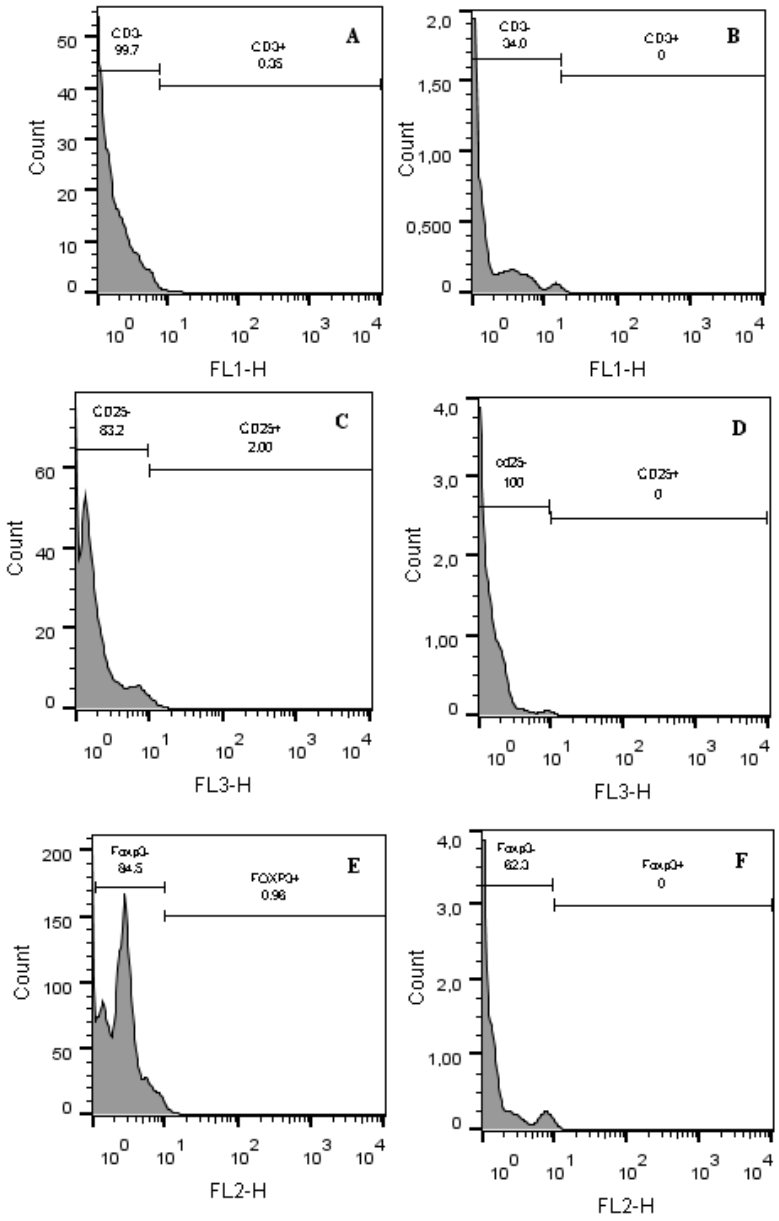

Figure 27 – Representative histograms of flow cytometry analysis for lymphocytes characterization. The histograms FL1-H *vs* number of events (count), FL2-H *vs* number of events and FL3-H *vs* number of events were used to determine $CD3^+$ (A and B), $FoxP3^+$ (E and F) and $CD25^+$ (C and D) cell subsets.

3.6.1. Magnetic separation demonstrated to be efficient

Control Samples of magnetic separation were analyzed and demonstrated that this technique presents a high efficiency. Results indicated that $CD8^-$ cell fraction included approximately 80% of $CD3^+CD4^+$ cells, while in $CD8^+$ cell fraction, were included about 75% of $CD3^+CD8^+$. Thus, these results indicate that $CD8^-$ cell fraction is mainly constituted by $CD4^+$ T cells, while the $CD8^+$ cell fraction in primarily constituted by T cytotoxic lymphocytes.

3.6.2. *T. b. brucei* impairs lymphocyte proliferation

Cell marker CD3 is a protein complex that acts as a T-cell co-receptor in association with T cell receptor. Therefore, anti-CD3 Abs can be used as T cell markers, ensuring that the cells that are being analyzed correspond to T lymphocytes.

Analyzing the results from $CD8^-$ enriched fraction, it was found out that ConA (positive control) induced a significant expansion of $CD3^+CD8^-$ cell subset ($p = 0.0078$, **Fig. 28B and 29A**), when compared to non-stimulated lymphocytes (**Fig. 28A and 29A**), indicating that cells were viable and functioning. On the other hand, *T. b. brucei* exposure caused a significant contraction of $CD3^+CD8^-$ cell subpopulation ($p = 0.0078$, **Fig 28C and 29A**). However, parasite extract (**Fig. 28D and 29A**) and parasite exosomes (**Fig. 28E and 29A**) induced a significant expansion of $CD3^+CD8^-$ lymphocytes ($p_{extract,\ exosomes} = 0.0156$) when compared with non-stimulated lymphocytes. Even so, in the case of exosomes stimulation, the increase observed was significantly lower in comparison to ConA-stimulated lymphocytes ($p = 0.0156$).

Relatively to $CD8^+$ enriched fraction, as expected ConA (**Fig. 28G and 29B**) caused a significant expansion of $CD3^+CD8^+$ cell subset ($p = 0.0078$) when compared with non-stimulated lymphocytes (**Fig. 28F and 29B**). Also, in this cell fraction the parasite ($p = 0.0078$, **Fig. 28H and 29B**) caused a significant contraction of $CD3^+CD8^+$ cells, while exosomes caused a significant increase in $CD3^+CD8^+$ cells ($p = 0.0234$, **Fig. 28J and 29B**).

In the case of *T. brucei* exposure, T lymphocyte significantly decrease to values inferior to non-stimulated lymphocytes. This unexpected low amount of $CD3^+$ cells

could be caused by a technical issue, as is the case of cells remained in the column or be a direct consequence of the contact with mobile parasites that could cause cell damage.

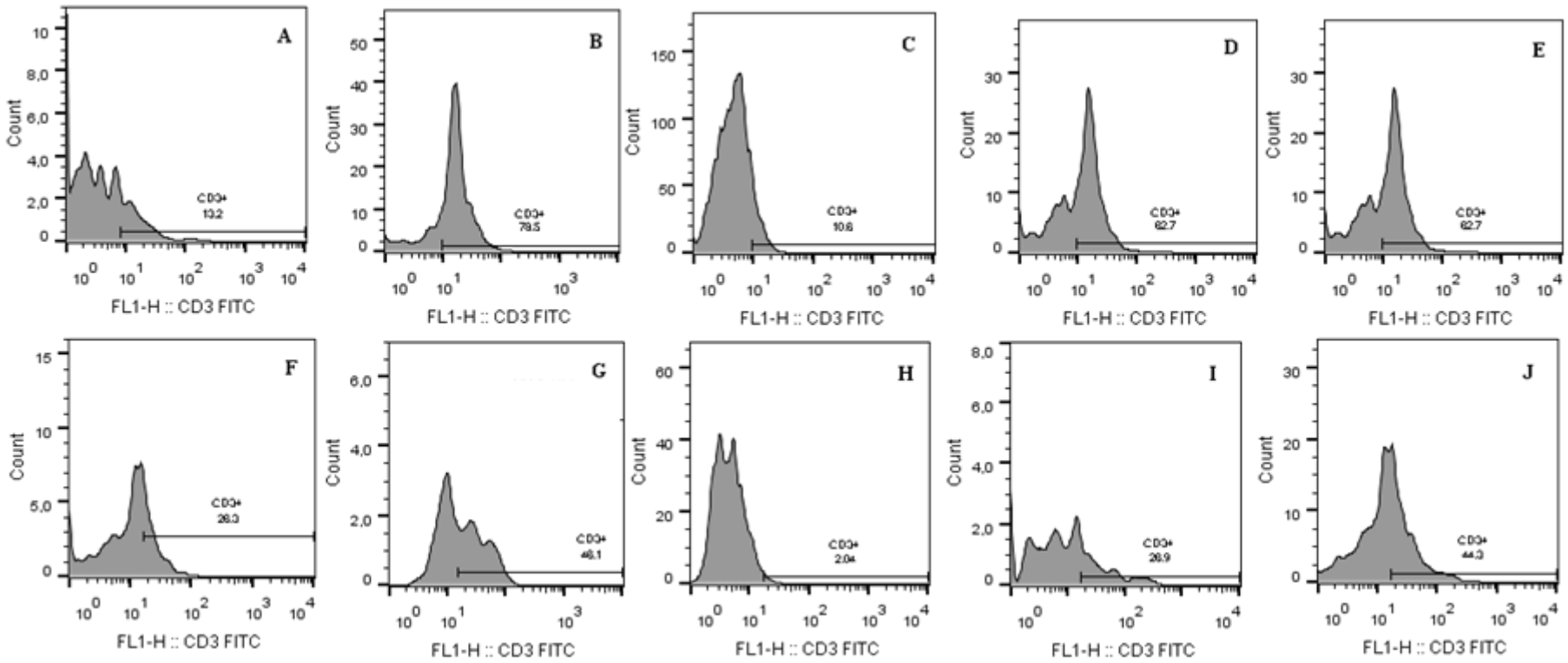

Figure 28 – Representative histograms of CD3$^+$ cells after contacted *T. b. brucei*, parasite extract or exosomes. Resting lymphocytes (A and F), Con A-stimulated lymphocytes (B and G), *T. b. brucei*-exposed lymphocytes (C and H), *T. b. brucei* extract-stimulated lymphocytes (D and I) and *T. brucei* exosomes-stimulated lymphocytes (E and J) were magnetically separated in CD8$^-$ (A- E) and CD8$^+$ (B - J) cell fractions. Cells were stained with CD3 marker and evaluated by flow cytometry. Histograms indicate CD3$^+$ cells at both CD8$^-$ and CD8$^+$ cell fractions.

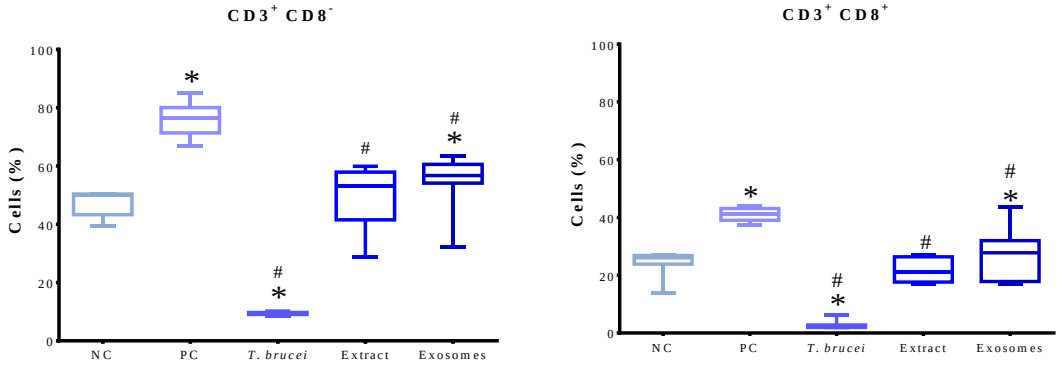

Figure 29 – T cell subsets induced by *T. b. brucei*. Mouse lymphocytes incubated with parasites, parasite extract and parasite exosomes were magnetically separated in $CD8^-$ (A) and $CD8^+$ (B) cell fractions. Cells were stained with CD3 monoclonal antibody and evaluated by flow cytometry. Results of three independent experiments performed in triplicate are represented by whisker box-plot, median, minimum and maximum values. The non-parametric Wilcoxon test was used for statistical comparisons ($p<0.05$). * indicates significant values when comparing non-stimulated lymphocytes (NC) *vs* the other conditions, and # indicates significant differences when comparing ConA stimulated lymphocytes (PC) *vs* the other conditions.

3.6.3. Lymphocyte fluorescence intensity decreases after *T. b. brucei* stimulation

The intensity of fluorescence was another parameter assessed to better understand the effect of parasite in lymphocytes, and consequently in the immune response.

Relatively to $CD8^-$ fraction, CD3 fluorescence intensity increased significantly after ConA stimulation, when comparing with non-stimulated lymphocytes ($p = 0.0313$). Similarly, also parasite exosomes seemed to increase CD3 fluorescent intensity ($p = 0.0313$). However, after *T. b. brucei* exposure fluorescence reduced significantly ($p = 0.0156$, **Fig. 30A**).

Analyzing $CD8^+$ fraction, it was observed that only parasite extract and parasite exosomes induced significant increases in CD3 fluorescent intensity, when compared with resting lymphocytes ($p_{extract,\ exosomes} = 0.0313$, **Fig. 30B**).

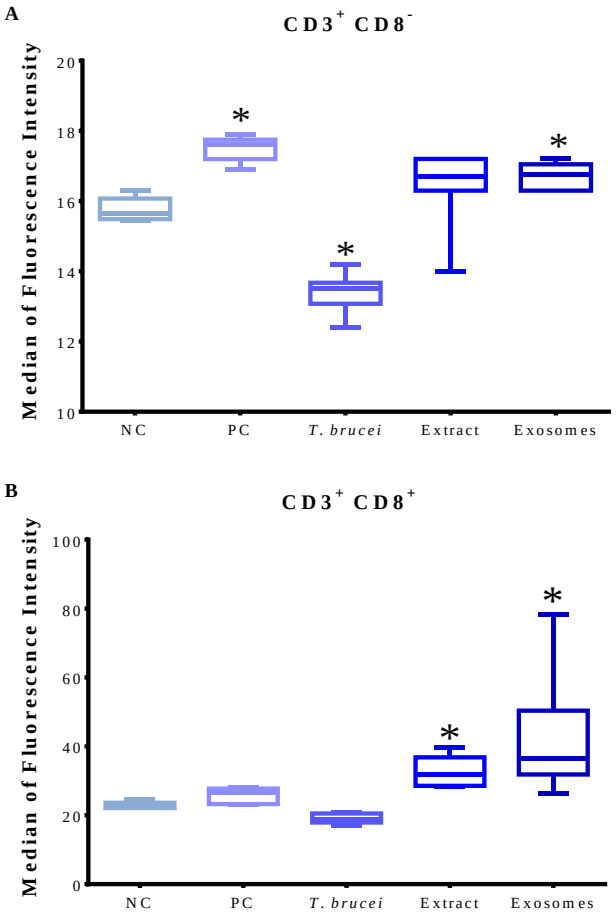

Figure 30 – Density levels of CD3 cells on *T. b. brucei*-exposed lymphocytes. $CD8^-$ (A) and $CD8^+$ (B) lymphocytes exposed to *T. brucei* and stimulated by parasite extract and parasite exosomes were used to evaluate CD3 fluorescence intensity. Resting-lymphocytes (NC) and ConA-stimulated lymphocytes (PC) were also evaluated. Results of three independent experiments and triplicates of each sample are represented by box-plot, median, minimum and maximum values. The non-parametric Wilcoxon test was used for statistical comparisons ($p<0.05$). * represents statistical significance when comparing resting-lymphocytes *vs* the other conditions.

3.6.4. Frequency of $CD3^+$ cells and fluorescence intensity are positively correlated in cells exposed to *T. brucei*

In order to understand the correlation between T cell frequencies and fluorescence intensities, linear regression of these two independent parameters was generated. In the case of $CD8^+$ cells exposed to *T. b. brucei* (**Fig. 31A**) or stimulated by parasite extract (**Fig. 31C)** or parasite exosomes (**Fig. 31E)** and in the case of $CD8^-$ cells exposed to parasites (**Fig. 31B**), positive correlations were found, although more

expressive in *T. brucei* exposed $CD8^-$ cells. These correlations indicate that the increase of $CD3^+$ cells is associated with an augment of CD3 molecules. On the other hand, in $CD8^+$ cells stimulated by parasite extract **(Fig. 31D)** or parasite exosomes **(Fig. 31F)** negative correlations were observed, that was more accentuated in the exosomes-stimulated cells. These correlations indicate that T cell increase was associated with a reduction of CD3 molecules on lymphocyte membrane.

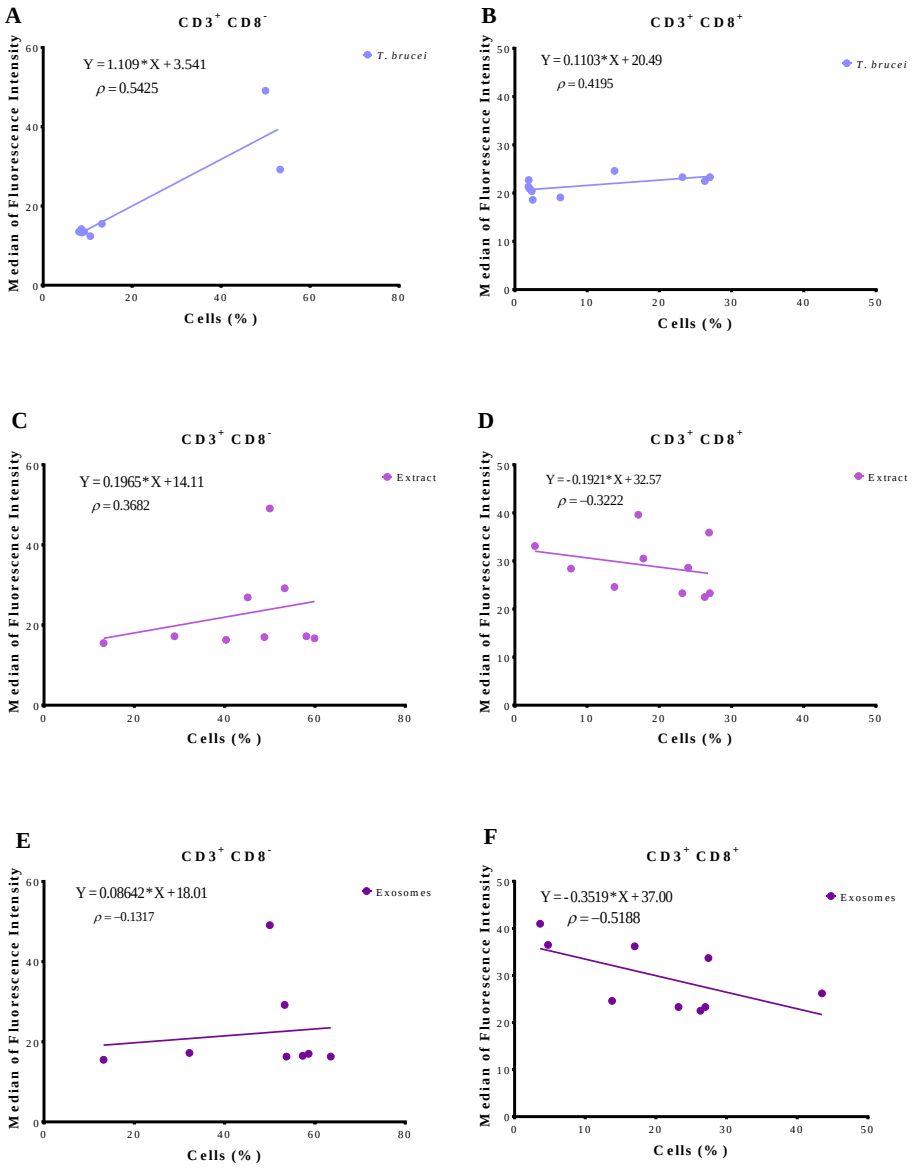

Figure 31 - Correlation between the frequency of $CD3^+$ cells and the intensity of CD3 molecules. A linear regression was generated using the frequencies of the $CD3^+$ $CD8^-$ (A, C and E) and $CD3^+$ $CD8^+$ (B, D and F) cells exposed to *T. brucei* (A and B), stimulated by parasite antigen (C and D) or by parasite exosomes (E and F) and the respective density of CD3 molecules.

3.6.5. A predominance of T helper cells is observed in the presence of *T. b. brucei*

In order to characterize the role of helper T cells and cytotoxic T cells in African trypanosomiasis, frequency of $CD8^-$ and $CD8^+$ cells were compared for different stimulus. $CD8^-/CD8^+$ rates were assessed, and a significant increase was observed after *T. brucei* exposure and after stimulation by *T. brucei* extract ($p_{parasite,\ extract} = 0.0078$). After parasite exposure and after extract and exosome stimulation, $CD8^-$ T cells predominated (mean, 4.00, 4.22, 2.08) and increased relative to non-stimulated lymphocytes (mean, 1.50, **Fig. 32A**). These results were confirmed, when analyzing flow cytometry histograms (**Fig. 32B and C**).

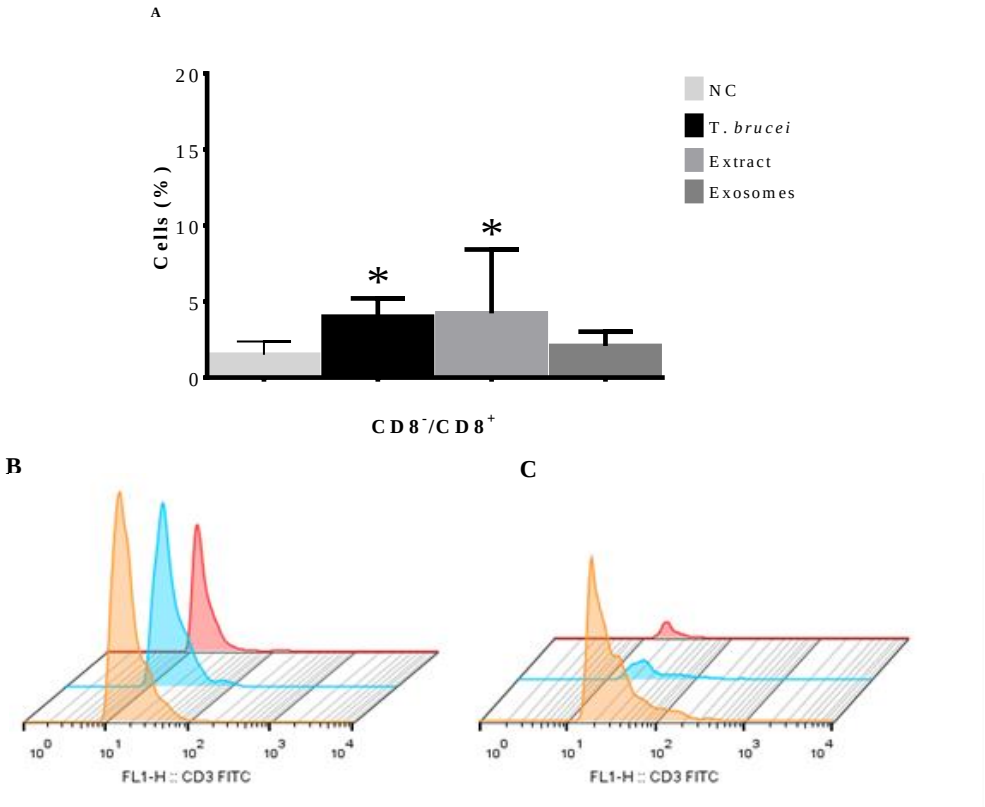

Figure 32 – $CD8^-$ / $CD8^+$ T cell ratios after *T. b. brucei* exposure and stimulated by parasite extract and parasite exosomes. $CD8^-$ / $CD8^+$ T cell ratios are represented by graphical bars as means and standard deviation (A). The non-parametric Wilcoxon test was used for statistical comparisons ($p<0.05$). * represents values of statistical significance when comparing resting-lymphocytes with the other conditions. Histograms comparing the relative dimension of $CD3^+$ $CD8^-$ (B) and $CD3^+$ $CD8^+$ (C) cell populations when exposed to *T. b. brucei* (red) and when stimulated by parasite extract (blue) and by parasite exosomes (orange) are shown.

To evaluate retraction or increment of lymphocyte populations, values of non-stimulated lymphocytes were subtracted to the values of exposed or stimulated-lymphocytes. Results indicated that in the $CD8^-$ cell fraction, the exposure to *T. b. brucei* parasites caused an accentuated reduction of lymphocyte population (mean, -25.18%). However, parasite extract (mean, 14.81%) and parasite exosomes (mean, 20.13%) induced the expansion of cell subset. In $CD8^+$ T cells, *T. b. brucei* was also responsible for a reduction of the cell subset (mean, -21.69%), while parasite extract (mean, 1.08%) and parasite exosomes (mean, 2.15%) caused a slight augment of lymphocytes (**Fig. 33**).

Taken together, these results indicate that *T. brucei* is responsible for the depletion of $CD3^+CD8^+$ and $CD3^+CD8^-$ T cells, more evident in $CD8^-$ fraction. On the other hand, parasite extract and parasite exosomes triggered lymphocyte proliferation, that was more accentuated in the $CD8^-$ cell fraction.

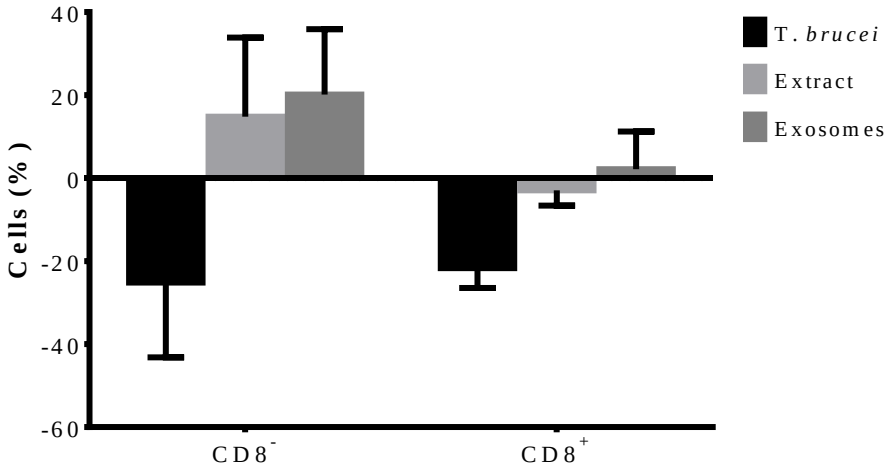

Figure 33 – Retraction of $CD8^-$ and $CD8^+$ T cell subsets caused by *T. brucei* parasites. Frequency of non-stimulated lymphocytes were subtracted to the frequency of cells exposed to alive parasites or stimulated by parasite extract or parasite exosomes**.** The results are expressed as means plus standard errors.

3.6.6. *T. b. brucei* promotes the expansion of $CD25^+$ $FoxP3^-$ subset in both $CD8^-$ and $CD8^+$ T cells

Treg cells are a $CD25^+$ lymphocyte subset that plays a key role in the immune system. Therefore the surface biomarker CD25 was used in the current study to better understand the effect of African trypanosomes in Treg population. Furthermore, $CD25^-$ cells were also evaluated, since they represent effector T cells that are crucial in immune response. Also, to better characterize the role of T cells in immune regulation, the nuclear transcription factor FoxP3 was evaluated within $CD25^+$ T and $CD25^-$ T cells.

When analyzing $CD3^+$ $CD8^-$ cell fraction of non-stimulated lymphocytes, it was observed a small percentage of $CD25^-$ $FoxP3^+$ and $CD25^+$ $FoxP3^+$ cells (**Fig. 34A and 35A and B**). When stimulated with ConA, it was observed a significant expansion in $CD25^-$ $FoxP3^+$ cell subset ($p = 0.0078$, **Fig. 34B and 35A**) that was more accentuated in $CD25^+$ $FoxP3^+$ cell subset ($p = 0.0156$). This huge increase of the above subset justifies the depletion observed in $CD25^+$ $FoxP3^-$ ($p = 0.0156$) and $CD25^-$ $FoxP3^-$ cell subsets ($p = 0.0078$), relative to non-stimulated lymphocytes (**Fig. 34A and B and, 35C and D**).

After *T. b. brucei* stimulation, it was observed a significant impairment in $CD25^-$ $FoxP3^+$ cell subset relative to non-stimulated lymphocytes ($p = 0.0156$, **Fig. 34C and 35A**). A significant increase in $CD25^+$ $FoxP3^-$ cell subset ($p = 0.0313$, **Fig. 34C and 35C**) was also observed. Although not significant changes occurred in $CD25^-$ $FoxP3^-$ cell subset, is seems that parasite induced the differentiation of two different subpopulations, one expressing high CD25 fluorescence, and the other expressing high FoxP3 fluorescence, when comparing with non-stimulated lymphocytes (**Fig. 34A and C**).

In the case of cells stimulated with *T. b. brucei* extract, it was observed a significant increase of $CD25^-$ $FoxP3^+$ ($p = 0.0156$, **Fig. 34D and 35A**) and $CD25^-$ $FoxP3^-$ ($p = 0.0078$, **Fig. 34D and 35D**) cell subsets. These increments were associated to a significant depletion of $CD25^+$ $FoxP3^-$ cells ($p = 0.0078$, **Fig. 34D and 35C**). *T. b. brucei* exosomes seemed to have an effect similar to parasite extract. Significant increases of $CD25^-$ $FoxP3^+$ ($p = 0.0156$, **Fig. 34E and 35A**) and $CD25^-$ $FoxP3^-$ ($p = 0.0156$, **Fig. 34E and 35D**) cell subsets and a significant retraction of $CD25^+$ $FoxP3^-$

cell subset (p = 0.0078, **Fig. 34E and 35C**) was observed. In both antigen and exosomes lymphocyte stimulation, $CD25^+$ $FoxP3^+$ cell subset was unchanged.

Relatively to $CD8^+$ fraction, it was observed that $CD25^-$ $FoxP3^+$ cell subset was almost null (**Fig. 34F and 35E**) in the non-stimulated cells, but after ConA stimulation, this subset increased significantly (p = 0.0156, **Fig. 34G and 35E**). A significant increase was also observed in $CD25^+$ $FoxP3^+$ (**Fig. 34G and 35F**) and $CD25^+$ $FoxP3^-$ cell subsets (p = 0.0078, **Fig. 34G and 35G**). On the other hand, an important reduction of $CD25^-$ $FoxP3^-$ cells (p = 0.0313) was observed (**Fig. 34G and 35H**).

After *T. b. brucei* exposure, it was observed a complete depletion of cells with $CD25^-$ $FoxP3^+$ phenotype when comparing with non-stimulated lymphocytes (p = 0.0078, **Fig. 34H and 35E**). Also $CD25^+$ $FoxP3^+$ (p = 0.0313, **Fig. 34H and 35F**) and $CD25^-$ $FoxP3^-$ (p = 0.0313, **Fig. 34H and 35H**) cell subsets were significantly impaired. On the contrary, $CD25^+$ $FoxP3^-$ cells constitute the major subset (p = 0.0156, **Fig. 34H and 35G**).

$CD8^+$ cells stimulated by *T. b. brucei* extract evidenced a significant increment of $CD25^+$ $FoxP3^+$ (p = 0.0313, **Fig. 34I and 35F**) and of $CD25^-$ $FoxP3^+$ (p = 0.0313, **Fig. 34I and 35G**) cell subsets when compared with non-stimulated cells. Moreover, $CD8^+$ lymphocytes exhibiting a $CD25^-$ $FoxP3^-$ phenotype were highly depleted (p = 0.0156, **Fig. 34I and 35G**). Moreover, it seemed that in $CD25^+$ $Foxp3^+$ cell subset two subpopulations were differentiated, one with lower and the other with higher fluorescence, and in $CD25^+$ $Foxp3^-$, three different subpopulations, with different fluorescence levels were observed (**Fig. 34I).**

T. b. brucei exosomes caused a significative expansion of $CD25^-$ $FoxP3^+$ (p = 0.0156, **Fig. 34J and 35E**) and $CD25^+FoxP3^+$ (p = 0.0313, **Fig. 34J and 35F**) cell subsets when compared with non-stimulated cells. Additionally, $CD25^-$ $FoxP3^-$ cell subset was significantly depleted (p = 0.0313, **Fig. 34J and 35G**).

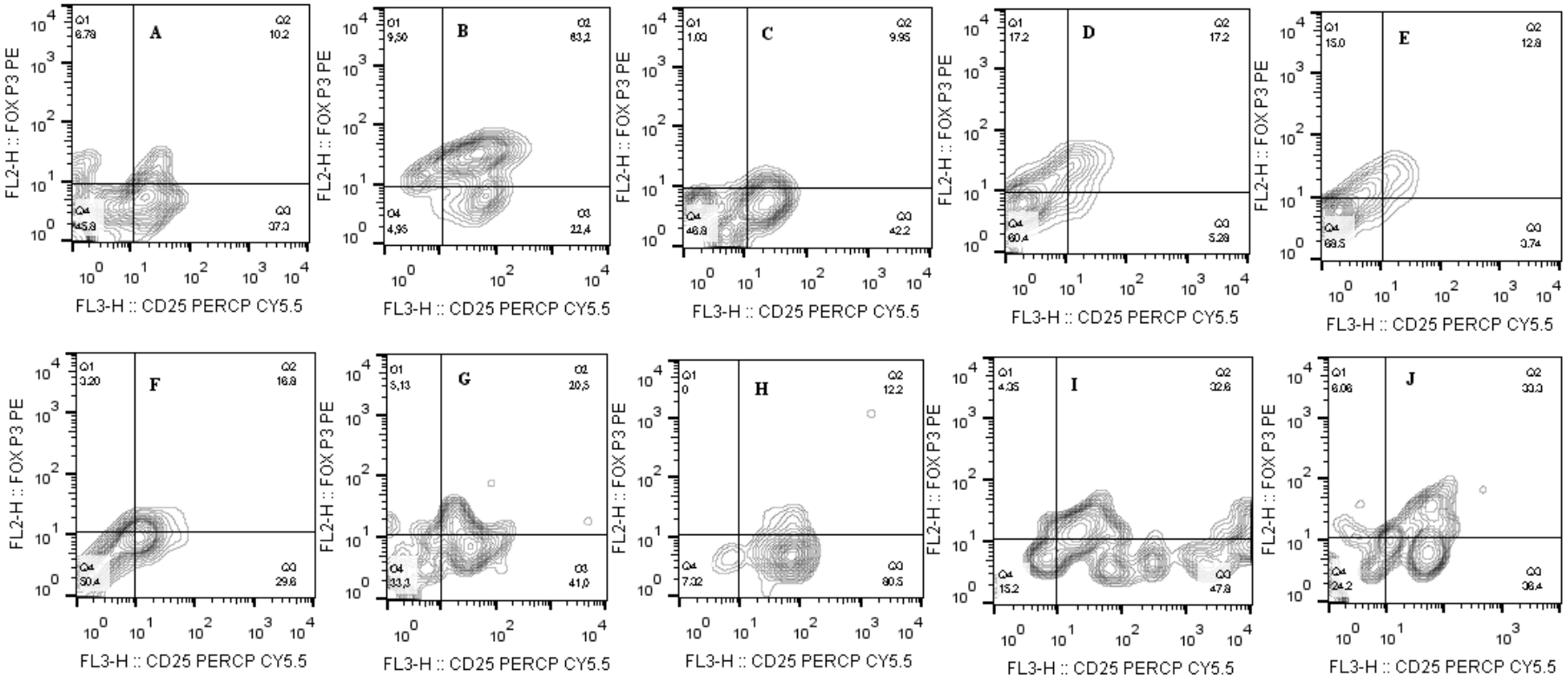

Figure 34 - Representative contour plots of CD25$^+$FoxP3$^+$ T lymphocytes after exposure to *T. brucei* parasites. Lymphocytes (CD8$^-$, CD8$^+$) exposed to *T. b. brucei* (C and H) and, stimulated by parasite antigen (D and I) and by parasite exosomes (E and J) 72 h were marked for CD25 and FoxP3. Cells were then evaluated by flow cytometry. In parallel, non-stimulated lymphocytes (negative control, A and F) and ConA-stimulated lymphocytes (positive control, B and G) were also assessed.

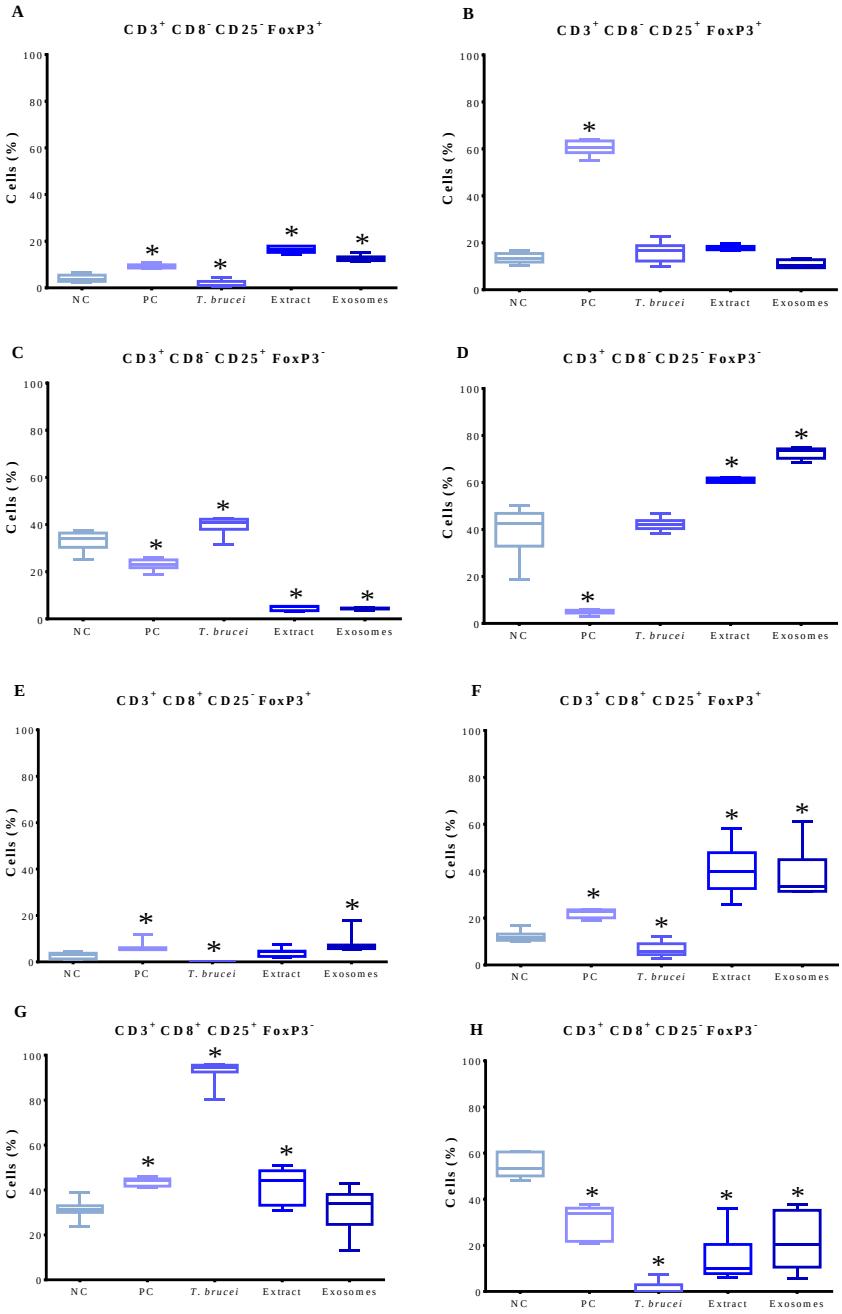

Figure 35 – T cell subsets induced by *T. b. brucei* were immunophenotyped for CD25 and FoxP3 biomarkers. Mouse lymphocytes incubated with parasites, parasite extract and parasite exosomes were magnetically separated in $CD8^-$ (A, B, C and D) and $CD8^+$ (E, F, G and H) cell fractions, labeled with CD3, CD25 and FoxP3 monoclonal antibodies and evaluated by flow cytometry. In parallel, non-stimulated cells (NC) and cells stimulated with ConA (PC) were also evaluated. $CD3^+$ cells were gated and the frequency of cells positive for CD25 and FoxP3 were estimated. Results of three independent experiments performed in triplicate are represented by box-plot, median, minimum and maximum values. The non-parametric Wilcoxon test was used for statistical comparisons ($p<0.05$). * indicates significant values when comparing non-stimulated lymphocytes (NC) *vs* the other conditions.

These results demonstrated that *T. b. brucei* decreases naturally occurring FoxP3 in both $CD8^-$ and $CD8^+$ cells. In $CD8^-$ lymphocytes, antigenic extract and parasite exosomes seem to stimulate effector T cells, while in $CD8^+$ cells antigenic extract and parasite exosomes demonstrated to be responsible for Treg expansion.

Taken together, these results allow us to indicate that the major lymphocyte subset in sleeping sickness is the effector subset ($CD25^-$ $FoxP3^-$), followed by the regulatory subset ($CD25^+$ $FoxP3^+$) and lastly, regulatory population ($CD25^-$ $FoxP3^+$) in $CD8^-$ cells. In $CD8^+$ cells, it was observed that the major subset corresponds to Treg cells ($CD25^+$ $FoxP3^-$, **Table 6**).

Table 6 – Blood T-cell subsets in African trypanosomiasis.

Phenotype		Mean ± SEM	
		$CD8^-$	**$CD8^+$**
$CD25^+FoxP3^+$ T cells (Activated Treg-cells)	T	10.54 ± 1.30	6.55 ± 1.31
	A	17.92 ± 0.41	41.30 ± 4.03
	E	10.90 ± 0.60	39.81 ± 4.13
$CD25^+FoxP3^-$ (Non-activated Treg-cells)	T	39.68 ± 1.66	94.65 ± 0.45
	A	4.60 ± 0.39	41.90 ± 3.21
	E	4.35 ± 0.14	31.53 ± 4.18
$CD25^-FoxP3^+$ (Treg-cells)	T	1.87 ± 0.53	0.01 ± 0.01
	A	16.40 ± 0.61	7.91 ± 1.68
	E	12.53 ± 0.54	4.73 ± 1.19
$CD25^-FoxP3^-$ (Effector T cells)	T	42.22 ± 1.14	1.63 ± 1.04
	A	60.93 ± 0.34	14.26 ± 4.51
	E	72.63 ± 0.90	21.73 ± 5.19

SEM: Standard error of mean; **T**: *T. brucei* trypomastigotes; **A**: *T. brucei* antigen; **E**: *T. brucei* exosomes

3.6.7. *T. b. brucei* triggers the increase in CD25 molecules on T cells

In order to better characterize $CD25^+$ cell subset and understand the role of Treg in sleeping sickness, density of CD25 molecules in cell membrane was evaluated through the respective fluorescent intensity.

$CD8^-$ T cells stimulated by ConA, parasite extract and parasite exosomes presented a high density of CD25 molecules when compared to non-stimulated lymphocytes ($p = 0.0313$). Furthermore, cells exposed to *T. b. brucei* parasites also evidenced a significant increase ($p = 0.0078$) of CD25 molecules (**Fig. 36A**).

$CD8^+$ T cells stimulated by ConA, parasite extract and parasite exosomes showed significant increase of CD25 molecules when comparing with non-stimulated lymphocytes ($p = 0.0313$). An even more accentuated increase was observed in *T. b. brucei*-stimulated lymphocytes ($p = 0.0156$, **Fig. 36B**).

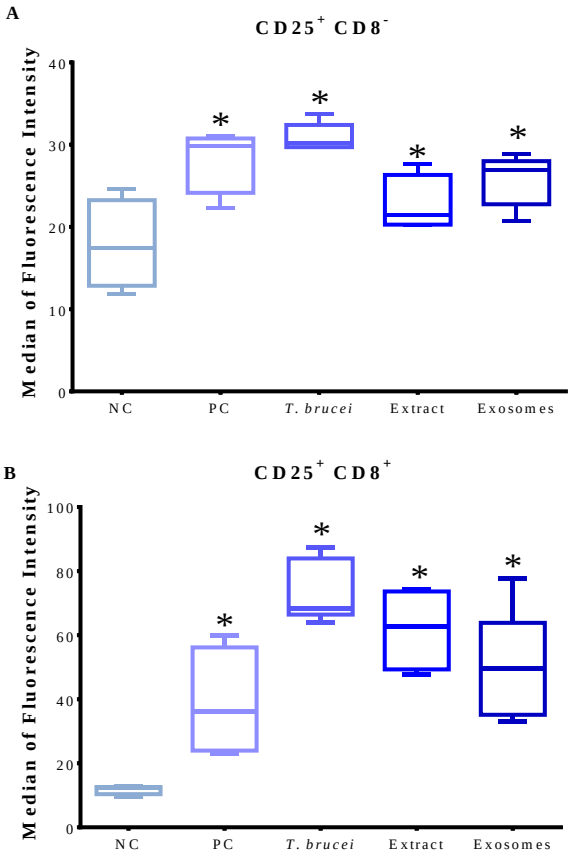

Figure 36 - **Density levels of CD25 molecules on *T. b. brucei*-exposed lymphocytes.** $CD8^-$ (A) and $CD8^+$ lymphocytes (B) exposed to *T. brucei* and stimulated by parasite extract and parasite exosomes were used to evaluate CD25 fluorescence intensity. Non-stimulated lymphocytes (NC) and ConA-stimulated lymphocytes (PC) were also evaluated. Results of three independent experiments and three replicates per sample are represented by box-plot, median, minimum and maximum values. The non-parametric Wilcoxon test was used for statistical comparisons ($p<0.05$). * represents significant differences when comparing non-stimulated lymphocytes *vs* the other conditions.

3.6.8. $CD25^+$ cell frequency and fluorescent intensity are positive correlated

In order to understand the correlation between cell proliferation and fluorescent intensity, linear regression of these two parameters was performed in $CD8^+$ and $CD8^-$ T cells. Positive correlations were obtained in the case of *T. b. brucei*-exposed lymphocytes. This indicates that when $CD25^+$ cell frequency is increased, the fluorescence intensity of CD25 molecules at lymphocyte surface also increase (**Fig. 37A and B**). In the case of parasite extract (**Fig. 37C and D**) and parasite exosomes ($p=0.0480$, **Fig. 37E and F**), it was observed in $CD8^-$ fraction a negative correlation,

indicating that despite their impairment in $CD25^+$ cell subset, they are able to stimulate CD25 surface molecules. However, for $CD8^+$ fraction, a positive correlation was observed, indicating that when $CD25^+$ cell subset expands also increase the density of CD25 molecules ($p_{parasite,\ extract}$=0.0011, $p_{exosomes}$=0.0045).

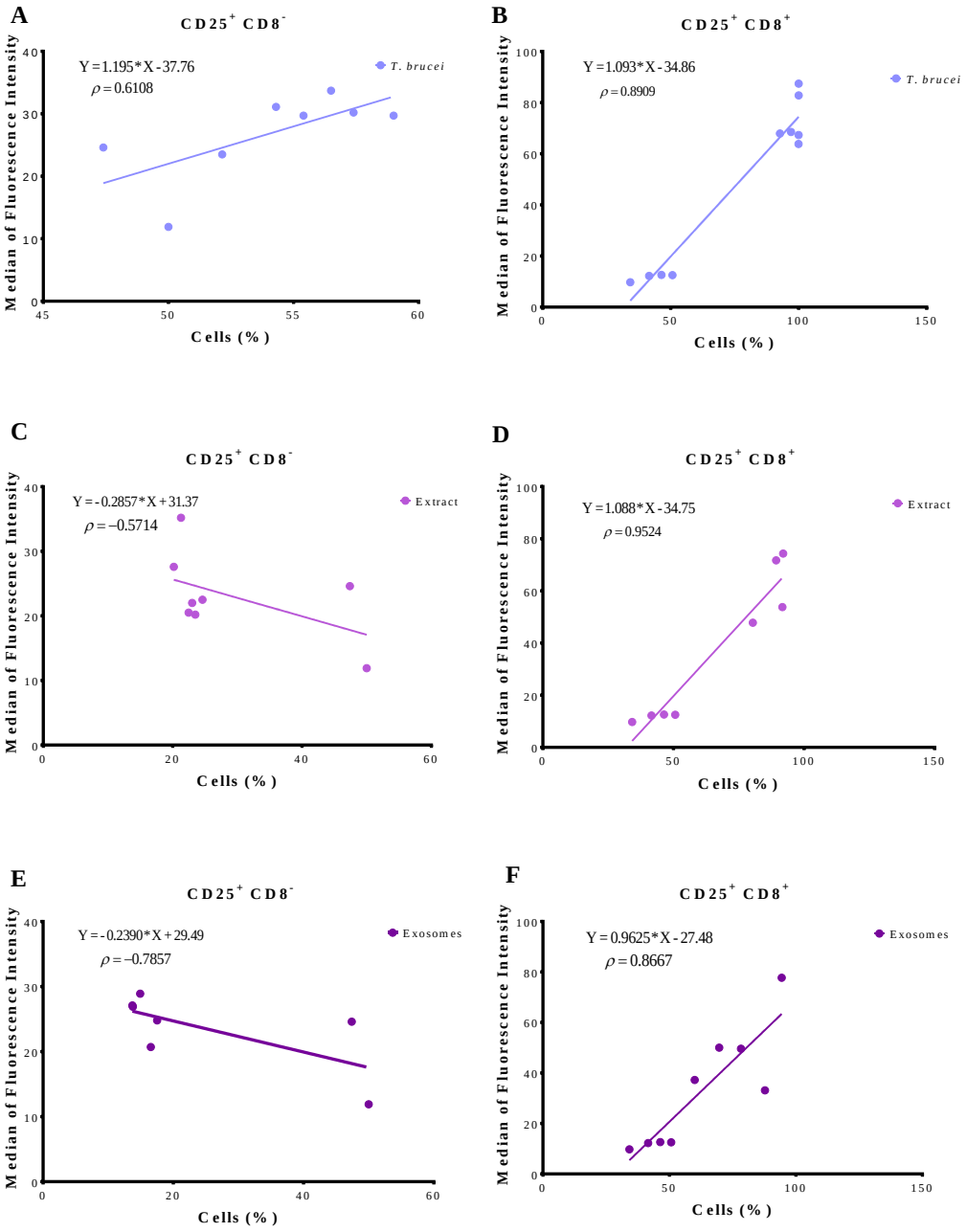

Figure 37 - Correlation between $CD25^+$ cell percentage and fluorescence intensity. A linear regression was generated using the frequency of $CD25^+$ $CD8^-$ (A, C and E) and $CD25^+$ $CD8^+$ (B, D and F) T cell fractions exposed to *T. brucei* (A and B), stimulated by parasite antigen (C and D) or by parasite exosomes (E and F) and the respective density of CD25 molecules.

3.6.9. *T. b. brucei* enhances FoxP3 molecules on $CD25^+$ $CD8^-$ T cells

In order to better characterize $CD25^+$ subset and understand the role of Treg in sleeping sickness, FoxP3 fluorescent intensity was evaluated, reflecting the expression level of these nuclear molecules.

Non-stimulated $CD8^-$ cells exhibited low levels of FoxP3 fluorescent intensity. ConA- ($p = 0.156$) parasite extract- and parasite exosomes-stimulated lymphocytes ($p_{extract,\ exosomes} = 0.0156$) significantly increased FoxP3 levels. When exposed to *T. b. brucei* trypomastigotes, lymphocytes also increased significantly FoxP3 molecules ($p = 0.0313$, **Fig. 38A**).

Non-stimulated and antigen-stimulated $CD8^+$ cells presented low fluorescent intensity. However, ConA and exosomes promoted a fluorescence increase ($p = 0.0313$). Lymphocytes exposed to parasites revealed a low level of FoxP3 molecules (**Fig. 38B**).

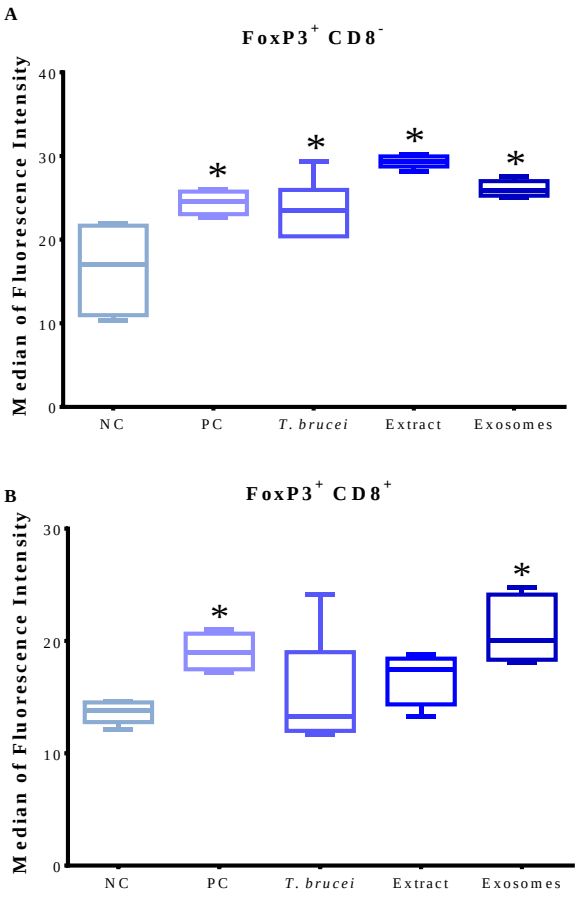

Figure 38 - Density levels of FoxP3 molecules on *T. b. brucei*-exposed lymphocytes. $CD8^-$ (A) and $CD8^+$ (B) lymphocytes exposed to *T. brucei* and stimulated by parasite extract and parasite exosomes were used to evaluate FoxP3 fluorescent intensity. Non-stimulated (NC) and ConA-stimulated lymphocytes (PC) were also evaluated. Results of three independent experiments and three replicates per sample are represented by box-plot, median, minimum and maximum values. The non-parametric Wilcoxon test was used for statistical comparisons ($p<0.05$). * represents statistical significant values when comparing non-stimulated lymphocytes *vs* the other conditions.

3.6.10. *T. b. brucei* triggers a negative correlation between $FoxP3^+$ cell frequency and fluorescence intensity

In order to understand the correlation between the expression of FoxP3 and proliferation of $FoxP3^+$ cells, linear regression of these two independent parameters was generated for $CD8^-$ and $CD8^+$ T cells. When exposed to parasites, both cell fractions evidenced a negative correlation, indicating a slight increase of FoxP3 molecules associated with cell decrease (**Fig. 39A and B**). However, in cells stimulated by parasite extract (**Fig. 39C and D**) and parasite exosomes (**Fig. 39E and F**) positive correlations

were found for both cell fractions, indicating that proliferation of FoxP3$^+$ cells was associated with the increase of FoxP3 molecules.

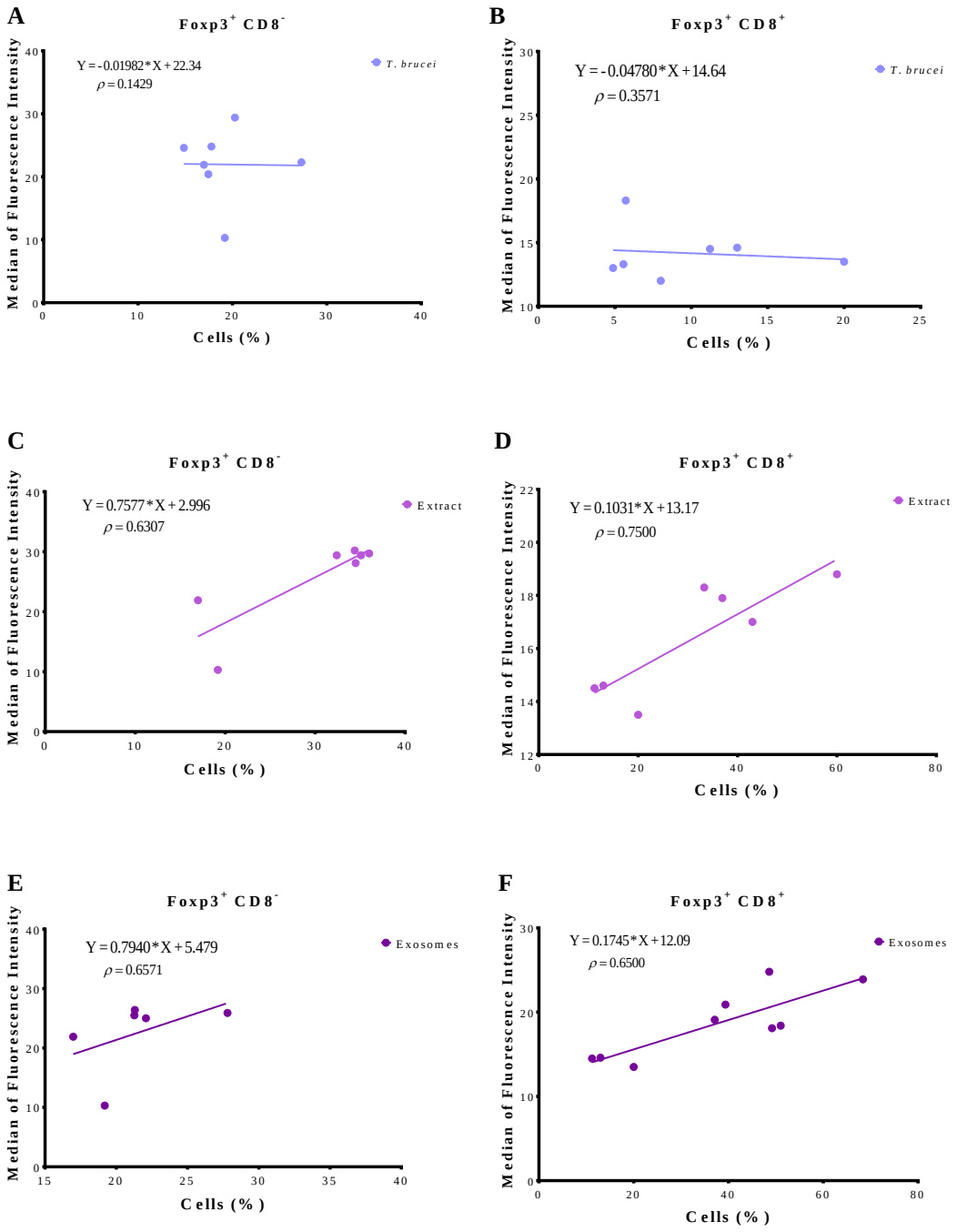

Figure 39 - Correlation between the frequency of CD3$^+$ cells and the intensity of CD3 molecules. A linear regression was generated using the frequency of FoxP3$^+$CD8$^-$ T cells (A, C and E) and FoxP3$^+$ CD8$^+$ (B, D and F) exposed to *T. brucei* (A and B), stimulated by parasite antigen (C and D) or by parasite exosomes (E and F) and the respective density of FoxP3 molecules.

4.DISCUSSION AND CONCLUDING REMARKS

African trypanosomes have been extensively studied, since they are responsible for diseases that are important in both medical and veterinary contexts. Several are the mechanisms that this extracellular protozoan uses to evade the immune system. However, since the parasite need to avoid their host mortality in order to ensure the conclusion of the life cycle, it is crucial to achieve an equilibrium between the level of infection (parasitemia) and intensity of the inflammatory immune response.

Since safe and efficient anti-trypanosomal drugs and vaccines are lacking, many are the studies performed to understand the underlying mechanisms associated with this parasite and the host immune response. Although different approaches have been performed and several results have been reported, there are some questions that remain unanswered and some mechanisms that are not entirely understood or still controversial. Therefore, the current work aimed to find an answer to some of these questions by evaluating leukocyte response to *T. brucei* trypomastigotes, *T. brucei* extract and *T. brucei* exosomes.

Transmission of African trypanosomes occurs during blood-feeding of both male and female tsetse flies. It is reported that the female deposits fully developed larva into the soil, triggering the development of an adult fly in just one month. Given this rapid spreading, vector also needs future control interventions (Brun et al., 2010). After feeding on an infected mammalian host, the fly becomes infected and parasites enter their digestive track. Upon the bite of a tsetse fly, there are components present in the saliva that triggers NO production and induce mast cell degranulation with consequent release of histamine and vasodilation, triggering parasite dissemination into bloodstream (Reviewed by Stijlemans et al., 2016).

NO is known to be involved in different cellular and organ function in the body. Regulates blood flow, participates in leukocyte adhesion and platelet aggregation, modulates physiological processes in the brain that affect cognitive functions and is vital for neuronal survival. Moreover, NO is also implicated in cellular immunity and acts as a toxic agent, regulating innate immune response (Bogdan, 2001, Coleman, 2001, Luiking et al., 2010). Since it regulates several processes, NO synthesis need to be highly regulated, otherwise different kind of damages can occur. Indeed, NO is

implicated in septic shock, and its overproduction is associated with neurodegenerative processes (Luiking et al., 2010).

A large expansion of MΦ in different organs (such as liver, spleen and bone marrow) has been described in *T. b. brucei*-infected mice (Gobert et al., 2000). NOS2 that were also found in these cells can oxidize L-arginine, originating L-citrulline and NO. When produced, NO undergoes a set of reactions that generate nitrite (NO_2^-) and nitrate (NO_3^-) (Gobert et al., 2000, Paulnock et al., 2010). The commercial kit used in the present study allows the indirect measurement of NO, through the joint detection of NO_2^- and NO_3^- .

In the present work, PMA was used to stimulate MΦ, assuring that cells were viable and functional by transforming arginase into NO through the enzymatic activity of NOS2. Thus, the use of a MΦ-like cell line in *in vitro* studies allows to evaluate the role of MΦ in a trypanosome infection, minimizing the need for murine models.

High levels of *de novo* NO were produced by MΦ when exposed to parasites or when stimulated by parasite extract or by parasite exosomes. In a previous study with *T. b. brucei*-infected mice, NO_2^- levels were measured and results reported that those levels peaked 6 days post-infection (Gobert et al., 2000). In the current work, high levels were observed than those that were reported, though both NO_2^- and NO_3^- were measured. In order to understand if NO_3^- might have been responsible for the MΦ-over activation that was observed, measurement of nitrate levels with Griess method should be performed hereafter. Furthermore, *T. brucei* exosomes also trigger the activation of MΦ metabolism, suggesting a role for these nanovesicles at the early-stage of sleeping sickness. Thus, these results indicate that in the first 24 h of parasitemia, high levels of NO are produced, with consequent mast cell degranulation, so the parasite can establish their infection and guarantee that their life cycle is maintained. However, it constitutes a disadvantage to host, given the large spectra of disorders that are associated with NO metabolism dysregulation.

L-arginine can instead be hydrolyzed by arginase, originating the production of ornithine, urea, proline and polyamines that are associated with tissue repair (Gordon and Martinez, 2010). In the present study, it was also found that the parasite, the extract

and exosomes induce MΦ to produce *de novo* urea. A previous study performed in *T. b. brucei*-infected mice indicate that type 1-MΦ predominate in the early stage of infection while type 2-MΦ appear in late stage of infection (1 - 4 weeks) (Stijemans et al., 2007). Positive correlation between urea and NO indicate that *in vitro* parasites can activate both MΦ L-arginine pathways. Although positive correlations were also found for parasite extract and parasite exosome stimulated-MΦ the joint amounts of urea and NO evidenced a steady pattern of low growth during the 24 h of observation. Taken together, these findings indicate that the effect of live parasites in MΦ activation is more intense that the parasite extract or the parasite exosomes.

It is described that the persistence of type 1-MΦ is associated with features like anemia of chronic disease (ACD) and systemic immune response syndrome (SIRS) that are features of sleeping sickness (Bertero and CaligarisCappio, 1997, Davies and Hagen, 1997, Stijemans et al., 2007). Since these clinical features are associated with late and chronic stages of infection, it is probable that type 1-MΦ be induced in both phases of disease. Moreover, to subvert NO effect it is also possible that African trypanosomes induce the activation of type 2-MΦ for their own benefit, since products or arginase metabolic degradation are known to induce parasite growth (Lott et al., 2014). It is known that African trypanosomes release kinesin heavy chain-1 (TbKHC-1), which induces the activation of arginine pathway, leading to polyamine production that is known as trypanosome essential nutrients (De Muylder et al., 2013).

The predomination of type 2-MΦ during infection onset and the continuous urea production described in African trypanosomiasis ensure parasite survival, leading to the establishment of a chronic infection. Given the fact that high NO levels were accumulated in 24 h of exposure of African trypanosomes and respective exosomes, it is normal to expect activation of aa-MΦ in order to prevent tissue lesions, that could also be associated with the activation of ca-MΦ as it was found in the present study.

During the course of infection, *T. brucei* releases stumpy induction factor (TSIF) that has been associated with the impairment of T cell proliferation (Gomez-Rodriguez et al., 2009). A previous study performed in HAT patients infected with *T. b. gambiense* has shown that T ($CD3^+$) cells were significantly lower when compared with controls

(non-HAT patients) (Lejon et al., 2014). In agreement with these findings, reduction of both $CD3^+CD8^-$ (which includes T helper cells) and $CD3^+CD8^+$ (T cytotoxic cells) cell subsets caused by trypomastigote parasites was demonstrated in the present study. These findings suggest the involvement of one or more parasite molecules that down-regulate lymphocyte subset expansion, as is the case of TSIF that was shown to be essential for parasite persistence (Stijlemans et al., 2016). However, lymphocyte population not only did not expand, as a significant contraction was found. Although not completely understood in the case of extracellular African trypanosomes, it is thought that these parasites develop different mechanisms that may induce apoptotic death of host immune cells (Elmore, 2007, Geiger et al., 2016,). Apoptosis is a process of programmed cell death, which major role is to maintain cellular homeostasis, controlling cell populations in the tissues, and has been previously described in T lymphocytes (Elmore, 2007, Krammer et al., 2007). In the case of *T. brucei* it was only reported an association with B cell apoptosis that culminates into lack of memory response (Radwanska et al., 2008). Therefore, take into account the above considerations and findings of the present study the hypothesis that African trypanosomes promote T cell apoptosis can be raised, leading to further studies by evaluating more specifically the apoptotic process. For example, the expression of CD95 can be assessed, since it is associated with Fas/Fas ligand, an apoptotic pathway, that was previously described in *T. cruzi* (Guillermo et al., 2007). On the contrary, *T. brucei* extract and *T. brucei* exosomes triggered an increase in $CD3^+CD8^-$ lymphocyte population, while in the case of $CD3^+CD8^+$ cells, only exosomes were responsible for cell expansion. Taking together, these findings indicate that parasites are able to negatively modulate both cytotoxic and helper T cells while exosomes seems to promote the spread of cytotoxic T cells and drive the expansion of helper T cells.

When analyzing expression of $CD8^-$ and $CD8^+$ T cells in all the evaluated cases (parasite exposure, parasite extract and parasite exosomes) a reduction of CD8 molecules was found. Since parasites promote depletion of $CD8^+$ T cells, and exosomes seem to cause a slight change in $CD8^+$ T cell subset, it is expected an enhancement of $CD8^-$ T cell activity. Early studies associated the increase of $CD4^+$: $CD8^+$ T cells ratio (healthy mice and human beings present a 2:1 ratio) with self-cure (Onah et al., 1999). However, low levels of $CD8^+$ T cells and the expected abrogation of IFN-α, described

as a *Trypanosome* grown factor, could lead to the suppression of parasite growth, contributing for host survival. Moreover, it has been demonstrated that this cytokine is not released in an environment rich in $CD8^+$ T cells, but becomes secreted by $CD4^+$ T cells (Liu et al., 2015). In the present study, $CD8^-$: $CD8^+$ T cell ratio was higher when lymphocytes were exposed to parasites or to parasite antigens, suggesting that the parasite or its antigens promote the preferential expansion of T helper cells in sleeping sickness. On the other hand, exosomes seem to have a minor effect. Even so, extracellular vesicles secreted by *T. brucei* need further investigation for instance, in the context of an IFN-α evaluation, to better understand their role in host immune response.

It is known that foreign antigens are presented to $CD8^+$ T cells when complex with MHCI molecules. However, an impairment of these molecules on MΦ membrane was found in cells exposed to *T. brucei*. At the parasitic point of view, delay of host mortality ensures parasite life-cycle conclusion and, consequently the transmission to its invertebrate vector and then to other mammal hosts. Thus, it is expected that the parasite has developed mechanisms able to subvert $CD8^+$ T cell activation, given the host mortality associated. According to Liu et al., (2015), $CD8^+$ T cells mediate mortality of *T. brucei*- infected BALB/c mice.

One of the mechanisms might be the impairment of MHCI molecules, reducing the probability of foreign antigens be recognized by cytotoxic T cells. To generate antigens, there is a biologic system, known as ubiquitin-proteasome. Briefly, proteasome is a protein complex, that performs protein degradation, generating peptides able to be complex with MHCI molecules. It has been reported that *T. cruzi* developed mechanisms to avoid the degradation of its own proteins and the consequent generation of parasite peptides, making the infection undetectable to host immune cells (Camargo et al., 2014). Although this mechanism is not clearly understood, the findings of the current study raise the hypothesis that *T. brucei* could have involved identical mechanisms.

Despite MΦ, also NK cells possess receptors for MHCI molecules. When recognize membrane MHCI molecules NK cells stay inactive, but in the absence of MHCI molecules or in the case of low levels of these molecules, NK cells become activated, being competent to induce a cytotoxic immune response. Since in the current

study it was observed a very reduced amount of cells expressing MHCI molecules when exposed to parasites, it would be possible to assume that NK will be active, for further infection control. However, it was previously reported that after nine days of infection, NK activity is severely reduced in *T. brucei*-infected mice (Vincendeau and Bouteille, 2006). As demonstrated in the present study, parasites cause an accentuated reduction in the differentiation of $MHCI^{+}M\Phi$ although induced an increase in the expression of MHCI molecules at the cell membrane. Therefore, antigen presentation to cytotoxic T cells becomes impaired and African trypanosomes can escape to the immune activity of $CD8^{+}$ T cells. Thus, reduction of NK activity might be a secondary effect derived from impairment of antigen presentation via MHCI.

Despite the low percentage of $MHCI^{+}$ cells, the amount of molecules on cell-surface presented a considerable increase. This might be an effect of host immune response to revert the parasite effect on cell reduction, enhancing parasite antigen presentation to $CD8^{+}$ T cells.

$MHCII^{+}$ MΦ were also at very low levels when exposed to *T. brucei* parasites and to parasite antigens, suggesting an impairment of APC functions. A decrease in the affinity of MHCII molecules for *T. brucei* antigen was reported (Namangala et al., 2000). However, in this particular case the fluorescence intensity did not indicate an increase of MHCII expression, suggesting that African trypanosomes may inhibit APC expansion and antigen presentation to $CD4^{+}$ T cells, exerting a negative modulation in host immune response.

The MHCI / MHC II ratio allowed to perform an indirect correlation with major stimulation of $CD8^{+}$ or $CD8^{-}$ respectively. The results indicated that African trypanosomes stimulate $CD8^{-}$ cells rather than $CD8^{+}$. Given the host mortality associated to $CD8^{+}$, as mentioned before, it might fully justify the depletion of $CD8^{+}$ T cells and the low MHCI / MHC II ratio found in the present study after parasite exposure and antigen stimulation. However, in the case of *T. brucei* exosomes, high MHCI / MHCII ratio suggested the involvement of both $CD4^{+}$ and $CD8^{+}$ T cells. These findings are in agreement with the differentiation of $MHCI^{+}$ and $MHCII^{+}M\Phi$ cells induced by exosomes. Moreover, when analyzing T cell subsets, also a proliferation of

$CD4^+$ and $CD8^+$ was observed, thus suggesting an involvement of both T cell populations.

Taken into consideration that parasite and parasite exosomes seem to have opposite roles in inducing cytotoxic T cell activity, the hypothesis that during sleeping sickness exosomes can function as a decoy, attracting the host immune cells while parasites stay free to establish disease should be considered.

During chronic parasite infections, uncontrolled inflammation is one of the most clinical features observed. It is known that an inflammatory response against parasite can become lethal if not balanced by Treg cells, since this T cell population is known to protect the host from collateral tissue damage (Vignali et al., 2008, Corthay, 2009). Previous evidences have suggested that naturally occurring $CD3^+CD4^+CD25^+FoxP3^+$ cells constitutes 5-10% of peripheral $CD4^+$ T cells in normal mice (Hsieh et al., 2004). Several studies in pathogenic diseases have been done and many pathogens have been reported to trigger the expansion of Treg cells (reviewed in Belkaid, 2007). In African trypanosomiasis, the expansion of Treg seems to occur from parasite establishment to chronic stage, being associated with parasite tolerance (reviewed in Adalid-Peralta et al., 2011). In trypanotolerant C57BL/6 mice, it was demonstrated the expansion of $CD4^+CD25^+FoxP3^+$ T cell subset after the first peak of parasitemia (Guilliams et al., 2007). More recently, the same group showed that the lack of expansion of Treg cell subset is associated with tissue damage and impaired survival of infected mice (Guilliams et al., 2008). In the current study, *T. b. brucei* seem to induce the expansion of $CD25^+$ cells in both $CD8^-$ and $CD8^+$ T cell subpopulations. However, in agreement with Guilliams et al. (2008) it was verified in the current study that naturally FoxP3 levels decrease. In fact, a positive correlation between $CD25^+$ cells and the density of CD25 molecules in cell membrane occurs, but the density of FoxP3 molecules slightly increase at the same time that $CD8^-$ $FoxP3^+$ and $CD8^+$ $FoxP3^+$ T cells decrease. Taken together, these findings suggest that when the parasite induces the expansion of $CD25^+$ T cell subset also increases the density of CD25 molecules on lymphocyte surface. However, *T. b. brucei* impairs $FoxP3^+$ cells while increase the expression of FoxP3 molecules.

In both $CD8^-$ and $CD8^+$ cell fractions a significant increase in CD25 cells was found. However, it is described that in human peripheral blood only $CD25^{+\ (high)}$ are recognized as regulatory T cells (Ermann and Fathman, 2003, Baecher-Allan and Hafler, 2004). There is also the fact that CD25 cell marker is not only specific to regulatory T cells (Kmieciak et al., 2009), thus the high levels observed specially in $CD8^+$ T cells might not be associated with regulation. In fact, despite high $CD25^+$ cell expansion, levels of FoxP3 were low. Although not completely defined, some authors describe that Treg cells are only activated in the presence of this transcription factor. The fact that the production of immunoregulatory cytokines by $CD25^+$ T cells is depending of FoxP3 expression and that an association between lack of FoxP3 and the origin of autoimmune diseases (Kmieciak et al., 2009) support the regulatory role of these cells. Other authors consider that $CD25^-$ $FoxP3^+$ constitutes another Treg cell subset (Zelenay et al., 2005). It was verified for both cell fractions that these cell subsets decreased, indicating that African trypanosomes may have mechanisms to retract this regulatory cells. Taken together the above considerations, is possible to suggest that African trypanosomes do not favor regulation of immune response, promoting anemia reduction and prolonged the survival of infected mice as Guilliams et al. (2008) previously suggested. However, in order to understand if high levels of CD25 that were observed in $CD8^+$ are really associated to regulation, further characterization of Treg should be done, using another cell markers, as is the case of cytotoxic T lymphocyte-associated antigen 4 (CTLA-4), glucocorticoid-induced tumour necrosis factor receptor family-related gene (GITR), lymphocyte activation gene-3 (LAG-3) or CD127, that were previously described as markers for Treg cells (Corthay, 2009). Despite this, to understand the significance of $CD8^-$ $CD25^+$ $FoxP3^-$ cell subset expansion, also further analysis with CD62L should be done, since high levels of this cell marker are associated with better characterization of Treg cells in $CD4^+$ $CD25^+$ T cells (Ermann and Fathman., 2003, Fu et al., 2004). Furthermore, an increase of FoxP3 molecules was found, suggesting that this might be an effect of immune system cells to subvert the lack of regulation that African trypanosomes seemed to favor.

On the other hand, *T. brucei* extract and exosomes induce the growth of $CD8^-$ $CD25^+FoxP3^+$ T cell subset and the expansion of $CD8^+CD25^+FoxP3^+$ T cell subset was

caused only by exosomes, indicating that in sleeping sickness T cell regulation can be mediated by parasite antigens and by exosomes released by parasites.

Several virulence factors have been associated with African trypanosomes. Flagellar proteins GPI-phospholipase C (GPI-PLC), calflagins and metascaspase-4 are the most studied and their presence in *T. brucei* exovesicle proteome was recently confirmed (Langousis and Hill, 2014, Szempruch et al., 2016). Taken together, these virulence factors increase parasite infectivity and consequently reduce host survival. Moreover, Szempruch et al. (2016) also reported that exovesicles contain AdC. It has been demonstrated that AdC is associated with the activation of protein kinase A, responsible for reducing TNF-α (Salmon et al., 2012). Like mentioned before, this cytokine is related to meningoencephalitis and tissue necrosis, which constitutes an advantage for the parasite and the host. However, it has been reported that natural Treg cells require TNF-α to maintain their functions (Housley et al., 2011). More specifically, this cytokine is known as an activator of $CD4^+$ $FoxP3^+$ Treg cells (Chen et al, 2010). With TNF-α levels decrease due to AdC activity, Treg might be impaired. In fact, when analyzing the results obtained, a significant increase of $CD8^-CD25^-FoxP3^+$ was observed when compared to resting lymphocytes. However, the subset $CD8^-CD25^+FoxP3^+$ cells is reduced after exosome stimulation. Although not measured, it is possible that TNF-α decreased after 24 h of infection when a decrease of NO production by MΦ was found, thus justifying the low levels of this subset. Given the fact that MΦ need this pro-inflammatory cytokine to activate NOS2, a reduction in the activity of this enzyme lead to NO reduction. Therefore, it is also possible that at 24 h of infection higher levels of $FoxP3^+$ cells would be found. Taken into account the above considerations, it is expected reduced levels of TNF-α at the early-stage of infection since this cytokine is described to be involved in parasite entrance in the liver, that is the major clearance organ for trypanosomes (Salmon et al., 2012). Thus, TNF-α high levels would favor low parasitemias, impairing trypanosome life cycle (Magez et al., 1999). Hence, exosomes-exposed lymphocytes should be studied within the course of infection, also as TNF-α levels, but with these results is possible to suggest that the low regulation that occurs in sleeping sickness might be associated with the release of AdC. If an association is confirmed, then this can originate new studies in order to find an

inhibitor of AdC and analyze the effects in T cell subsets, and the associated consequences.

To complement this work, several attempts were made to visualize the possible interactions that parasites could establish with MΦ. It was previously described that bloodstream forms of *T. brucei* did not adhere to coverslips used, or poly-L-lysine-coated coverslips (Gluenz et al., 2015). In this current work were used glass poly-D-lysine-coated coverslips and in fact, few were the parasites acquired. However, this may indicate that the protocol established in this study can be a potential alternative option to the cooper-coated coverslips Thermanox (Thermo Scientific), where bloodstreams forms seems to adhere (Gluenz et al., 2015). Yet, it requires a more refined optimization to accomplish a new successful adherence method for *T. brucei* bloodstream forms. However, unexpectedly, several difficulties were faced that lead to changes in technical procedure. At the end of this study, it was verified that in comparison with *Leishmania* promastigotes or mammal cells, like neutrophils, MΦ or hepatocytes, trypomastigotes are very fragile parasites that become almost fully destroyed during metallization process. In fact, only the flagellum that is constituted by a canonical 9 + 2 microtubules of tubulin (Ralston et al., 2009) rests intact. Therefore, the above considerations raised the hypothesis that trypomastigote cell body exhibits a faint microtubule cytoskeleton.

In summary, the current work allowed to characterize the role of MΦ and lymphocytes, in the context of an early stage of African trypanosome infection (**Fig. 40**). To the best of our knowledge, this was the first time that a correlation between cell subset and density of cell markers was evaluated in the context of sleeping sickness. Moreover, it was also the first time that the role of *T. brucei* exosomes was evaluated in leukocyte response. Even so, the findings of the present study should be complemented by future research in the context of cytokine profile, allowing to clarify some mechanism underlaying of both innate and adaptive immune responses in African trypanosomiasis.

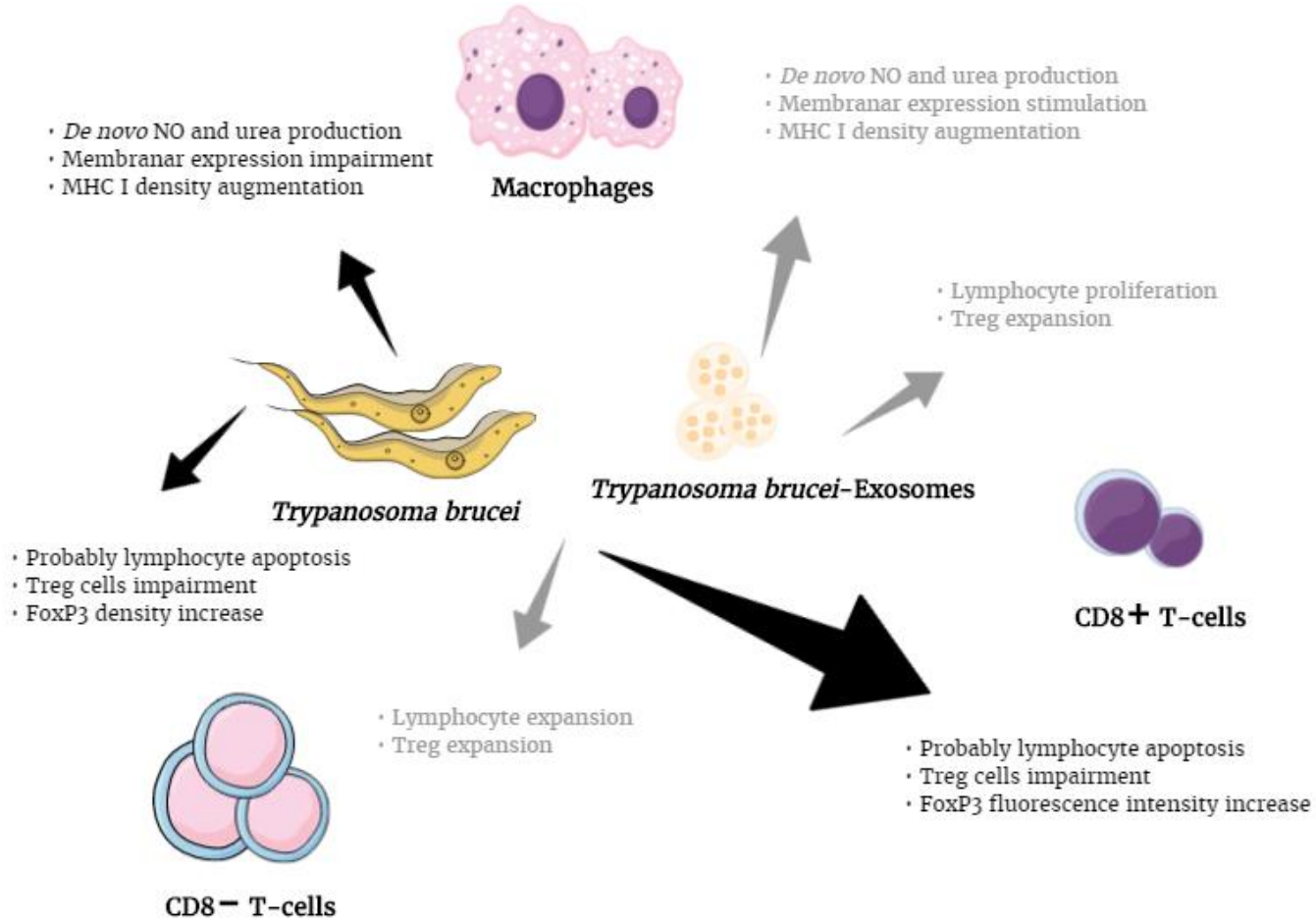

Figure 40 - Proposed mechanisms for *T. brucei* and *T. brucei*-exosomes interaction with the host immune system, in the early-stage of African trypanosome infection. The differentiation of T lymphocyte subsets, macrophage activation and potential for antigen presentation (bridging innate and adaptive immune response) when cells were exposed to parasites (black arrows and text) and exosomes (gray arrows and text) are represented.

5. REFERENCE LIST

ACHCAR, F., KERKHOVEN, E. J. & BARRETT, M. P. 2014. *Trypanosoma brucei*: meet the system. *Current Opinion in Microbiology,* 20**,** 162-169.

ADALID-PERALTA, L., FRAGOSO, G., FLEURY, A. & SCIUTTO, E. 2011. Mechanisms underlying the induction of regulatory T cells and its relevance in the adaptive immune response in parasitic infections. *International Journal of Biological Sciences,* 7**,** 1412-1426.

BAECHER-ALLAN, C. & HAFLER, DA. 2004. Supressor T cells in human diseases. *The Journal of Experimental Medicine,* 200(3):273-6

BARAL, T. N. 2010. Immunobiology of African Trypanosomes: Need of Alternative Interventions. *Journal of Biomedicine and Biotechnology***,** 24.

BARRETT, M. P., BOYKIN, D. W., BRUN, R. & TIDWELL, R. R. 2007. Human African trypanosomiasis: pharmacological re-engagement with a neglected disease. *British Journal of Pharmacology,* 152**,** 1155-1171.

BARRETT, M. P., BURCHMORE, R. J. S., STICH, A., LAZZARI, J. O., FRASCH, A. C., CAZZULO, J. J. & KRISHNA, S. 2003. The trypanosomiases. *Lancet,* 362**,** 1469-1480.

BARRY, J. D., GRAHAM, S. V., FOTHERINGHAM, M., GRAHAM, V. S., KOBRYN, K. & WYMER, B. 1998. VSG gene control and infectivity strategy of metacyclic stage *Trypanosoma brucei*. *Molecular and Biochemical Parasitology,* 91**,** 93-105.

BASU, S., HORAKOVA, E. & LUKES, J. 2016. Iron-associated biology of *Trypanosoma brucei*. *Biochimica Et Biophysica Acta-General Subjects,* 1860**,** 363-370.

BELKAID, Y. 2007. Regulatory T cells and infection: a dangerous necessity. *Nature Reviews Immunology,* 7**,** 875-888.

BERTERO, M. T. & CALIGARIS-CAPPIO, F. 1997. Anemia of chronic disorders in systemic autoimmune diseases. *Haematologica,* 82**,** 375-381.

BOCKSTAL, V., GUIRNALDA, P., CALJON, G., GOENKA, R., TELFER, J. C., FRENKEL, D., RADWANSKA, M., MAGEZ, S. & BLACK, S. J. 2011. *T.brucei* infection reduces B lymphopoiesis in bone marrow and truncates compensatory splenic lymphopoiesis through transitional B-cell apoptosis. *Plos Pathogens,* 7**,** 14.

BOGDAN, C. 2001. Nitric oxide and the immune response. *Nature Immunology,* 2**,** 907-916.

BREIDBACH, T., NGAZOA, E. & STEVERDING, D. 2002. *Trypanosoma brucei*: *in vitro* slender-to-stumpy differentiation of culture-adapted, monomorphic bloodstream forms. *Experimental Parasitology,* 101**,** 223-230.

BRUN, R., BLUM, J., CHAPPUIS, F. & BURRI, C. 2010. Human African trypanosomiasis. *Lancet,* 375**,** 148-159.

BUUS, S., SETTE, A. & GREY, H. M. 1987. The Interaction between protein-derived immunogenic peptides and Ia. *Immunological Reviews,* 98**,** 115-141.

CAMARGO, R., FARIA, L. O., KLOSS, A., FAVALI, C. B. F., KUCKELKORN, U., KLOETZEL, P. M., DE SA, C. M. & LIMA, B. D. 2014. *Trypanosoma cruzi* infection down-modulates the immunoproteasome biosynthesis and the MHC class I cell surface expression in HeLa cells. *Plos One,* 9**,** 12.

CATTAND, P., JANNIN, J. & LUCAS, P. 2001. Sleeping sickness surveillance: an essential step towards elimination. *Tropical Medicine & International Health,* 6**,** 348-361.

CHAPLIN, D. D. 2010. Overview of the immune response. *Journal of Allergy and Clinical Immunology,* 125**,** S3-S23.

CHEN, X., OPPENHEIM, JJ. 2010. TNF-alpha: an activator of $CD4^{+}FoxP3^{+}TNFR2^{+}$ regulatory T cells. *Current directions in autoimmunity,* 11:199-34

CNOPS, J., DE TREZ, C., BULTE, D., RADWANSKA, M., RYFFEL, B. & MAGEZ, S. 2015. IFN- mediates early B-cell loss in experimental African trypanosomosis. *Parasite Immunology,* 37**,** 479-484.

CNOPS, J., KAUFFMANN, F., DE TREZ, C., BALTZ, T., KEIRSSE, J., RADWANSKA, M., MURAILLE, E. & MAGEZ, S. 2016. Maintenance of B cells during chronic murine *Trypanosoma brucei gambiense* infection. *Parasite Immunology,* 38**,** 642-647.

COCHRANE, J. C. 1996. An introduction to scanning electron microscopy. *Microscopy Research and Technique,* 33**,** 87-87.

COLEMAN, J. W. 2001. Nitric oxide in immunity and inflammation. *International Immunopharmacology,* 1**,** 1397-1406.

CORTHAY, A. 2009. How do regulatory T cells work? *Scandinavian Journal of Immunology,* 70**,** 326-336.

DAVIES, M. G. & HAGEN, P. O. 1997. Systemic inflammatory response syndrome. *British Journal of Surgery,* 84**,** 920-935.

DE MUYLDER, G., DAULOUEDE, S., LECORDIER, L., UZUREAU, P., MORIAS, Y., VAN DEN ABBEELE, J., CALJON, G., HERIN, M., HOLZMULLER, P., SEMBALLA, S., COURTOIS, P., VANHAMME, L., STIJLEMANS, B., DE BAETSELIER, P., BARRETT, M. P., BARLOW, J. L., MCKENZIE, A. N. J., BARRON, L., WYNN, T. A., BESCHIN, A., VINCENDEAU, P. & PAYS, E. 2013. A *Trypanosoma brucei* kinesin heavy chain promotes parasite growth by triggering host arginase activity. *Plos Pathogens,* 9**,** 14.

DEVINE, D. V., FALK, R. J. & BALBER, A. E. 1986. Restriction of the alternative pathway of human complement by Intact *Trypanosoma brucei* subsp. *gambiense*. *Infection and Immunity,* 52**,** 223-229.

DRENNAN, M. B., STIJLEMANS, B., VAN DEN ABBEELE, J., QUESNIAUX, V. J., BARKHUIZEN, M., BROMBACHER, F., DE BAETSELIER, P., RYFFEL, B. & MAGEZ, S. 2005. The induction of a type 1 immune response following a *Trypanosoma brucei* infection is MyD88 dependent. *Journal of Immunology,* 175**,** 2501-2509.

ECKLE, S. B. G., TURNER, S. J., ROSSJOHN, J. & MCCLUSKEY, J. 2013. Predisposed alpha beta T cell antigen receptor recognition of MHC and MHC-I like molecules? *Current Opinion in Immunology,* 25**,** 653-659.

ELMORE, S. 2007. Apoptosis: A review of programmed cell death. *Toxicologic Pathology,* 35**,** 495-516.

ENANGA, B., BURCHMORE, R. J. S., STEWART, M. L. & BARRETT, M. P. 2002. Sleeping sickness and the brain. *Cellular and Molecular Life Sciences,* 59**,** 845-858.

ENGSTLER, M., PFOHL, T., HERMINGHAUS, S., BOSHART, M., WIEGERTJES, G., HEDDERGOTT, N. & OVERATH, P. 2007. Hydrodynamic flow-mediated protein sorting on the cell surface of trypanosomes. *Cell,* 131**,** 505-515.

ERMANN, J. & FATHMAN, C. G. 2003. Regulatory $CD4^{+}CD25^{+}$ T cells are 'suppressor' T cells. *Nature Reviews Immunology,* doi:10.1038/nri1043

FARGEAS, C., WU, C. Y., NAKAJIMA, T., COX, D., NUTMAN, T. & DELESPESSE, G. 1992. Differential effect of transforming growth factor-beta on the synthesis of Th1- and Th2-Lymphokines by human T lymphocytes. *European Journal of Immunology,* 22**,** 2173-2176.

FENN, K. & MATTHEWS, K. R. 2007. The cell biology of *Trypanosoma brucei* differentiation. *Current Opinion in Microbiology,* 10**,** 539-546.

FIELD, M. C., HORN, D., FAIRLAMB, A. H., FERGUSON, M. A. J., GRAY, D. W., READ, K. D., DE RYCKER, M., TORRIE, L. S., WYATT, P. G., WYLLIE, S. & GILBERT, I. H. 2017. Anti-trypanosomatid drug discovery: an ongoing challenge and a continuing need. *Nature Reviews Microbiology,* 15**,** 15.

FRANCO, J. R., SIMARRO, P. P., DIARRA, A. & JANNIN, J. G. 2014. Epidemiology of human African trypanosomiasis. *Clinical Epidemiology,* 6**,** 257-275.

FU, S., YOPP, A. C., MAO, X., CHEN, D. M., ZHANG, N., CHEN, D., MAO, M. W., DING, Y. Z. & BROMBERG, J. S. 2004. CD4(+) CD25(+) CD62(+) T-regulatory cell subset has optimal suppressive and proliferative potential. *American Journal of Transplantation,* 4, 65-78.

GEIGER, A., BOSSARD, G., SERENO, D., PISSARRA, J., LEMESRE, J. L., VINCENDEAU, P. & HOLZMULLER, P. 2016. Escaping deleterious immune response in their hosts: lessons from Trypanosomatids. *Frontiers in Immunology,* 7**,** 21.

GIORDANI, F., MORRISON, L. J., ROWAN, T. G., DE KONING, H. P. & BARRETT, M. P. 2016. The animal trypanosomiases and their chemotherapy: a review. *Parasitology,* 143**,** 1862-1889.

GLUENZ, E., WHEELER, R. J., HUGHES, L. & VAUGHAN, S. 2015. Scanning and three-dimensional electron microscopy methods for the study of *Trypanosoma brucei* and *Leishmania mexicana flagella*. *In:* BASTO, R. & MARSHALL, W. F. (eds.) *Methods in Cilia & Flagella.* San Diego: Elsevier Academic Press Inc.

GOBERT, A. P., DAULOUEDE, S., LEPOIVRE, M., BOUCHER, J. L., BOUTEILLE, B., BUGUET, A., CESPUGLIO, R., VEYRET, B. & VINCENDEAU, P. 2000. L-arginine availability modulates local nitric oxide production and parasite killing in experimental trypanosomiasis. *Infection and Immunity,* 68**,** 4653-4657.

GOMEZ-RODRIGUEZ, J., STIJLEMANS, B., DE MUYLDER, G., KORF, H., BRYS, L., BERBEROF, M., DARJI, A., PAYS, E., DE BAETSELIER, P. & BESCHIN, A. 2009. Identification of a parasitic immunomodulatory protein triggering the development of suppressive M1 macrophages during African Trypanosomiasis. *Journal of Infectious Diseases,* 200**,** 1849-1860.

GORDON, S. & MARTINEZ, F. O. 2010. Alternative activation of macrophages: mechanism and functions. *Immunity,* 32**,** 593-604.

GUILLERMO, L. V. C., SILVA, E. M., RIBEIRO-GOMES, F. L., DE MEIS, J., PEREIRA, W. F., YAGITA, H., DOSREIS, G. A. & LOPES, M. F. 2007. The Fas death pathway controls coordinated expansions of type 1 CD8 and type 2 CD4 T cells in *Trypanosoma cruzi* infection. *Journal of Leukocyte Biology,* 81**,** 942-951.

GUILLIAMS, M., BOSSCHAERTS, T., HERIN, M., HUNIG, T., LOI, P., FLAMAND, V., DE BAETSELIER, P. & BESCHIN, A. 2008. Experimental expansion of the regulatory T cell population increases resistance to African trypanosomiasis. *Journal of Infectious Diseases,* 198**,** 781-791.

GUILLIAMS, M., OLDENHOVE, G., NOEL, W., HERIN, M., BRYS, L., LOI, P., FLAMAND, V., MOSER, M., DE BAETSELIER, P. & BESCHIN, A. 2007. African trypanosomiasis: Naturally occurring regulatory T cells favor trypanotolerance by limiting pathology associated with sustained type 1 inflammation. *Journal of Immunology,* 179**,** 2748-2757.

HAMADIEN, M., LYCKE, N. & BAKHIET, M. 1999. Induction of the trypanosome lymphocyte-triggering factor (TLTF) and neutralizing antibodies to the TLTF in experimental African trypanosomiasis. *Immunology,* 96**,** 606-611.

HARTY, J. T., TVINNEREIM, A. R. & WHITE, D. W. 2000. $CD8^+$ T cell effector mechanisms in resistance to infection. *Annual Review of Immunology,* 18**,** 275-308.

HERTZ, C. J., FILUTOWICZ, H. & MANSFIELD, J. M. 1998. Resistance to the African trypanosomes is IFN-gamma dependent. *Journal of Immunology,* 161**,** 6775-6783.

HORN, D. 2014. Antigenic variation in African trypanosomes. *Molecular and Biochemical Parasitology,* 195**,** 123-129.

HOUSLEY, W. J., ADAMS, C. O., NICHOLS, F. C., PUDDINGTON, L., LINGENHELD, E. G., ZHU, L., RAJAN, T. V. & CLARK, R. B. 2011. Natural but not inducible regulatory T cells require TNF-alpha signaling for *in vivo* function. *Journal of Immunology,* 186**,** 6779-6787.

HSIEH, C. S., LIANG, Y. Q., TYZNIK, A. J., SELF, S. G., LIGGITT, D. & RUDENSKY, A. Y. 2004. Recognition of the peripheral self by naturally arising CD25(+) CD4(+) T cell receptors. *Immunity,* 21**,** 267-277.

HUNTER, C. A., GOW, J. W., KENNEDY, P. G. E., JENNINGS, F. W. & MURRAY, M. 1991. Immunopathology of experimental African sleeping sickness: detection of cytokine mRNA in the brains of *Trypanosoma brucei brucei*-infected mice. *Infection and Immunity,* 59**,** 4636-4640.

JAMONNEAU, V., ILBOUDO, H., KABORE, J., KABA, D., KOFFI, M., SOLANO, P., GARCIA, A., COURTIN, D., LAVEISSIERE, C., LINGUE, K., BUSCHER, P. & BUCHETON, B. 2012. Untreated human infections by *Trypanosoma brucei gambiense* are not 100% fatal. *Plos Neglected Tropical Diseases,* 6**,** 7.

JAMONNEAU, V., RAVEL, S., GARCIA, A., KOFFI, M., TRUC, P., LAVEISSIERE, C., HERDER, S., GREBAUT, P., CUNY, G. & SOLANO, P. 2004. Characterization of *Trypanosoma brucei* s.l. infecting asymptomatic sleeping-sickness patients in Cote d'Ivoire: a new genetic group? *Annals of Tropical Medicine and Parasitology,* 98**,** 329-337.

JOINER, K. A. 1988. Complement evasion by bacteria and parasites. *Annual Review of Microbiology,* 42**,** 201-230.

JONGEJAN, F., OOIJEN, C., ZIVKOVIC, D. & TERHUURNE, A. 1988. Quantitative correlation of parasitological and serological techniques for the diagnosis of *Trypanosoma congolense* infection in cattle. *Veterinary Quarterly,* 10**,** 42-47.

KEATING, J., YUKICH, J. O., SUTHERLAND, C. S., WOODS, G. & TEDIOSI, F. 2015. Human African trypanosomiasis prevention, treatment and control costs: A systematic review. *Acta Tropica,* 150**,** 4-13.

KEITA, M., BOUTEILLE, B., ENANGA, B., VALLAT, J. M. & DUMAS, M. 1997. *Trypanosoma brucei brucei*: A long-term model of human African trypanosomiasis in mice, meningo-encephalitis, astrocytosis, and neurological disorders. *Experimental Parasitology,* 85**,** 183-192.

KENNEDY, P. G. E. 2013. Clinical features, diagnosis, and treatment of human African trypanosomiasis (sleeping sickness). *Lancet Neurology,* 12**,** 186-194.

KMIECIAK, M., GOWDA, M., GRAHAM, L., GODDER, K., BEAR, H. D., MARINCOLA, F. M. & MANJILI, M. H. 2009. Human T cells express CD25 and Foxp3 upon activation and exhibit effector/memory phenotypes without any regulatory/suppressor function. *Journal of Translational Medicine,* 7**,** 7.

KRAMMER, P. H., ARNOLD, R. & LAVRIK, I. N. 2007. Life and death in peripheral T cells. *Nature Reviews Immunology,* 7**,** 532-542.

KURIAKOSE, S. M., SINGH, R. & UZONNA, J. E. 2016. Host intracellular signaling events and pro-inflammatory cytokine production in African Trypanosomiasis. *Frontiers in Immunology,* 7**,** 10.

LANGOUSIS, G. & HILL, K. L. 2014. Motility and more: the flagellum of *Trypanosoma brucei*. *Nature Reviews Microbiology,* 12**,** 505-518.

LANHAM, S. M. & GODFREY, D. G. 1970. Isolation of salivarian trypanosomes from man and other mammals using DEAE-cellulose. *Experimental Parasitology,* 28**,** 521-&.

LECORDIER, L., UZUREAU, P., TEBABI, P., PEREZ-MORGA, D., NOLAN, D., BURKARD, G. S., RODITI, I. & PAYS, E. 2014. Identification of *Trypanosoma brucei* components involved in trypanolysis by normal human serum. *Molecular Microbiology,* 94**,** 625-636.

LEJON, V., NGOYI, D. M., KESTENS, L., BOEL, L., BARBE, B., BETU, V. K., VAN GRIENSVEN, J., BOTTIEAU, E., TAMFUM, J. J. M., JACOBS, J. & BUSCHER, P. 2014. Gambiense human African Trypanosomiasis and immunological memory: Effect on phenotypic lymphocyte profiles and humoral immunity. *Plos Pathogens,* 10**,** 10.

LIU, G. G., SUN, D. L., WU, H., ZHANG, M. S., HUAN, H. X., XU, J. J., ZHANG, X. Q., ZHOU, H. & SHI, M. Q. 2015. Distinct contributions of CD4(+) and CD8(+) T cells to pathogenesis of *Trypanosoma brucei* infection in the context of gamma interferon and interleukin-10. *Infection and Immunity,* 83**,** 2785-2795.

LOTT, K., ZHU, L., FISK, J. C., TOMASELLO, D. L. & READ, L. K. 2014. Functional interplay between protein arginine methyltransferases in *Trypanosoma brucei*. *Microbiologyopen,* 3**,** 595-609.

LUCAS, R., MAGEZ, S., SONGA, B., DARJI, A., HAMERS, R. & DEBAETSELIER, P. 1993. A role for TNF during African trypanosomiasis: involvement in parasite control, immunosuppression and pathology. *Research in Immunology,* 144**,** 370-376.

LUCKHEERAM, R. V., ZHOU, R., VERMA, A. D. & XIA, B. 2012. CD4(+)T cells: Differentiation and functions. *Clinical & Developmental Immunology***,** 12: 925135.

LUIKING, Y. C., ENGELEN, M. & DEUTZ, N. E. P. 2010. Regulation of nitric oxide production in health and disease. *Current Opinion in Clinical Nutrition and Metabolic Care,* 13**,** 97-104.

LUNDKVIST, G. B., KRISTENSSON, K. & BENTIVOGLIO, M. 2004. Why trypanosomes cause sleeping sickness. *Physiology,* 19**,** 198-206.

MAGEZ, S., RADWANSKA, M., BESCHIN, A., SEKIKAWA, K. & DE BAETSELIER, P. 1999. Tumor necrosis factor alpha is a key mediator in the regulation of experimental *Trypanosoma brucei* infections. *Infection and Immunity,* 67**,** 3128-3132.

MAGEZ, S., SCHWEGMANN, A., ATKINSON, R., CLAES, F., DRENNAN, M., DE BAETSELIER, P. & BROMBACHER, F. 2008. The role of B-cells and IgM antibodies in parasitemia, anemia, and VSG switching in *Trypanosoma brucei*-infected mice. *Plos Pathogens,* 4**,** 12.

MAGEZ, S., STIJLEMANS, B., BARAL, T. & DE BAETSELIER, P. 2002. VSG-GPI anchors of African trypanosomes: their role in macrophage activation and induction of infection-associated immunopathology. *Microbes and Infection,* 4**,** 999-1006.

MALVY, D. & CHAPPUIS, F. 2011. Sleeping sickness. *Clinical Microbiology and Infection,* 17**,** 986-995.

MARCILLA, A., MARTIN-JAULAR, L., TRELIS, M., MENEZES-NETO, A., OSUNA, A., BERNAL, D., FERNANDEZ-BECERRA, C., ALMEIDA, I. C., & DEL PORTILLO, H. A. 2014. Extracellular vesicles in parasitic diseases. *Journal of Extracellular Vesicles,* 3, 10.3402

MASLOV, D. A., VOTYPKA, J., YURCHENKO, V. & LUKES, J. 2013. Diversity and phylogeny of insect trypanosomatids: all that is hidden shall be revealed. *Trends in Parasitology,* 29**,** 43-52.

MATTHEWS, K. R. 2005. The developmental cell biology of *Trypanosoma brucei. Journal of Cell Science,* 118**,** 283-290.

MCGETTRICK, A. F., CORCORAN, S. E., BARRY, P. J. G., MCFARLAND, J., CRES, C., CURTIS, A. M., FRANKLIN, E., CORR, S. C., MOK, K. H., CUMMINS, E. P., TAYLOR, C. T., O'NEILL, L. A. J. & NOLAN, D. P. 2016. *Trypanosoma brucei* metabolite indolepyruvate decreases HIF-1 alpha and glycolysis in macrophages as a mechanism of innate immune evasion. *Proceedings of the National Academy of Sciences of the United States of America,* 113**,** E7778-E7787.

MILLS, C. D. 2001. Macrophage arginine metabolism to ornithine/urea or nitric oxide/citrulline: A life or death issue. *Critical Reviews in Immunology,* 21**,** 399-425.

MOGENSEN, T. H. 2009. Pathogen recognition and inflammatory signaling in innate immune defenses. *Clinical Microbiology Reviews,* 22**,** 240.

NAMANGALA, B. 2011. How the African trypanosomes evade host immune killing. *Parasite Immunology,* 33**,** 430-437.

NAMANGALA, B. 2012. Contribution of innate immune responses towards resistance to African Trypanosome infections. *Scandinavian Journal of Immunology,* 75**,** 5-15.

NAMANGALA, B., BRYS, L., MAGEZ, S., DE BAETSELIER, P. & BESCHIN, A. 2000. *Trypanosoma brucei brucei* infection impairs MHC class II antigen presentation capacity of macrophages. *Parasite Immunology,* 22**,** 361-370.

NARE, B., WRING, S., BACCHI, C., BEAUDET, B., BOWLING, T., BRUN, R., CHEN, D. T., DING, C., FREUND, Y., GAUKEL, E., HUSSAIN, A., JARNAGIN, K., JENKS, M., KAISER, M., MERCER, L., MEJIA, E., NOE, A., ORR, M., PARHAM, R., PLATTNER, J., RANDOLPH, R., RATTENDI, D., REWERTS, C., SLIGAR, J., YARLETT, N., DON, R. & JACOBS, R. 2010. Discovery of novel orally bioavailable oxaborole 6-carboxamides that demonstrate cure in a murine model of late-stage central nervous system African Trypanosomiasis. *Antimicrobial Agents and Chemotherapy,* 54**,** 4379-4388.

NEWPORT, G. R., PAGE, C. R., ASHMAN, P. U., STIBBS, H. H. & SEED, J. R. 1977. Alteration of free serum amino acids in voles Infected with *Trypanosoma brucei gambiense*. *Journal of Parasitology,* 63**,** 15-24.

NORIS, M. & REMUZZI, G. 2013. Overview of complement activation and regulation. *Seminars in Nephrology,* 33**,** 479-492.

OKWOR, I., ONYILAGHA, C., KURIAKOSE, S., MOU, Z. R., JIA, P. & UZONNA, J. E. 2012. Regulatory T cells enhance susceptibility to experimental *Trypanosoma congolense* infection independent of mouse genetic background. *Plos Neglected Tropical Diseases,* 6**,** 9.

ONAH, D. N., HOPKINS, J. & LUCKINS, A. G. 1999. Changes in peripheral blood lymphocyte subpopulations and parasite-specific antibody responses in *Trypanosoma evansi* infection of sheep. *Parasitology Research,* 85**,** 263-269.

PAULNOCK, D. M. & COLLER, S. P. 2001. Analysis of macrophage activation in African trypanosomiasis. *Journal of Leukocyte Biology,* 69**,** 685-690.

PAULNOCK, D. M., FREEMAN, B. E. & MANSFIELD, J. M. 2010. Modulation of innate immunity by African Trypanosomes. *Parasitology,* 137**,** 2051-2063.

PAYS, E. & VANHOLLEBEKE, B. 2009. Human innate immunity against African trypanosomes. *Current Opinion in Immunology,* 21**,** 493-498.

PEACOCK, L., FERRIS, V., SHARMA, R., SUNTER, J., BAILEY, M., CARRINGTON, M. & GIBSON, W. 2011. Identification of the meiotic life cycle stage of *Trypanosoma brucei* in the tsetse fly. *Proceedings of the National Academy of Sciences of the United States of America,* 108**,** 3671-3676.

PONTE-SUCRE, A. 2016. An overview of *Trypanosoma brucei* infections: An intense host-parasite interaction. *Frontiers in Microbiology,* 7**,** 12.

RADWANSKA, M., GUIRNALDA, P., DE TREZ, C., RYFFEL, B., BLACK, S. & MAGEZ, S. 2008. Trypanosomiasis-induced B cell apoptosis results in loss of protective anti-parasite antibody responses and abolishment of vaccine-induced memory responses. *Plos Pathogens,* 4**,** 11.

RAPOSO, G. & STOORVOGEL, W. 2013. Extracellular vesicles: Exosomes, microvesicles, and friends. *Journal of Cell Biology,* 200**,** 373-383.

ROCHA, G., MARTINS, A., GAMA, G., BRANDAO, F. & ATOUGUIA, J. 2004. Possible cases of sexual and congenital transmission of sleeping sickness. *Lancet,* 363**,** 247-247.

ROCHE, P. A. & FURUTA, K. 2015. The ins and outs of MHC class II-mediated antigen processing and presentation. *Nature Reviews Immunology,* 15**,** 203-216.

ROCK, K. L., REITS, E. & NEEFJES, J. 2016. Present yourself by MHC class I and MHC class II molecules. *Trends in Immunology,* 37**,** 724-737.

SALMON, D., VANWALLEGHEM, G., MORIAS, Y., DENOEUD, J., KRUMBHOLZ, C., LHOMME, F., BACHMAIER, S., KADOR, M., GOSSMANN, J., DIAS, F. B. S., DE MUYLDER, G., UZUREAU, P., MAGEZ, S., MOSER, M., DE BAETSELIER, P., VAN DEN ABBEELE, J., BESCHIN, A., BOSHART, M. & PAYS, E. 2012. Adenylate cyclases of *Trypanosoma brucei* inhibit the innate immune response of the host. *Science,* 337**,** 463-466.

SCHLOSSMAN, S. F. 1984. Nomenclature for clusters of differentiation (CD) of antigens defined on human-leukocyte populations. *Bulletin of the World Health Organization,* 62**,** 809-811.

SCHROEDER, H. W. & CAVACINI, L. 2010. Structure and function of immunoglobulins. *Journal of Allergy and Clinical Immunology,* 125**,** S41-S52.

SCHWEDE, A. & CARRINGTON, M. 2010. Bloodstream form trypanosome plasma membrane proteins: antigenic variation and invariant antigens. *Parasitology,* 137**,** 2029-2039.

SHARMA, R., GLUENZ, E., PEACOCK, L., GIBSON, W., GULL, K. & CARRINGTON, M. 2009. The heart of darkness: growth and form of *Trypanosoma brucei* in the tsetse fly. *Trends in Parasitology,* 25**,** 517-524.

SHI, M. Q., PAN, W. L. & TABEL, H. 2003. Experimental African trypanosomiasis: IFN-gamma mediates early mortality. *European Journal of Immunology,* 33**,** 108-118.

STERNBERG, J. M. 2004. Human African trypanosomiasis: clinical presentation and immune response. *Parasite Immunology,* 26**,** 469-476.

STEVERDING, D. 2008. The history of African trypanosomiasis. *Parasites & Vectors,* 1**,** 8.

STIJEMANS, B., GUILLIAMS, M., RAES, G., BESCHIN, A., MAGEZ, S. & DE BAETSELIER, P. 2007. African trypanosomosis: From immune escape and in-immunopathology to immune intervention. *Veterinary Parasitology,* 148**,** 3-13.

STIJLEMANS, B., BESCHIN, A., MAGEZ, S., VAN GINDERACHTER, J. A. & DE BAETSELIER, P. 2015. Iron Homeostasis and *Trypanosoma brucei* associated immunopathogenicity development: A battle/quest for iron. *Biomed Research International***,** 15.

STIJLEMANS, B., CALJON, G., VAN DEN ABBEELE, J., VAN GINDERACHTER, J. A., MAGEZ, S. & DE TREZ, C. 2016. Immune evasion strategies of *Trypanosoma brucei* within the mammalian host: Progression to Ppathogenicity. *Frontiers in Immunology,* 7**,** 14.

STIJLEMANS, B., RADWANSKA, M., DE TREZ, C. & MAGEZ, S. 2017. African Trypanosomes undermine humoral responses and vaccine development: link with inflammatory responses? *Frontiers in Immunology,* 8**,** 14.

STOORVOGEL, W., KLEIJMEER, M. J., GEUZE, H. J. & RAPOSO, G. 2002. The biogenesis and functions of exosomes. *Traffic,* 3**,** 321-330.

SZEMPRUCH, A. J., SYKES, S. E., KIEFT, R., DENNISON, L., BECKER, A. C., GARTRELL, A., MARTIN, W. J., NAKAYASU, E. S., ALMEIDA, I. C., HAJDUK, S. L. & HARRINGTON, J. M. 2016. Extracellular vesicles from *Trypanosoma brucei* mediate virulence factor transfer and cause host anemia. *Cell,* 164**,** 246-257.

TACHADO, S. D. & SCHOFIELD, L. 1994. Glycosylphosphatidylinositol toxin of *Trypanosoma brucei* regulates IL-1 alpha and TNF-alpha expression in macrophages by protein tyrosine kinase mediated signal transduction. *Biochemical and Biophysical Research Communications,* 205**,** 984-991.

TURNER, C. M. R., ASLAM, N. & DYE, C. 1995. Replication, differentiation, growth and the virulence of *Trypanosoma brucei* infection$_s$. *Parasitology,* 111**,** 289-300.

VICKERMAN, K., TETLEY, L., HENDRY, K. A. K. & TURNER, C. M. R. 1988. Biology of African trypanosomes in the tsetse fly. *Biology of the Cell,* 64**,** 109-119.

VIGNALI, D. A. A., COLLISON, L. W. & WORKMAN, C. J. 2008. How regulatory T cells work. *Nature Reviews Immunology,* 8**,** 523-532.

VINCENDEAU, P. & BOUTEILLE, B. 2006. Immunology and immunopathology of African trypanosomiasis. *Anais Da Academia Brasileira De Ciencias,* 78**,** 645-665.

WEI, G. J. & TABEL, H. 2008. Regulatory T cells prevent control of experimental African trypanosomiasis. *Journal of Immunology,* 180**,** 2514-2521.

WHERRY, E. J. 2011. T cell exhaustion. *Nature Immunology,* 12**,** 492-499.

WORLD-HEALTH-ORGANIZATION 2012. Research Priorities for Chagas Disease, Human African Trypanosomiasis and Leishmaniasis. *Research Priorities for Chagas Disease, Human African Trypanosomiasis and Leishmaniasis: Technical Report of the Tdr Disease Reference Group on Chagas Disease, Human African Trypanosomiasis and Leishmaniasis.* Geneva: World Health Organization.

ZELENAY, S., LOPES-CARVALHO, T., CARAMALHO, I., MORAES-FONTES, M. F., REBELO, M. & DEMENGEOT, J. 2005. Foxp3(+) CD25(-) CD4 T cells constitute a reservoir of committed regulatory cells that regain CD25 expression upon homeostatic expansion. *Proceedings of the National Academy of Sciences of the United States of America,* 102**,** 4091-4096.

ZHU, J. F., YAMANE, H. & PAUL, W. E. 2010. Differentiation of effector CD4 T Cell populations. *In:* PAUL, W. E., LITTMAN, D. R. & YOKOYAMA, W. M. (eds.) *Annual Review of Immunology, Vol 28.* Palo Alto: Annual Reviews.